Copyright Warning & Restrictions

The copyright law of the United States (Title 17, United States Code) governs the making of photocopies or other reproductions of copyrighted material.

Under certain conditions specified in the law, libraries and archives are authorized to furnish a photocopy or other reproduction. One of these specified conditions is that the photocopy or reproduction is not to be "used for any purpose other than private study, scholarship, or research." If a, user makes a request for, or later uses, a photocopy or reproduction for purposes in excess of "fair use" that user may be liable for copyright infringement,

This institution reserves the right to refuse to accept a copying order if, in its judgment, fulfillment of the order would involve violation of copyright law.

Please Note: The author retains the copyright while the New Jersey Institute of Technology reserves the right to distribute this thesis or dissertation

Printing note: If you do not wish to print this page, then select "Pages from: first page # to: last page #" on the print dialog screen

NJIT New Jersey's Science & Technology University

The Van Houten library has removed some of the personal information and all signatures from the approval page and biographical sketches of theses and dissertations in order to protect the identity of NJIT graduates and faculty.

U·M·I

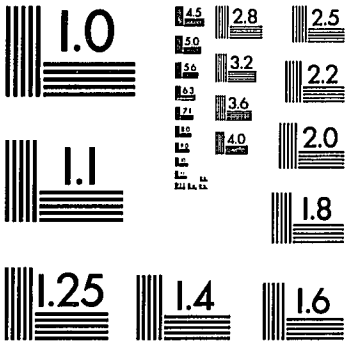

MICROCOPY RESOLUTION TEST CHART
NATIONAL BUREAU OF STANDARDS
STANDARD REFERENCE MATERIAL 1010a
(ANSI and ISO TEST CHART No. 2)

University Microfilms International
A Bell & Howell Information Company
300 N. Zeeb Road, Ann Arbor, Michigan 48106

INFORMATION TO USERS

While the most advanced technology has been used to photograph and reproduce this manuscript, the quality of the reproduction is heavily dependent upon the quality of the material submitted. For example:

- Manuscript pages may have indistinct print. In such cases, the best available copy has been filmed.
- Manuscripts may not always be complete. In such cases, a note will indicate that it is not possible to obtain missing pages.
- Copyrighted material may have been removed from the manuscript. In such cases, a note will indicate the deletion.

Oversize materials (e.g., maps, drawings, and charts) are photographed by sectioning the original, beginning at the upper left-hand corner and continuing from left to right in equal sections with small overlaps. Each oversize page is also filmed as one exposure and is available, for an additional charge, as a standard 35mm slide or as a 17"x 23" black and white photographic print.

Most photographs reproduce acceptably on positive microfilm or microfiche but lack the clarity on xerographic copies made from the microfilm. For an additional charge, 35mm slides of 6"x 9" black and white photographic prints are available for any photographs or illustrations that cannot be reproduced satisfactorily by xerography.

8701905

Chen, Win-Chung Tony

DEPOSITION OF PARTICLES IN TUBES DUE TO GRAVITY AND ELECTROSTATIC CHARGES

New Jersey Institute of Technology D.ENG.SC. 1986

University
Microfilms
International 300 N. Zeeb Road, Ann Arbor, MI 48106

PLEASE NOTE:

In all cases this material has been filmed in the best possible way from the available copy. Problems encountered with this document have been identified here with a check mark __√__.

1. Glossy photographs or pages _____
2. Colored illustrations, paper or print _____
3. Photographs with dark background _____
4. Illustrations are poor copy _____
5. Pages with black marks, not original copy _____
6. Print shows through as there is text on both sides of page _____
7. Indistinct, broken or small print on several pages __√__
8. Print exceeds margin requirements _____
9. Tightly bound copy with print lost in spine _____
10. Computer printout pages with indistinct print _____
11. Page(s) _____ lacking when material received, and not available from school or author.
12. Page(s) _____ seem to be missing in numbering only as text follows.
13. Two pages numbered _____. Text follows.
14. Curling and wrinkled pages _____
15. Dissertation contains pages with print at a slant, filmed as received _____
16. Other _____

_____

_____

University
Microfilms
International

DEPOSITION OF PARTICLES IN TUBES
DUE TO
GRAVITY AND ELECTROSTATIC CHARGES

By

Win-Chung Chen

A DISSERTATION
PRESENTED IN PARTIAL FULFILLMENT OF
THE REQUIREMENTS FOR THE DEGREE
OF
DOCTOR OF ENGINEERING SCIENCE
IN
MECHANICAL ENGINEERING
AT
NEW JERSEY INSTITUTE OF TECHNOLOGY

THIS DISSERTATION IS TO BE USED ONLY WITH DUE REGARD TO THE RIGHTS OF THE AUTHOR. BIBLIOGRAPHICAL REFERENCES MAY BE NOTED, BUT PASSAGES MUST NOT BE COPIED WITHOUT PERMISSION OF THE INSTITUTE AND WITHOUT CREDIT BEING GIVEN IN SUBSEQUENT WRITTEN OR PUBLISHED WORK.

NEWARK, NEW JERSEY, U.S.A.
1986

TITLE of THESIS : Deposition of Particles in Tubes Due to Gravity and Electrostatic Charges

Win-chung Chen, Doctor of Engineering Science, October, 1986

Thesis directed by: Professor Rong-Yaw Chen

ABSTRACT

The deposition of particles in a parallel-plate channel and a circular tube under the influence of inertia, fluid viscosity, gravity and electrostatic image forces was studied by analytical and numerical methods. A laminar flow with uniform and parabolic velocity profiles was investigated with a particle initial velocity of zero as well as that of the local fluid velocity.

The governing equations were solved by the Lagrangian approach to obtain the particle trajectories from which the fraction of deposition was calculated. Closed form solutions for particle trajectory and a complete deposition of particles in a finite length of the flow passage were obtained for the gravity force alone. When both gravity and image forces are present, the deposition increases greatly. However, a complete deposition cannot be attained, theoretically, in a finite length of the flow passage due to the balance of the downward gravity force and the upward image force in the flow field.

In general, the particle deposition is high for particles with small inertia forces and high image forces. It is also higher for uniform flow than for a parabolic flow and is higher for particles with zero initial velocity than that for particles with the initial velocity of the local fluid.

APPROVAL OF DISSERTATION

DEPOSITION OF PARTICLES IN TUBES

DUE TO

GRAVITY AND ELECTROSTATIC CHARGES

BY

WIN-CHUNG CHEN

FOR

DEPARTMENT OF MECHANICAL ENGINEERING

NEW JERSEY INSTITUTE OF TECHNOLOGY

BY

FACULTY COMMITTEE

APPROVED: _____ Chairman

_____

_____

_____

_____

NEWARK, NEW JERSEY

OCTOBER, 1986

ACKNOWLEDGEMENTS

The author wishes to express his sincere gratitute to his advisor, professor Rong-Yaw Chen, who provided many valuable suggestions, constant supervison, continuous guidance and encouragement throughout the course of investigation.

The author wishes also to express his sincere gratitute to Dr. John V. Droughton, Dr. Robert P. Kirchner, Dr. Hans E. Pawel and Dr. Bernard Koplik who have kindly read through the original manuscript and provided valuable suggestions. Also, a special thanks to my friend, Reginald Chen, for his patience of reading the first draft.

Further acknowledgement is given to Mechanical Engineering Department of the New Jersey Institute of Technology for the teaching assistantship during the academic years of 1983-1986.

TABLE OF CONTENTS

	PAGE
ABSTRACT	ii
APPROVAL PAGE	iv
ACKNOWLEGEMENTS	v
TABLE OF CONTENTS	vi
LIST OF TABLES	viii
LIST OF FIGURES	ix
NOMENCLATURE	xi
CHAPTER	
1. INTRODUCTION	1
2. LITERATURE SURVEY	5
3. ANALYSIS	16
3.1 DESCRIPTION OF ANALYSIS	17
3.2 ASSUMPTIONS	18
3.3 GOVERNING EQUATION	19
3.4 COMPUTATION OF FRACTIONAL DEPOSITION IN PARALLEL-PLATE CHANNELS	25
3.4.1 INFLUENCE OF PARTICLE SIZE ON THE MAGNITUDES OF CHARGE, INERTIA, AND IMAGE FORCES . .	25
3.4.2 SOLUTIONS FOR CHANNEL FLOW WITH INERTIA AND GRAVITY FORCES	26
3.4.3 COMPUTATION OF FRACTION OF DEPOSITION . .	30
3.4.4 DEPOSITION DUE TO VISCOUS, INERTIA, GRAVITY AND IMAGE FORCES	37
3.5 COMPUTATION OF FRACTIONAL DEPOSITION IN CIRCULAR TUBES	41

3.5.1 INFLUENCE OF PARTICLE SIZE ON THE MAGNITUDES OF CHARGE, INERTIA AND IMAGE FORCES . . . 41
3.5.2 SOLUTIONS FORFLOW WITH INERTIAAND GRAVITY FORCES 43
3.5.3 COMPUTATION OF FRACTION OF DEPOSITION . . 48
3.5.4 DEPOSITION DUE TO VISCOUS, INERTIA, GRAVITY AND IMAGE FORCES 57
4. RESULTS AND DISCUSSIONS 62
4.1 DEPOSITION IN PARALLEL-PLATE CHANNELS 62
4.1.1 VISCOUS, INERTIA AND GRAVITY IMAGES . . . 63
4.1.2 VISCOUS, INERTIA, GRAVITY AND IMAGE FORCES 68
4.2 DEPOSITION IN CIRCULAR TUBES 72
4.2.1 VISCOUS, INERTIA AND GRAVITY FORCES . . . 73
4.2.2 VISCOUS, INERTIA, GRAVITY AND IMAGE FORCES 78
5. CONCLUSIONS 81
6. RECOMMENDATION 85
REFERENCE 87
APPENDICES 91
A. NUMERICAL COMPUTATION METHODS FOR CIRCULAR TUBES 91
B. NUMERICAL COMPUTATION METHODS WITH ADDITIONAL IMAGE FORCES 101
TABLES 105
FIGURES 108
VITA 133

LIST OF TABLES

Table		Page
3.1	The Magnitudes of Charge, Gravity and Inertia Parameters	105
3.2	The Magnitudes of Image Force, Gravity and Inertia in a Parallel-Plate Channel ; h = 2 cm, uo = 30 cm/sec	105
3.3	The Magnitudes of Image Force, Gravity and Inertia in a Parallel-Plate Channel; h = .1 cm, uo = 30 cm/sec	106
3.4	The Magnitudes of Image Force, Gravity and Inertia in a Circular Tube; h = 2 cm, uo = 30 cm/sec	106
3.5	The Magnitudes of ImageForce, Gravity and Inertia in a Circular Tube; h = .1 cm, uo = 30 cm/sec	107
3.6	Summary of Analysis on the Particle Deposition due to Viscous, Inertia, Gravity and Electrostatic Charge Forces in Parallel-plate Channels and Circular Tubes	108

LIST OF FIGURES

Figure		Page
3.1	Cartensian Coordinate System Employed in the Analysis	108
3.2	Deposition Route of Particles in a Fluid of Uniform Velocity Profile Confined by a Parallel-Plate Channel	109
3.3	Deposition Route of Particles in a Fluid of Parabolic Velocity Profile Confined by a Parallel-Plate Channel	110
3.4	Deposition Route of Particles in Parallel-Plate Channels with Additional Image Force . . .	111
3.5	Typical Equi-penetration Curves in a Circular Tube for a Uniform Flow with Gravity and Inertia Forces Involved	112
3.6	Typical Equi-penetration Curve (CDB) Lied above the Z-axis	113
3.7	Typical Equi-penetration Curves in a Circular Tube for a Parabolic Flow with Gravity and Inertia Forces Involved	114
3.8	Deposition Route of Particles in a Circular Tube with Additional Image Force Involved . .	115
3.9	Typical Data Points on an Inlet Plane of a Circular Tube	116
4.1	Effect of Gravity and Inertia on Deposition for Uniform Flow in a Parallel-Plate Channel; Up_o = 0, G = 1	117
4.2	Effect of Gravity and Inertia on Deposition for Uniform Flow in a Parallel-Plate Channel; Up_o = U_f, G = 1	118
4.3	Generalized Deposition Curve in a Parallel-Plate Channel for $X^* < 200$ in a Uniform Flow; Up_o = Uf, G = 1, ($X^* = X/Q$, $DEPO^* = DEPO/Q$)	119
4.4	Generalized Deposition Curve in a Parallel-Plate Channel for $X^* < 3$ in a Uniform Flow; Up_o = Uf, G = 1, ($X^* = X/Q$, $DEPO^* = DEPO/Q$)	120

4.5 Effect of Gravity and Inertia on Deposition for Parabolic Flow in a Parallel-Plate Channel; $Up_o = 0$, G = 1 121

4.6 Effect of Gravity and Inertia on Deposition for Parabolic Flow in a Parallel-Plate Channel; $Up_o = U_f$, G = 1 122

4.7 Effect of Gravity, Inertia and Image Force on Deposition for Uniform Flow in a Parallel-Plate Channel; $Up_o = 0$, G = 1, Fp = 1 123

4.8 Effect of Gravity, Inertia and Image Force on Deposition for Uniform Flow in a Parallel-Plate Channel; $Up_o = U_f$, G = 1, Fp = 1 124

4.9 Effect of Gravity, Inertia and Image Force on Deposition for Parabolic Flow in a Parallel-Plate Channel; $Up_o = 0$, G = 1, Fp = 1 125

4.10 Effect of Gravity, Inertia and Image Force on Deposition for Parabolic Flow in a Parallel-Plate Channel Channel; $Up_o = U_f$, G = 1, Fp = 1 126

4.11 Effect of Gravity and Inertia on Deposition for Uniform Flow in a Circular Tube; $Up_o = 0$, G = 1 127

4.12 Effect of Gravity and Inertia on Deposition for Uniform Flow in a Circular Tube; $Up_o = U_f$, G = 1 128

4.13 Effect of Gravity and Inertia on Deposition for Parabolic Flow in a Circular Tube; $Up_o = 0$, G = 1 129

4.14 Effect of Gravity and Inertia on Deposition for Parabolic Flow in a Circular Tube; $Up_o = U_f$, G = 1 130

4.15 Effect of Gravity, Inertia and Image Force on Deposition for Uniform Flow in a Circular Tube; $Up_o = U_f$, G = 1, Fp = 1 131

4.16 Effect of Gravity, Inertia and Image Force on Deposition for Parabolic Flow in aCircular Tube; $Up_o = U_f$, G = 1, Fp = 1 132

NOMENCLATURE

Symbol

a	particle radius
D	Brownian diffusion coefficient
D_p	particle diameter
f	Stoke's drag force
Fx,Fy,Fz	dimentionless particle image force in the axial and vertical components
F_p	charge parameter
g	gravity acceleration constant
G	gravitational force parameter
K	constant parameter, 1/(Q G)
H	half of the dimensionless channel width
h	half the channel width
m	mass of a particle
n	particle concentration
n_o	inlet particle concentration
N	dimensionless particle concentration
N_o	dimensionless inlet particle concentration
Ix,Iy	particle image force in the axial and vertical
q	electric charge per particle
Q	Stocke's number or particle inertia parameter
R	dimensionless radial distance
R_i	dimensionless radial distance at step i
R_o	dimensionless radius
Rs	radial distance of the new coordinate S

t	time variable
T	dimensionless time variable
T"	dimensionless time variable (T/Q)
u,v,w	x, y, z component of fluid velocity
u_p, v_p, w_p	x, y, z component of particle velocity
u_o	inlet velocity of fluid (uniform)
u_{po}	inlet velocity of particle
U,V,W	dimensionless X, Y, Z component of fluid velocity
Up,Vp,Wp	dimensionless X, Y, Z component of particle velocity
Uo	dimensionless inlet velocity of fluid (uniform)
Up_o	dimensionless inlet velocity of particle
x,y,z	axial, vertical and horizontal coordinates
yo,zo	inlet particle coordinate
X,Y,Z	dimensionless axial, vertical and horizontal corordinates
Xl, X2	dimensionless channel length
Yo,Zo	dimensionless particle inlet coordinate
Ys,Zs	dimensionless vertical and horizontal component of new coordinate system S
Ym	origin of new coordinate system S
Yl	vertical component of the upper point deposited at a distance Xl
Y2	vertical component of the lower point deposited at a distance Xl

Greek Letters

ε''	permitivity of free space
θ	polar angle coordinate of inlet point
θ_w	polar angle coordinate of inlet point at the wall
μ	viscosity of the fluid of suspension
pi	3.14159...

Superscripts

"	dimensionless quantities as defined

Subscripts

i	the ith step (i = 1,2,3....)
o	initial or inlet condition
p	particle phase
w	condition at wall

CHAPTER 1 INTRODUCTION

Advances in science and technology have increased productivity and provided a luxurious life for mankind, yet these same advances have also accelerated the depletion of natural resources and polluted the environment. The major sources of pollutants are exhaust fumes and discharge liquid from chemical factories. The motion and deposition of such contaminants in suspension in a fluid moving through a conduit are, therefore, important subjects in recent years.

The investigation of the particle deposition process in a suspension of moving fluid is relevant to the design of dust collection equipment, aerosol spray devices and fluidic devices, and also to the understanding of the deposition process in the human respiratory system. A detailed knowledge of the mechanism of deposition would be helpful in understanding the deposition process, and controlling the particle deposition on these devices would result in better control of pollutants.

To predict the performance of deposition effectively, the significance of each mechanism or parameter involved has to be identified, and a mathematical model simulating the flow and deposition process must be developed.

The forces that affect the motion of the particles are

the inertia or the mass of the particle, the gravity acting on the particle, and the force exerted on the particle due to the velocity difference between the particle and the fluid.

For particles with electrostatic charges, the deposition forces are due to space charge repulsive forces and image forces. When particles having the same polarity of charge are distributed in a space, they tend to repel one another and drift toward the tube wall. This type of force is called the space charge repulsive force. The tube wall is generally considered grounded, i.e. it has zero electrostatic potential. When a particle is placed in front of a grounded wall, an attractive electrostatic force, the image force, between the particle and the wall is induced. At a particle concentration of greater than 1.0 E7 particles per cubic centimeter, the deposition is mainly due to space charge repulsive forces (see Yu [41]), while at a particle concentration of less than 1.0 E5, the deposition is mainly due to image forces.

Practically all aerosols or particles, natural or artificial, are eletrostatically charged. When particles capture free ions from the air, they become charge carriers. Particles may also acquire charge when they impact each other and the wall.

The purpose of this study is to investigate the deposition of particles in a channel and a circular tube due

to interia, gravity and charge image forces. The significance of each individual mechanism on the deposition is investigated first and the combined effect of each parameter on the deposition can, therefore , be assessed.

A steady incompressible laminar flow of fluid with uniformly charged particles in a parallel-plate channel and a circular tube are studied by a particle pathline method. The effects of inertia, gravity and image forces are considered, and parabolic and uniform velocity profiles are assumed. For uniform flow with inertia and gravity forces, a closed form solution can be obtained. In most cases numerical analysis of the non-linear differential equations is required.

The computer programs for the numerical method were executed on a UNIVAC VS/9, VAX 11/780. Programs in Univac and Vax systems were written in Fortran IV. The trajectory or pathline of each particle entering the tube inlet is calculated first, and then an equi-penetration line is determined as the inlet section is found. From the equi-penetration line the deposition can be calculated.

Two particle inlet velocities are studied. One is equal to the velocity of the fluid, the other is zero. This represents the limiting cases since the actual inlet velocity of a particle is, most likely, somewhat between zero and the fluid velocity.

In Chapter Two a summarized literature survey on the deposition of suspension under the effect of gravitational force, inertia, and image forces are presented.

In Chapter Three the trajectories of particles due to these forces are obtained analytically and numerically and are used to calculate the fractions of deposition. In chapter Four the results from all the forces involved are presented and discussed.

High particle deposition is obtained for particles with small inertia forces and high image forces and for uniform flow with zero initial velocity. Conclusions are presented in Chapter Five and recommendation are in Chapter Six.

CHAPTER 2 LITERATURE SURVEY

Investigations of particle deposition for laminar flow have been carried out by many authors. This survey focuses on the deposition of suspensions in parallel-plate channels and circular tubes due to gravity, inertia and electrostatic forces.

Gravitational Force Alone

For a submicron particle moving in a fluid, its inertial effect may be neglected and the particles can be maintained at the same velocity as that of the fluid. Deposition due to gravitational force alone has been studied by Walton [36] in 1954 and Thomas [33] in 1958. These studies are included in The Mechanics of Aerosol by Fuchs [16].

By means of the concept of the particle trajectory function, Pich [27] derived an equi-penetration curve of particles at the inlet plane. The particles below the equi-penetration curve are considered deposited on the wall. The deposition efficiency is found by integrating the product of particle velocity and the area between the equi-penetration curve and the boundary of the channel wall.

Wang [37] further developed the concept of particle trajectory in an inclined channel in a laminar flow. Analytical solutions for gravitational deposition of

particles were derived for the uphill and downhill flows. At zero inclination (i.e. in a horizontal tube) Wang obtained the same solution as that derived by Pich [27]. In an uphill flow with parabolic velocity profile, the axial component of particle velocity at the entrance region is negative; hence these particles are not able to enter the tube. Therefore, in the calculation of particle deposition, those particles are not included while in a downhill flow, this situation does not happen since the axial components of particle velocity in the entrance region are all positive. It was found that the deposition is dependent upon the sedimentation parameter, which is the product of the particle terminal velocity, the diameter of tube, and the angle of inclination.

When the settling velocity component in the axial direction of the tube was small in comparison with the axial flow velocity, Heyder and Gebhart [19] obtained a solution which is applicable to both uphill and downhill flow directions. By visualization of the small airways in the human respiratory tract as a system of randomly oriented circular tubes, it was found that the deposition efficiency was equal to $vt/2r$, where v is the terminal settling velocity, t is the mean residence time of aerosol particles in these tubes, and r is the radius of these tubes. Two He-Ne laser photometers were used to measure gravitational deposition of particles in laminar flows of air through inclined tubes.

The deposition of particles from flows in a system of finite tubes in random orientation was further studied by Thiagarajan and Yu [32] to include the case of a large settling velocity.

Gravitational Force and Particle Inertia

Taulbee [31] studied the effects of gravity on deposition in the entrance region of a developing flow in a circular tube. The developing flow field was calculated numerically using the boundary layer equations. It was found that deposition at a very small settling velocity is essentially the same as that of fully developed flow. In this case, most of the particles settle out after the flow becomes fully developed. For a very large settling parameter, the solution with developing flow approached that for constant uniform flow. For this case, the particles settle out relatively near the entrance where the flow profile is flat.

In addition, Taulbee [31] studied the effects of particle inertia on the deposition and found that the deposition rate decreases with increasing inertia forces. The results show that the deposition is smaller near the tube entrance when the inertia parameter was introduced. The introduction of inertia causes the initial axial momentum of the particles to carry them farther downstream before the

vertical gravitational settling velocity carries the particles toward the tube surface. The inertia effects could be neglected if the inertia parameter, which is defined as the square of particle radius divided by the product of kinematic viscosity and the particle relaxation time, is less than 1000.

Electrostatically Charged Particles

It has been known that all dust particles become electrostatically charged upon being dispersed into a cloud. Cheng and Soo [10] indicated that the basic mechanism of particle being charged is due to impact or collision. The charge redistribution during impact was described in terms of the particle dynamics, and the properties of the materials of the contacting surfaces.

When electrostatically charged particles are suspended in a fluid, the deposition is due to both the space charge repulsive force and the image force. Yu and Chandra [44] analysed these forces seperately and compared the results with existing experimental data. It was found that at 1.0E05 particles per cubic centimeter, the space charge force can only lead to a small effect on the deposition and the predominant effect is due to image forces exerted on the particles. In the image force model, the interactive forces between particles is neglected and the deposition is independent of the particle density.

Yu [41] studied the precipitation from still air in cylindrical and spherical vessels due to either space charge repulsion or image force. It was found that for the product of number density and cubic power of the vessel radius much greater that 100, the mutual repulsion gives a larger fractional deposition than that obtained by the image force, and for a product much less than 10 the image force is the predominant factor for deposition.

Chen [6] studied the deposition of aerosol in a two-dimensional parallel-plate channel due to diffusive and space charge effects by an integral method. The fluid phase was assumed to be either uniform flow or fully developed flow. Two models of particle density profiles, a third order polynomial and a fully developed particle density profile were employed.

Comparison between fully developed and slug flows which are equivalent to the series solutions given by Carslaw and Jaeger[4] showed that the fully developed density profile gives better results. The inverse of the centerline particle density was found to increase linearly with the product of space charge parameter and axial distance near the channel inlet. The centerline particle density, penetration and electric field force were found to decrease near the channel inlet. At far downstream, those factors decrease exponentially with the axial distance.

The analysis on the deposition from charged aerosol passing through a pipe bend was presented by Diu and Yu [13]. The analysis for the case of $t'/T << 1$ and h/r were considered, where $t' = m/f$ is the particle relaxation time and $T = \theta/a'$ is the residence time, where θ is the bend angle and a' is a constant.

Three parameters which are related to inertia, image force, and tube geometry were introduced to analyse the particle collecting efficiency. Results are given for charged and uncharged particles at varying inertia. Significant increase of collecting efficiency due to the increase of the electrostatic image force were observed.

Experimental results by Diu and Yu [13] for flow of particles of 1 μm diameter in a 90-degree pipe bend for neutral particles and charged particles with electron charge density of 300 el./particle were presented and agreement between theory and experiment made by Chan et al. [5] appeared to be good.

Yu and Chandra [44] investigated theoretically the deposition of charged particles by their image forces from laminar flows in rectangular and cylindrical channels. They considered the case in which particles of 1 μm diameter and 100 el./particle were breathed into the lung with 1000 cc tidal volume and 12 respirations per minute. It was found

that the image force contributes approximately the same amount of deposition as the gravitational force does.

Using a series expansion Ingham [20] obtained an analytical expression for the concentration of particles at small duration as a function of the governing parameter and residual distance. The deposition at very small value of time is about 15 % less than that of Yu and Chandra [40].

Thiagarajan and Yu [32] studied the deposition of aerosol from laminar flow in parallel-plate and cylindrical channels due to the simultaneous effect of gravitational and electrostatic image forces. The equations of particle motion are solved numerically to obtained the particle trajectories in 3-dimensions. It was found that the deposition is considerably lower than that obtained by adding the deposition due to gravity alone and that due to the image force alone.

An analytical solution of the deposition of charged particles near the entrance of a cylindrical tube has been studied by Ingham [20]. In the analysis both plug and Poiseuille flow were considered and the axial diffusion force were neglected.

In the analysis outside the boundary layer, the value of density parameter is independent of radial distance which is consistent with the assumption by Chen [7]. By using a series

expansion form and assuming a small time duration, solutions of the particle density and electrostatic force can be derived for a small axial distance. The two solutions are functions of time and radial distance. The results of the electrostatic charge effect, therefore, can be obtained by using the two functions.

The analysis indicates that in the aerosol generating process, the electrification of particles will affect the deposition efficiency of particles flowing in the tube.

Application of the deposition mechanism on the research of deposition process in the human respiratory system has been studied by many authors. Detailed analyses on the experimental and calculated data for the total and regional depositions in the human lung were investigated by Ferron et al [15]. Calculations with different mathematical deposition models were compared with the experimental data obtained in the region of the extrathoracic, bronchial and pulmonary area.

The influence of the electric charge carried by airbone particles on airway deposition was studied theoretically by many authors; Yu, 1977 [41]; Yu and Chandra, 1978 [44], Pich 1972 [27]; Ingham, 1981 [20]. Successive experimental works have also been investigated by Vincent et al., 1981 [35], Jones et al., 1982 [24] on experimental animals.

Recently, Melandri [25] performed a series of measurements on volunteers' airway with unipolar charged monodisperse aerosols of both polarities. For the charge concentration tested, the increase in deposition was due to image forces between the wall and the particle. For particle sizes of 0.3, 0.6 and 1.0 μm and concentrations within 10^5 #/cc, charged particles attracted to the walls of a spherical volume with size at same order as the alveoli is satisfied as described by Fuchs [15] and Yu [41] that the charge force effect is dominant the deposition process.

The magnitude of the ratio of the space charge force to the image force in a cylindrical cavity with radius R was discussed by Yu [41] . The ratio of these two magnitudes is equal to $A = (32/3)^{1/3} pi\ N\ R^3 (Te)^{2/3}$ where N is particle concentration and Te is dimensionless time which is related to axial distance. As Yu has pointed out, when $A << 1$ the deposition of a suspension flow is contributed predominantly by the image force. A detailed analysis is given to an aerosol of 1 μm particle diameter carried with 100 elementary charges breathed into a Weibel's lung at 1000 cm^3 tidal volume and 15 respiration per minute. The results showed that for $N = 10^5$ particles cm^{-3}, the value of A is very small compared with unity everywhere in the lung.

The effect of electrostatically charged aerosol particles on the lung deposition of human being and rats were tested at <u>in vivo</u> condition by Prodi and Mularoni [28]. A

significant deposition increase was found for particle charges exceeding a threshhold charge q_c, which is dependent on the particle size but not on the individual volunteer at the charge concentration used. This increase is due to image forces between the wall and particle and depends on the magnitude of charge carried by each individual particle and not on the collective behavior of the charged particle cloud. The electrostatic deposition efficiency is a function of $(Bq)^{1/3}$, where B is the mechanical mobility and q is the charge.

The electrostatic properties of work place aerosol and their implications in relation to occupational hygiene were discussed by many authors, such as Yu, 1977 [41], Vincent et al., 1981 [35]; Melandri et al., 1983 [25]; Jones et al., 1983 [24]; Prodi and Mularoni, 1985 [28]. The theoretical studies supported the finding that the main factor enhancing the deposition process is the image force acting on an airborne charged particle. The survey indicated that most aerosols found in ambient and workplace enviroments have relatively insignificant space charge forces for particle concentration and amount of charge pertained on the aerosol.

Vincent [34] conducted the observations in animal studies and found that electrostatic enhancement of lung deposition is small for inhaled isometric polydisperse mineral dusts, but is potentially large for similarly

disposed fine fibrous asbestos aerosols. Further study by Vincent [34] suggested that for particles of diameter 1 μm and density 1 gm per cubic centimeter inhaled by human subjects breathing under normal conditions, the threshold charge is found to be about 50 electrons, more than that studied by Schevchenko [29] which suggested that in some case the workplace aerosols are charged to levels substantially above Boltzman equilibrium.

Recent attention is focused on the possibility that electric charged particles produced on industrial aerosols during the dispersal process might cause significantly enhanced deposition in the lungs of exposed workers. Concern was expressed about the effect this might have on the relationship between the measured concentration and the lung dose received, and about whether it might therefore be appropriate in some instances - in order to properly reflect health risk - to monitor not only the dust concentration but also the charge level.

In reviewing the contributions related to lung deposition, John and Vincent [22] concluded that, in most industrial workplaces, aerosol charge levels are not high enough to warrant changes in occupational hygiene practice. However, for airbone asbestos fibers, the charges carried by respirable particles of long aspect ratio are large enough to suggest that a significant electrostatic effect on the lung deposition might occur.

CHAPTER 3 ANALYSIS

All aerosols are, in reality, more or less polydisperse, so it is necessary to assume in such studies that the properties of a polydisperse aerosol with the mean particle radius "a" coincide with the corresponding properties of a monodisperse aerosol with the same particle radius. Monodispersed particles are, therefore, assumed in the analysis.

In this analysis, our interest is focused on the efficiency of deposition due to inertia, gravity, and charge forces. For charge carriers larger than molecules or atoms are simply called charged particles. Based on Davies's [12] suggestion, the particle diameter considered is greater than 15 A and a mobility of about 0.1 cm/sec/v/cm. Usually the electrical characteristics of an aerosol particle can be defined by specifying any two of the three properties: particle size, number of unit charges, and mobility.

In practice, the electrical force which can be exerted on a small electrically charged particle in an electrical field or simply due to space charge, is many times that of gravity. This is apparent from Table 3.1 where the ratio of the electric force to that of gravity is compared with other forces that are exerted on aerosol particles. The analysis

is presented by Chen(4).

From this analysis it is to be shown that, when the particle concentration is less than 10^5 #/cc, the image force is shown to be dominant. When the particle size is increased, the influence of gravity or inertia become more important.

3.1 Description of Analysis

The deposition of particles in suspension due to the effects of image charge, inertia, and gravitational forces are analyzed by analytical and numerical methods. The analysis is divided into two categories: (1) Deposition due to viscous, inertia, and gravity forces; (2) Deposition due to viscous, inertia, gravity, and image forces. Two initial particle velocities and two flow velocity profiles are employed to calculate the fractional deposition efficiency.

For cases of inertia and gravity forces, the deposition of particles in a uniform flow can be obtained analytically. The deposition of particles in a flow of parabolic velocity profile is calculated numerically by the trapezoidal rule. In the numerical methods, equi-penetration points and curves over the inlet plane are constructed, and the fraction of deposition is obtained by integrating the product of the particle's initial velocity and its concentration over the

area enclosed by the equi-penetration curve and the boundary wall. In this case, the equi-penetration curve is constructed from the time dependent solutions which are obtained analytically by solving the governing equations.

In the case of additional image forces, a set of data is chosen to calculate the particle trajectories by the Runge-Kutta Method. The deposition lengths of particles are interpolated by regression analysis to construct the functions of the equi-penetration curve. Once the equi-penetration curve is obtained, the fraction of deposition can be obtained by numerical integration. The results for both cases are presented in Chapter 4 for both parallel-plate channels and circular tubes.

3.2 ASSUMPTIONS

For flows of suspensions in a parallel-plate channel and a circular tube, the following assumptions are made:

(1) Incompressible, steady flow
(2) Two-dimensional, laminar flow
(3) Dilute suspension
(4) No diffusion forces are involved
(5) Stoke's Drag law for viscous forces applies
(6) Interaction between particles is negligible
(7) A constant velocity profile which is either uniform or parabolic

(8) No chemical reactions take place

(9) Negligible temperature effects

The rectangular cartesian coordinate system as shown in Fig. 3.1 is employed in the analysis. The x-axis, is along the centerline of the channel and y-axis is parallel to the direction of gravity. The parallel-plate channel is made of two plates spaced by a distance of 2h apart, while the tube has a radius of h.

3.3 GOVERNING EQUATIONS

The fluid flowing in the constant area conduit is treated as a continuum and its velocity profile is assumed to be either uniform or parabolic. Thus, the continuity and momentum equations are satisfied by the fluid. From Newton's second law of motion, the governing equations for a particle moving in a fluid subject to viscous and body forces can be expressed as follows:

$$m \frac{dU}{dT} = f\,(U_f - U_p) + F \qquad (3\text{-}1)$$

where m is the mass of particle, f is inverse of the particle mobility or f = 1/(6 pi u a) where u is the viscosity of fluid; F is the external force vector, and U_f and U_p are the fluid and particle velocity vector respectively.

In the cartesian coordinate system, the equations of motion under the influence of gravity and image force become

$$m \frac{du_p}{dt} = f (u - u_p) \quad (3\text{-}2)$$

$$m \frac{dv_p}{dt} = f (v - v_p) - mg + I_y \quad (3\text{-}3)$$

$$m \frac{dw_p}{dt} = f (w - w_p) + I_z \quad (3\text{-}4)$$

where u, v and w are the components of velocity vector U_f; g is the gravity force; I is the image charge force vector which varies with the geometry of the channel; and I_y and I_z are the components of image charge force in the y and z directions.

Since the flow profile is constant, the velocity components in the z-direction and y-direction are zero. The equations are simplified to

$$m \frac{du_p}{dt} = f (u - u_p) \quad (3\text{-}5)$$

$$m \frac{dv_p}{dt} = f (-v_p) - mg + I_y \quad (3\text{-}6)$$

$$m \frac{dw_p}{dt} = f (-w_p) + I_z \quad (3\text{-}7)$$

In this analysis the particles entering the channel are assumed to be uniformly distributed across the inlet section of the channel. The boundary conditions are

at $x = 0$ and $y = y_o$, $z = z_o$ (initial particle location)

$n = n_o$ = constant (particle concentration)

where n_o is the particle initial concentration.

At the entrance, two types of particle initial velocities are considered. One assumes that the particle velocity is the same as the fluid velocity. The other assumes that the particle is initially stationary. In the realistic flow condition, we would expect that the particle should be at a velocity between these assumed velocities. Therefore, in the analysis, we assume that the particle is either initially at the fluid velocity or zero velocity.

Two types of initial conditions are considered.

(i) At $t = 0$ and $x = 0$;

$u_p = 0$

$v_p = 0$

$w_p = 0$

(ii) At $t = 0$, $x = 0$;

$u_p = u$

$v_p = 0$

$w_p = 0$

For the fluid phase the velocity is either uniform or parabolic. Therefore, the profiles of the flow are

at $-h < y < h$, $-h < z < h$ and $y^2 + z^2 < h^2$

(i) slug flow

$u = u_o$

$v = 0$

$w = 0$

(ii) fully-developed flow

$u = 1.5\ u_o\ (1 - (y/h)^2)$

(parallel-plate channel)

$= 2\ u_o\ (1 - (y/h)^2 - (z/h)^2)$

(circular tube)

$v = 0$

$w = 0$

where uo is the mean velocity in the x-direction and h is the boundary of the channel considered.

The following dimensionless parameters are introduced in the analysis to simplify the equations and reduce the number of variables involved.

$$Y = \frac{y}{h}$$

$$X = \frac{x}{h}$$

$$Z = \frac{z}{h}$$

$$T = \frac{t\ uo}{h}$$

$$Q = \frac{m\ uo}{f\ h} \qquad \text{(Inertia Parameter)} \qquad (3\text{-}8)$$

$$G = \frac{m\ g}{f\ uo} \qquad \text{(Gravity Parameter)} \qquad (3\text{-}9)$$

$$F_p = \frac{q^2}{4\ pi\ e"\ h^2\ f\ uo} \qquad \text{(Charge Parameter) (Parallel-Plate Channel)} \qquad (3\text{-}10)$$

$$= \frac{q^2}{16\ pi\ e"\ h^2\ f\ uo} \qquad \text{(Circular Tube)} \qquad (3\text{-}10a)$$

Using Lagrangian approach, a particle at time t is located at (x,y,z). The velocity components are

$$U_p = \frac{dx}{dt} \qquad (3\text{-}11)$$

$$V_p = \frac{dy}{dt} \qquad (3\text{-}12)$$

$$W_p = \frac{dz}{dt} \qquad (3\text{-}13)$$

The dimensionless equations of motion are

$$Q\ \frac{d^2X}{dT^2} = U - \frac{dX}{dT} \qquad (3.14)$$

$$Q\ \frac{d^2Y}{dT^2} = - \frac{dY}{dT} - G + F_y \qquad (3.15)$$

$$Q\ \frac{d^2Z}{dT^2} = - \frac{dZ}{dT} + F_z \qquad (3.16)$$

where F_y and F_z are the dimensionless image forces in the Y

and Z-directions, respectively. The equation of the image force given are discussed in Sections 3.4.4 and 3.5.4.

The dimensionless boundary conditions become

at $X = 0$ and $Y = Yo$ (particle initial location)

$Z = Zo$

$N_o = 1$ (particle concentration)

and the two types of flow are

(1) slug flow

$U = 1$

$V = 0$

$W = 0$

(2) fully developed flow

$U = 1.5\ (1 - Y^2)$

(parallel-plate channel)

$= 2\ (1 - Y^2 - Z^2)$

(circular tube)

$V = 0$

$W = 0$

In the parallel-plate, $Y = 1, -1$ are the boundaries of the channel. While in the circular tube, $Y^2 + Z^2 = 1$ is the boundary of the tube.

The two dimensionless initial conditions become

(i) at $T = 0$ and $X = 0$;

$dX/dT = 0$

$dY/dT = 0$

$dZ/dT = 0$

(ii) at $T = 0$ and $X = 0$;

$dX/dT = U$

$dY/dT = 0$

$dZ/dT = 0$

For given velocity of a particle in a channel and body forces acting on the particle, the system of differential equations (3-8) - (3-10) along with the boundary and initial conditions can be solved analytically or numerically depending on the velocity profile of the fluid and the type of flow passage. In the analysis, we assumed that the particle is either at the fluid velocity or zero velocity initially.

Two types of flow passages are considered in this analysis: flow in a parallel-plate channel and that in a circular tube. They are analyzed individually in the following sections.

3.4 Computation of Fractional Deposition in Parallel-Plate Channels

Imposing the assumptions made in Section 3.2, the analysis of the deposition mechanism is discussed in the following schemes.

3.4.1 Influence of Particle Size on Magnitude of Charge, Inertia and Image Forces

Table 3.1 shows that the effects of particle sizes on the inertia, gravity and image forces. In Table 3.1, for a particle size of 1 μ m, the magnitude of charge, gravity and

inertia are 7.88E-2, 9.86E-5 and 4.55E-5 respectively. It is noted that the gravity and inertia parameters have the same magnitude. As particle size decreases, the relative magnitude of charge and gravity become closer. For example, the magnitude ratio of charge to gravity is 800 for a particle size of 1 μ m, while for a particle size of 0.1 μ m, the ratio is 80. Hence, when the charge force exists, the inertia effect on the process of deposition increases with decreasing particle size.

3.4.2 Solutions for Channel Flow with Inertia and Gravity Forces

The governing equations in a parallel-plate channel are

$$Q \frac{d^2X}{dT^2} = U - \frac{dX}{dT} \qquad (3\text{-}17)$$

$$Q\frac{d^2Y}{dT^2} = - \frac{dY}{dT} - G \qquad (3\text{-}18)$$

Eq. (3-18) can be integrated directly and solved for the initial conditions that Y = Yo and dY/dT = 0 at T = 0. However solutions to Eq. (3-17) depend on the velocity profile U and the given particle initial conditions. These solutions are presented in the following section.

(A) Particles with Zero Initial Velocity and Fluid with Uniform Velocity

Initial conditions:

At T = 0 : Y = Yo, dY/dT = 0, X = 0 and dX/dT = 0

At T > 0 : U = 1

Solutions:

$$Y(T) = Q\,G + Yo - G\,T - Q\,G\,Exp(-T/Q) \qquad (3\text{-}19)$$

$$X(T) = -\,Q + T + Q\;\;Exp(-T/Q) \qquad (3\text{-}20)$$

(B) Particles with Uniform Initial Velocity and Fluid with Uniform Velocity

Initial Conditions:

At T = 0 : Y = Yo, dY/dT = 0, X = 0 and dX/dT = 1

At T > 0 : U = 1

Solutions :

$$Y(T) = Q\,G + Yo - G\,T - Q\,G\,Exp(-T/Q) \qquad (3\text{-}21)$$

$$X(T) = T \qquad (3\text{-}22)$$

When the inertial effect becomes negligible, i.e. at Q = 0, the solutions of Eqs. (3-21) and (3-22) are reduced to the case of particles under the influence of gravity alone. The

special case is presented as follows:

$$Y(T) = Yo - G\,T$$

$$X(T) = T$$

The effect of gravity on the deposition are discussed by many authors such as Pich [27], Wang[37], and Carpenter [3].

(C) Particles with Zero Initial Velocity and Fluid with Parabolic Velocity Profile

Initial conditions :

At $T = 0$: $Y = Yo$, $dY/dT = 0$, $X = 0$ and $dX/dT = 0$

At $T > 0$: $U = 1.5\ (1 - Y^2)$

Solutions :

$$Y(T) = Q\,G + Yo - G\,T - Q\,G\,\mathrm{Exp}(-T/Q) \qquad (3\text{-}23)$$

$$\begin{aligned} X(T'') = 1.5\,G^2\,Q^3 \{\ & 4.5 + 6\,Yo\,K + k^2(1 - Yo^2) \\ & + [\ K^2(1 - Yo^2) - 4\,Yo\,K - 5\ ]\ T'' \\ & + (2 + Yo\,K)^2\,T''^2 - 1/3\,T''^3 \\ & + [\ K^2(1 - Yo^2) - 6\,Yo\,K - 4\ ]\ \mathrm{Exp}(-T'') \\ & - 2\,Yo\,K\,T''\,\mathrm{Exp}(-T'') + T''^2\,\mathrm{Exp}(-T'') \\ & - 0.5\,\mathrm{Exp}(-2\,T'')\ \} \end{aligned} \qquad (3\text{-}24)$$

where $K = 1/Q/G$

$T'' = T/Q$

(D) Particles with Initial Velocity of 1.5 (1 - Yo^2) and Fluid with Parabolic Velocity Profile

Initial conditions :

At T = 0 : Y = 0, dY/dT = 0, X = 0

and dX/dT = 1.5 (1 - Yo^2)

At T > 0 : U = 1.5 (1- Y^2)

Solutions:

$$Y(T) = Q\,G + Yo - G\,T - Q\,G\,Exp(-T/Q) \qquad (3\text{-}25)$$

$$X(T") = 1.5\,G^2\,Q^3\,\{\,4.5 + 6\,Yo\,K + [K^2(1 - Yo^2) - 4\,Yo\,K - 5\,]\,T" + (2 + Yo\,K)\,T"^2 - 1/3\,T"^3 - 2\,(2 + 3\,Yo\,K)\,Exp(-T") - 2\,Yo\,K\,T"\,Exp(-T") + T"^2\,Exp(-T") - 0.5\,Exp(-2T")\,\} \qquad (3\text{-}26)$$

Again, when the inertial effect becomes negligible, i.e. at Q = 0, the solutions of Eqs. (3-25) and (3-26) become

$$Y(T) = Yo - G\,T$$

$$X(T) = 1.5\,G\,T^2\,(\,1 - G\,T/3\,)$$

These solutions are for the case of particles under the influence of gravity alone.

In summary, based on these solutions obtained from the case of gravity and inertia involved, the fraction of

deposition at any axial location can be calculated for the given conditions. The analysis of deposition is presented in the following paragraphs.

3.4.3 Computation of Fraction of Deposition

In a 2-dimensional parallel-plate channel, the fraction of deposition is the ratio of the total number of particles entering the channel, Q_t, to the number of particles deposited on the wall, Q_d, at a given axial distance. The deposition is expressed as

$$\text{DEPO} = \frac{Q_d}{Q_t} = \frac{\int_{A'} \text{No } Up_o \, d\,A}{\int_{A} \text{No } Up_o \, d\,A} \qquad (3\text{-}27)$$

where A is the cross sectional area of the flow passage, A' is the area for which particles penetrate through the channel. Thus, DEPO varies with flow passage and particle initial velocity. Discussion for the fractional deposition, therefore, is divided into four categories.

(A) Particles with Zero Initial Velocity and Fluid with Uniform Velocity Profile

1) Description of Deposition Process

The fraction of deposition at any axial distance X1 is

defined as the ratio of the number of particles deposited between X = 0 and X = X1 to the total number of particle entering the channel at X = 0. The schematic diagram shown as in Figure 3.2 depicts a trajectory of a particle which enters the channel at point A and is deposited on the wall at X = X1 and another particle which enters at point B and is deposited on the wall at X = X2 for a uniform flow in a channel.

For the case of a uniform flow all particles initially located between point A and the bottom wall C will deposit in the region 0 < X < X1. Particles initially located between point A and the upper wall D will deposit in the region X > X1. Assuming that the particle concentration n_o at the inlet is uniform, we may calculate the fraction of deposition at X1 based on the inlet condition of particles at point A (i.e. Y = Yo).

2) Computation of Fraction of Deposition

Since the total number of particles is the integral of the product of particle density and particle initial velocity along the Y-axis, the fraction of deposition is expressed as

$$DEPO = \frac{Qd}{Qt} = \frac{\int_{-1}^{Yo} N\ Up\ dY}{\int_{-1}^{1} N\ Up\ dY} = \frac{\int_{-1}^{Yo} dY}{\int_{-1}^{1} dY}$$

$$= 0.5\ (\ 1 + Yo\ ) \qquad (3\text{-}28)$$

where Y = -1 as particles deposit on the wall.

By substituting the boundary condition of Y = -1 into Eq. (3-19), we obtain

$$-1 = Q\ G\ + Yo - G\ T - Q\ G\ Exp(-T/Q) \qquad (3\text{-}29)$$

$$Yo = -1 - Q\ G + G\ T + Q\ G\ Exp(-T/Q)$$

$$= -1 + G\ (\ -Q + T + Q\ Exp(-T/Q))$$

From Eq. (3-20), we obtain

$$Yo = -1 + G\ X \qquad (3\text{-}30)$$

Substituting Eq. (3-30) into Eq. (3-28), we obtain

$$DEPO\ = 0.5\ (G\ X) \qquad (3\text{-}31)$$

From Eq. (3-31), at any given X, the fraction of deposition can be obtained. For example, at X = 0, the fraction of deposition is zero. The results are presented in Fig. 4.1.

(B) Particle with Uniform Initial Velocity and Fluid with Uniform Velocity Profile

1) Description of Deposition Process

The deposition process of particle is same as that stated in Case A. The analysis is divided into two parts (1) deposition with gravity and inertia, and (2) deposition with gravity only. The second part is utilized to verify the correctness of the approach.

2) Computation of Fraction of Deposition

For a particle entering the channel at Up = U = 1, the solution is obtained by combining Eqs. (3-21) and (3-22).

$$Y(T) = Q\ G + Yo - G\ X - Q\ G\ Exp(-X/Q)$$

By letting Y = -1 for deposition on the wall, we have

$$Yo = G\ X + Q\ G\ Exp(-X/Q) - Q\ G - 1$$

The fraction of deposition DEPO is 0.5 or

$$DEPO = 0.5\ (\ G\ X + Q\ G\ Exp(-X/Q) - Q\ G\ ) \qquad (3\text{-}32)$$

As X = 0, the deposition is equal to zero. When X increases, the deposition increases also. As Q = 0, the

fraction of deposition becomes

$$DEPO = 0.5\ G\ X \qquad (3\text{-}33)$$

which is the fraction of deposition given by gravity alone. The equation is same as stated by Pich [27].

(C) Particle with Zero Initial Velocity and Fluid with Parabolic Velocity Profile

1) Description of Deposition Process

For a uniform fluid velocity (Cases A and B), at a given axial distance, only one corresponding initial point is found; while for the case of particles entering with a parabolic velocity, two corresponding initial points of Y are computed. The schematic diagram shown in Fig. 3.3 depicts trajectories of two different particles entering at point B(0, Y1) and E(0, Y2) which are deposited on the wall at the same location of X = X1. Particles entering between location B and E will deposit farther than X1. Particles entering between points E and Y = 1, and B and Y = -1 will deposit in the region 0 < X < X1. Therefore, the fraction of deposition is proportional to the summation of two regions: the region between E and D and the region between B and C.

2) Computation of Fraction of Deposition

The fraction of deposition by definition is

$$DEPO = \frac{Q_d}{Q_t} = \frac{\int_{Y1}^{1} No\ Up_o\ dY + \int_{-1}^{Y2} No\ Up_o\ dY}{\int_{-1}^{1} No\ Up_o\ dY}$$

$$= 0.5\ (\ 1-\ Y1)\ +\ 0.5\ (Y2\ +1) \qquad (3\text{-}34)$$

where Up is a constant in the calculation of Q_d.

As given by initial conditions discussed in Section 3.4.2 (C), the initial location of the particle can be obtained by solving Eqs. (3-23) and (3-24) for a given axial distance. A numerical program (Appendix A) is used to calculate the values of Y1 and Y2 for a given dimensionless axial distance. The corresponding fractional deposition is then calculated from Eq. (3-33). It is noted that the value of Y1 is associated with the larger value of T.

It is observed that at points well below certain values of Yo, only one point for each corresponding axial distance is found. Thus the deposition of particle becomes

$$DEPO = 0.5\ (Y2\ +\ 1) \qquad (3\text{-}35)$$

Eq. (3-34) can be rearranged to

$$DEPO = 1.0 - 0.5\ (Y1 - Y2) \qquad (3\text{-}36)$$

In the analysis, if the values of Y1 obtained from the associated T value is greater than one, then only one corresponding point is found. Thus by assuming Y1 as one, the fraction of deposition can be calculated.

(D) Particles with Initial Velocity of $1.5(1- Yo^2)$ and Fluid with Parabolic Velocity Profile

Similarily, the initial locations of particle deposited for any given axial distance can be calculated from the time dependent solutions of Eqs. (3-25) and (3-26).

Since the total number of particles is the integral of the product of the particle concentration and particle initial velocity along the Y-axis, the fraction of deposition is

$$DEPO = \frac{Q_d}{Q_t} = \frac{\int_{Y1}^{1} N_o\, Up_o\, dY + \int_{-1}^{Y2} N_o\, Up_o dY}{\int_{-1}^{1} N_o\, Up_o\, dY}$$

$$= \frac{\int_{-1}^{Y1} (1)\ 1.5\ (1 - Y^2)\ dY \ + \ \int_{-1}^{Y2} (1)\ 1.5\ (1 - Y^2)\ dY}{\int_{-1}^{1} (1)\ 1.5\ (1 - Y^2)\ dY}$$

The equation can be simplified to

$$DEPO = 1.0 - 0.75\ (\ Y2 - Y1) + 0.25\ (Y2^3 - Y1^3) \quad (3\text{-}37)$$

In the numerical analysis, if the corresponding Y value is greater than one, then only one corresponding point exists for a given axial distance. To simplify Eq. (3-37) if only one particle is involved, the value of Y1 is set to one. The computation algorithm is given as discussed in Case A of Appendix A.

3.4.4 Deposition due to Viscous, Inertia, Gravity and Image Forces

When the particle concentration is sufficiently diluted, the image charge forces become important to the process of deposition (see Yu [42]). For flow in a parallel-plate channel, the magnitudes of dimensionless parameters are listed in Table 3-2 and Table 3-3. These parameters are based on particle material density of 1 gm/cc, a fluid velocity of Uo = 30 cm/sec and a channel width of h = 2 cm in Table 3-2 and h = 0.1 cm in Table 3-3. When the particle diameter is 1 μm, the gravity parameter G = 9.80 E-5, the

inertia parameter Q = 4.53E-5, the image force parameter Fy = 4.9E-7(at Y = 0.98) and Fy = 1.96E-6 (at Y = 0.99). When h = 0.1 cm , the image parameter becomes more significant.

2) Governing Equation

The dimensionless governing equation for a 2-dimensional parallel-plate channel with additional image forces are given as follows:

$$Q \frac{d^2X}{dT^2} = U - \frac{dX}{dT} \qquad (3\text{-}38)$$

$$Q \frac{d^2Y}{dT^2} = - \frac{dY}{dT} - G + F_Y \qquad (3\text{-}39)$$

where F_y is the dimensionless image force component in the Y-direction. The magnitude of charge force for monodisperse particle in the space of the parallel-plate from Yu [45] is given in Eq. (3-11).

For particles in a parallel-plate channel, the component of the dimensionless image force is

$$F_Y = \left(\frac{q2}{4\ pi\ e''\ f\ uo}\right)\left(\frac{Y}{h^2}\right)\left(\frac{1}{(1-Y^2)^2} + A\right) \qquad (3\text{-}40)$$

where q = electrostatic charge

e" = free space permitivity

pi = 3.14159

$$A = \sum_{n=1}^{\infty} \frac{2n+1}{((2n+1)^2 - Y^2)^2} \qquad (3\text{-}41)$$

In the numerical analysis only up to five terms of function A are needed to be considered for the image force to be accurate within 1 %.

3) Description of Deposition Process

As depicted in Fig. 3.4 for flow in a parallel-plate channel, for a given axial distance X1, two initial points A and B can be found. Particles entering at point A deposit on the top wall, while particles entering at point C deposit on the bottom wall. Points A and C are symmetric with respect to the X-axis, however, the particles will not deposit at the same axial distance due to the gravity and image forces acting in opposite direction for particles above the X-axis.

4) Computation of Fraction of Deposition

The fraction of deposition for particles with uniform inlet velocity is given by Eq. (3-36), while that for a parabolic inlet velocity is given by Eq. (3-37).

Therefore, the fraction of deposition for a given axial distance is, for a particle with constant inlet velocity

$$DEPO = 1 - 0.5\ (Y1 - Y2) \qquad (3\text{-}42)$$

and for a particle with parabolic inlet velocity

$$DEPO = 1.0 - 0.75\ (Y2 - Y1) + 0.25\ (Y2^3 - Y1^3) \qquad (3\text{-}43)$$

The particle trajectories in this case were calculated numerically by using the fourth order Runge Kutta method. A data set of 21 points located on the Y-axis is taken as initial points. The corresponding value of the axial distance for each particle deposited is computed and used in an N'th order regression curve fitting. In the analysis, the magnitude of image force parameter, F_p is assumed to be unity, i.e. $q^2/(4\ pi\ e") = 1$.

By using the functions obtained from the N'th order regression fitting method, the initial coordinates of those particles deposited at the same axial distance X can be determined. The predicted values of Y are substituted into the deposition Eq. (3-42) for a uniform velocity profile and Eq. (3-43) for a parabolic velocity profile.

The four different cases encountered in the previous analysis are studied. With the additional image force, the fraction of deposition is expected to be higher than that due to inertia and gravity alone. As the inertia increases, the rate of deposition decreases.

The fractional deposition for Q = 0.01, 0.1, 1, 10 and 100 are presented in Fig. 4.7 through Fig. 4.11 and are discussed in Chapter 4. The numerical methods used to compute the fractional deposition are presented in Appendix A.

3.5 Computation of Fractional Deposition in Circular Tubes

In practical applications, flows are more often encountered in the circular tube problem than in the 2-dimensional channel. The analytical technique, basically, is similar to that discussed in the 2-dimensional case, but it is more complicated due to 3-dimensional non-symmetrical effects. The boundary conditions, fluid velocity profiles and the initial conditions are similar to those in 2-dimensional flows as given in Section 3.3.

3.5.1 Influence of Particle Size on Magnitudes of Gravity, Inertia and Image Forces

The magnitudes of the forces of inertia, gravity and

charge for particles flowing in a tube are shown in TABLE 3.4 and TABLE 3.5. TABLE 3.4 shown the magnitude obtained with radius h = 2 cm. TABLE 3.5 shows the magnitude obtained at h = 0.1 cm. The charge number carried is based on Cheng and Soo's experimental findings [10] where the charge electron density was found to be 1 electron per 1.18 E-10 cm^2. Detailed analysis is discussed by Chen [12].

As is seen from Table 3.4 the magnitudes of gravity, inertia and image forces at Y = 0.98 and 0.99 are 9.86E-5, 9.06E-5, 2.0E-4 and 7.92E-4 respectively for particle size of 1 μm. These three forces have the same magnitude and therefore, the influence of each individual force on the process of deposition becomes equally important.

It is noted that the magnitude of the forces varies with particle size. In TABLE 3.4 for particle size less than 1 um, the inertia become significant when compared with the image force. The magnitude of the image force becomes larger as the particle size increases. This result is expected since a larger particle provides more surface area for carrying the charges, and therefore has higher image force. It is seen from these Tables that the magnitudes of gravity, inertia and image forces increase with increaing particle size. The levels of charges carried by different size of particles are shown in TABLE 3-4.

From the magnitude of image forcse and gravity given in TABLE 3-4, one discovers the ratio of gravity to image force increases with increasing particle size. The ratio of gravity to image force for 0.1 μm is 1, but decreases to 0.1 for particle size of 1 μm. Therefore, the size of particle considered in the analysis should be less than 0.1 μm if the image force is to be considered.

In order to investigate the mechanism of each individual force in the deposition process, the influence of inertia and image force on the deposition are analyzed in the following sections.

3.5.2 Solutions for Tube Flow with Viscous, Inertia and Gravity Forces

To better understand the mechanism of each individual force on the deposition, the gravity and inertia forces on the deposition are analyzed. However the effect of depositon due to gravity alone, is not included in the analysis, since it has been investigated by many authors such as Pich [27], Thomas [32], Wang [37] and Carpenter [3].

The governing equations for motion of a particle with the effects of gravity and inertia are as follows:

$$Q \frac{d^2X}{dT^2} = U - \frac{dX}{dT} \qquad (3\text{-}49)$$

$$Q \frac{d^2Y}{dT^2} = - \frac{dY}{dT} - G \qquad (3\text{-}50)$$

$$Q \frac{d^2Z}{dT^2} = - \frac{dZ}{dT} \qquad (3\text{-}51)$$

Eq. (3-50) can be integrated directly and solved for the initial conditions that $Y = Y_o$, $Z = Z_o$ and $dY/dT = 0$ at $T = 0$. Solutions to Eq. (3-49) depend on the velocity profile U and the initial conditions. These solutions are presented in the following section.

(A) Particles with Zero Initial Velocity and Fluid with Uniform Velocity Profile

Initial conditions:

At $T = 0$: $Y = Y_o$, $Z = Z_o$, $dY/dT = 0$, $dZ/dT = 0$,
$X = 0$ and $dX/dT = 0$

At $T \geq 0$: $U = 1$

Solutions:

$$Y(T) = Q\ G + Y_o - G\ T - Q\ G\ Exp(-T/Q) \qquad (3\text{-}47)$$

$$X(T) = - Q + T + Q\ \ Exp(-T/Q) \qquad (3\text{-}48)$$

$$Z(T) = Z_o \qquad (3\text{-}49)$$

(B) Particles with Uniform Initial Velocity and Fluid with Uniform Velocity Profile

Initial Conditions:

At $T = 0$: $Y = Y_o$, $Z = Z_o$, $dY/dT = 0$, $dZ/dT = 0$,

$X = 0$ and $dX/dT = 1$

At $T \geq 0$: $U = 1$

Solutions :

$$Y(T) = Q\ G + Y_o - G\ T - Q\ G\ Exp(-T/Q) \qquad (3\text{-}50)$$

$$X(T) = T \qquad (3\text{-}51)$$

$$Z(T) = Z_o \qquad (3\text{-}52)$$

When the inertia effect becomes negligible, i.e. at $Q = 0$, the solutions become that of particles under the influence of gravity alone. This special case is presented as follows:

$$Y(T) = Y_o - G\ T \qquad (3\text{-}53)$$

$$X(T) = T \qquad (3\text{-}54)$$

$$Z(T) = Z_o \qquad (3\text{-}55)$$

The effect of gravity has been discussed by many authors such as Pitch [27], Wang [37] and Carpenter [3].

(C) Particles with Zero Initial Velocity and Fluid with Parabolic Velocity Profile

Initial conditions:

At $T = 0$: $Y = Y_o$, $Z = Z_o$, $dY/dT = 0$, $dZ/dT = 0$,
$X = 0$ and $dX/dT = 0$

At $T \geq 0$: $U = 2\ (1 - Y^2 - Z^2)$

Solutions:

$$Y(T) = Q\ G + Yo - G\ T - Q\ G\ Exp(-T/Q) \qquad (3\text{-}56)$$

$$\begin{aligned} X(T") = 2\ G^2\ Q^3\ \{\ & 4.5 + 6\ Y_o\ K \\ & + K^2\ (1-Y_o^2-Z_o^2) \\ & + [K^2(1 - Y_o^2 - Z_o^2) - 4\ Y_o\ K - 5\ ]\ T" \\ & + (2 + Y_o\ K)^2\ T"^2 - 1/3\ T"^3 \\ & + [\ K^2(1-Y_o^2-Zo^2) - 6\ Y_o\ K - 4\ ]\ Exp(-T") \\ & - 2\ Y_o\ K\ T"\ Exp(-T") + T"^2\ Exp(-T") \\ & - 0.5Exp(-2\ T")\ \} \end{aligned} \qquad (3\text{-}57)$$

$$Z(T) = Z_o \qquad (3\text{-}58)$$

where $K = 1/Q/G$

$T" = T/Q$

(D) Particles with Initial Velocity of $2\ (1 - Y_o^2 - Z_o^2)$ and Fluid with Parabolic Velocity Profile

Initial conditions:

$$\text{At } T = 0 : \; Y = Y_o,\; Z = Z_o,\; dY/dT = 0,\; dZ/dT = 0,$$
$$X = 0 \text{ and } \; dX/dT = 2\,(1 - Y_o^2 - Z_o^2)$$

$$\text{At } T \geq 0 : \; U = 2\,(1 - Y^2 - Z^2)$$

Solutions:

$$Y(T) = Q\,G + Y_o - G\,T - Q\,G\,\mathrm{Exp}(-T/Q) \tag{3-59}$$

$$\begin{aligned} X(T") = 2\,G^2\,Q^3 \{ & \; 4.5 + 6\,Y_o\,K + K^2\,Z_o^2 \\ & + [\; K^2(1 - Y_o^2 - Z_o^2) - 4\,Y_o\,K - 5\;]\;T" \\ & + (2 + Y_o\,K)\,T"^2 - 1/3\,T"^3 \\ & - 2\,(\,2 + 3\,Y_o\,K\,)\,\mathrm{Exp}(-T") - 2\,Y_o\,K\,T"\,\mathrm{Exp}(-T") \\ & + T"^2\,\mathrm{Exp}(-T") - 0.5\mathrm{Exp}(-2T")\;\} \end{aligned} \tag{3-60}$$

$$Z(T) = Z_o \tag{3-61}$$

Again, when the inertia effect becomes negligible, i.e. at $Q = 0$, the solutions reduce to

$$Y(T) = Y_o - G\,T \tag{3-62}$$

$$X(T) = 2\,G\,T^2\,((1 - Z_o^2)^{1/2} - G\,T/3\,) \tag{3-63}$$

$$Z(T) = Z_o \tag{3-64}$$

Eqs. (3-62) through (3-64) are for the case of particles under the influence of gravity alone.

Based on these solutions, the fraction of deposition at

any axial location can be calculated for the given conditions. The analysis of deposition are discussed in the following paragraphs.

3.5.3 Computation of Fraction of Deposition

The expression of deposition is given in Eq. (3-27) which is

$$DEPO = \frac{Q_d}{Q_t} = \frac{Q_t - Q_p}{Q_t} \qquad (3\text{-}65)$$

where Q_p is the penetration at a given axial distance X.

The value of DEPO depends on the flow passage and the particle initial velocity. Discussion for the fractional deposition therefore, is divided into four categories.

(A) Particles with Zero Initial Velocity and Fluid with Uniform Velocity

1) Description of Deposition Process

The fraction of deposition at any axial distance X1 is defined as the ratio of the number of particles deposited between X = 0 and X = X1 to the total number of particle entering the tube at X = 0. The schematic diagram shown in

Fig.3-5 depicts a group of particles which enters the tube at points on the equi-penetration curve DB and deposited on the wall along the curve of D'B' at X = X1. As shown in the diagram, two particles entering at points D and B will deposit on the points D' and B,' respectively. For a uniform flow both points D and B have a distance of X1 from the inlet plane.

For a uniform flow all particles initially located between curve DB and the bottom wall D'B'B will deposit in the region 0 < X < X1. Particles initially located between curve DB and the upper wall BA will deposit in the region X > X1. Assuming that the particle concentration n at the inlet is uniform, the fraction of deposition at X1 can be caculated using the initial conditions of the particle on the equi-penetration curve.

Since the particle on the locus has the same initial velocity, the particles will take the same time T_f to reach the wall and all deposit at X = X1. With the assistance of the schematic diagram shown as in Figure 3-6, we can explain the process in physical term. The schematic diagram shows two unit circles intersecting at point A and B. The upper one is originated at $(0, 1+Y_o)$ and the lower one at (0,0). The deposition process can be seen as the upper unit circle moves downward at a velocity of V_p in the Y-direction. V_p is the velocity of particle in the Y-direction. As the two unit

circles coincide, the particle are said to be deposited on the wall. Therefore, the curve ACB is the equi-penetration curve for the particles having the same deposited axial distance.

2) Computation of Fraction of Deposition

To find the characteristics of the equi-penetration curve, the equations of two circles are given as

Upper one $$(Y - Y_d)^2 + Z^2 = 1 \qquad (3\text{-}66)$$

Lower one $$Y^2 + Z^2 = 1 \qquad (3\text{-}67)$$

The radius of each circle is unity.

The distance of Yd, Yw, Zw and angle 0w shown in Fig. 3.6 can be expressed in terms of Y_o as follow

$$Yd = Y_o + 1 \qquad (3\text{-}68)$$

$$\begin{aligned} Yw &= 0.5\ DA + Y_o \\ &= 0.5\ (1 + Y_o) \\ &= 0.5\ Y_d \end{aligned} \qquad (3\text{-}69)$$

so that the origin of upper circle is $(0,\ 1+Y_o)$ and

$$Zw = \cos \theta w \qquad (3\text{-}70)$$

$$Yw = \sin \theta w \qquad (3\text{-}71)$$

where

$$\theta w = \sin^{-1}(0.5(Y_o+1)) \qquad (3\text{-}72)$$

Then the fraction of deposition (DEPO) for the uniform inlet velocity U_{po} is

$$DEPO = \frac{Qd}{Qt} = \frac{\int_A N_o U_{po}\, dA}{N_o\, Pi\, U_{po}} = \frac{\int_A dA}{pi} \qquad (3\text{-}73)$$

where $\int dA$ = shaded area = $2\theta + \sin 2\theta$

Therefore, the fraction of deposition is

$$DEPO = \frac{2\theta + \sin 2\theta}{pi} \qquad (3\text{-}74)$$

Rearranging Eq. (5-53),

$$X + Q = T + Q\ Exp(-T) \qquad (3\text{-}75)$$

Substituting Eq. (3-75) into Eq. (3-47),

$$Y = (Q\ G + Y_o) - G\ X - G\ Q$$
$$= Y_o - G\ X \qquad (3\text{-}76)$$

As the particle fall on the bottom wall where Y = -1,

$$1 + Y_o = G\ X \tag{3-77}$$

From Eq. (3-69),

$$Yw = 0.5\ (\ 1 + Y_o)$$
$$= 0.5\ G\ X$$

From Eq. (3-71),

$$\sin \theta w = 0.5\ G\ X \tag{3-78}$$

Substituting Eq. (3-78) into (3-74), the fraction of deposition becomes

$$DEPO = \frac{2\ \sin^{-1}(0.5\ G\ X)\ +\ G\ X\ (1\ -\ 0.25\ G^2\ X^2)^{1/2}}{pi} \tag{3-79}$$

Thus, the fraction of deposition at X = 0 is zero and for G X = 2, the deposition is unity. Hence, a complete deposition takes place at X = 2/G. For G = 1, this relation gives X = 2.

(B) Particles with Uniform Initial Velocity and Fluid with Uniform Velocity Profile

1) Description of Deposition Process

The deposition process is similar to that described in

Case A. The analysis is presented in the following subsections.

2) Computation of Fraction of Deposition

The analyses are divided into two parts: deposition with gravity and inertia and deposition with gravity only. The second one is used to verify the validity of the approach.

(1) Fraction of Deposition due to Gravity and Inertia

Similarly, the fraction of deposition in this case can be obtained by arranging the associated time dependent solutions.

$$1 + Yo = - Q\ G + G\ X + Q\ G\ Exp(-X/Q)$$
$$= 2 \sin \theta w \qquad (3\text{-}80)$$

and

$$0w = 0.5 \sin^{-1}[- Q\ G + G\ X + Q\ G\ Exp(-X/Q)] \qquad (3\text{-}81)$$

Since the particle inlet velocity is assumed to be uniform, the fraction of deposition is the same as that given in Eq. (3-73). Thus the fraction of deposition becomes

$$DEPO = \frac{2 \sin^{-1}(0.5 (- Q G + G X + Q G \exp(-X/Q)))}{pi}$$

$$+ \frac{(1 - 0.25 (- Q G + G X + Q G \exp(-X/Q))^2)^{1/2}}{pi}$$

$$x \quad (- Q G + G X + Q G \exp(-X/Q)) \qquad (3\text{-}82)$$

With the parameters Q and G given, the fraction of deposition for a given axial distance can be obtained.

At X = 0, the fraction of deposition given by Eq. (3-82) is equal to zero. The fraction of deposition is unity when $- QG + GX + QG \exp(-X/Q) = 2$. When Q = G = 1, complete deposition takes place at X = 2.945.

(2) Fraction of Deposition with Gravity Only

For Q = 0, i.e. the inertia is neglected, the fraction of deposition becomes

$$DEPO = \frac{2 \sin^{-1}(0.5 (G X)) + G X (1 - 0.25 G^2 X^2)^{1/2}}{pi} \qquad (3\text{-}83)$$

which is the fraction of deposition under the influence of gravity alone. Eq. (3-83) can be obtained also from the time dependent solutions given in Eq. (3-53) through Eq. (3-55) for the case of gravity alone. The deposition equation is

the same as that obtained by Pich [27].

(C) Particle with Zero Initial Velocity and Fluid with Parabolic Velocity Profile

1) Description of Deposition Process

For a flow of uniform velocity profile described above (Cases A and B), there is only one initial point (0, Y_o, Z_o) corresponding to each axial point (X, 1- Z_o^2, Z_o) where the particle is deposited. For a flow of parabolic velocity profile, however there may be two initial points, D(0, Y_A, Z_o) and B(0, Y_C, Z_o) on the Y axis that will deposit at the same axial point (X, 1 - Zo^2, Zo) as shown in Fig. 3-7. In Fig. 3-7, those particles entering the tube along the curve DB (the equi-penetration curve) will deposit on the tube wall at X1 along the wall D'B'.

The dashed lines in Fig. 3-7 are the trajectories of particles moving in the tube. The shaded area is symmetrical to the Y-axis. All particles entering the tube through the shaded area will deposit in the region of X > X1, while particles entering the tube out of the shaded area will deposit in the region of 0 < X < X1. Two other types of penetration curves are shown in Figs. 3.10 and 3.11.

2) Computation of Fractional Deposition

For a particle entering at constant velocity, the deposition is expressed as

$$DEPO = \frac{Qd}{Qt} = \frac{\int_A N_o \, Up_o \, dA}{N_o \, pi \, Ro^2 \, Up_o} = \frac{\int dA}{pi} \qquad (3\text{-}86)$$

where $\int dA$ can be obtained by numerical integration.

Based on the location of the equi-penetration curve above or below the Z-axis, the fraction of deposition at any given X may be obtained by two numerical integrations. Detailed analysis is discussed in Appendix A.

(D) Particles with initial velocity of $2(1-Y_o^2-Z_o^2)$ and Fluid with Parabolic Velocity Profile

Similarly, at given initial and boundary conditions, the fraction of deposition for particles entering the tube with a parabolic velocity can be obtained by using the same numerical approach as described in Appendix A.

For a particle entering at parabolic velocity profile, the fraction of deposition is

$$Depo = 1 - \frac{Qd}{Qt}$$

where

$$\frac{Qd}{Qt} = \frac{\int_{A'} N_o \, Up_o \, dA}{\int_{A} N_o \, Up_o \, dA}$$

$$= \frac{\int_0^{\theta}\int_0^{R} 2\,(1 - R^2)\, R \, dR \, d\theta}{\int_0^{pi}\int_0^{R} 2\,(1 - R^2)\, R \, dR \, d\theta} = \frac{\int_0^{\theta} (R^2 - 0.5\, R^4)\, d\theta}{pi}$$

Two numerical integration methods are used to compute the fraction of deposition for the case with two types of penetration curves as shown in Fig. 3-7.

The characteristics of the equi-penetration curve can be obtained by numerically solving Eq. (3-59) through Eq. (3-61). Description of the analysis is discussed in Appendix A.

3.5.4 Deposition due to Viscous, Inertia, Gravity and Image Charge Forces

When the particle is sufficiently diluted, the image charge force becomes important to the process of deposition. The magnitude of associated parameters are listed in Tables

3-4 and 3-5 for density = 1 gm/cc and uo = 30 cm/s. Tables 3-4 and 3-5 have the geometry of a circular tube given as h = 0.1 cm and 2 cm. For h = 0.1 cm, at particle size of 1 μ m, the magnitude of gravity, inertia and image forces are 9.86e-5, 9.06e-4 and 1.96e-5 for Y =0.98 and 7.84 e-4 for Y = 0.99 respectively. As we can see from Tables 3-4 and 3-5, the magnitude of image forces compared with gravity and inertia cannot be neglected for particle sizes less than 1 μ m.

1) General Description

Again, the flow is assumed sufficiently diluted at a concentration of less than 10^5 particles per cubic centimeter. The deposition of a suspension flow is contributed predominantly by the image force.

2) Description of Deposition Process

As depicted in Fig. 3.8, the curve ACB is the equi-penetration curve for a given axial distance X1. The point E, where the gravity force acting downward is balanced off by the image force acting upward, has the maximum deposited distance. Particles entering along the curve ACE deposits on the bottom wall and is depicted as curve A'C' while those entering along curve EB excluding point E deposit on the top of wall and are indicated on curve B'E'. Particle entering through the shaded area are deposited in the region of X> X1.

3) Governing Equations

For a circular tube with radius h, the dimensionless governing equations with additional image force become

$$Q \frac{d^2X}{dT^2} = U - \frac{dX}{dT} \tag{3-88}$$

$$Q \frac{d^2Y}{dT^2} = - \frac{dY}{dT} - G + F_Y \tag{3-89}$$

$$Q \frac{d^2Z}{dT^2} = - \frac{dZ}{dT} + F_Z \tag{3-90}$$

where the parabolic velocity profile for circular tube is $U = 2\,(1 - X^2 - Y^2)$.

For a particle in a circular tube, the components of dimensionless image force are

$$F_Y = (F)\left(\frac{Y^2}{Y^2 + Z^2}\right) \tag{3-91}$$

$$F_Z = (F)\left(\frac{Z^2}{Y^2 + Z^2}\right) \tag{3-92}$$

where

$$F = \left(\frac{q^2}{16\ \text{pi}\ e''}\right)\left(\frac{R^2}{Ro^2}\right)\left(\frac{1}{1 - R^2}\right) \tag{3-93}$$

F_Y = Y-component of dimensionless image force

F_Z = Z-component of dimensionless image force

R = r/h

Ro = dimensionless radius which is equal to one

Instead of using time dependent solutions to find the initial particle location, the trajectory method accompanied with the curve-fitting method are used to determine the particle initial locations for which a particle entering the tube will deposit at the same axial distance. Since the particle trajectories are symmetrical to the Y-X plane, a typical analysis consists of calculating trajectories for 191 particles initially distributed over a right-side semi-circular inlet section ($-90 < 0 < 90$). When a particle trajectory intersects with the wall, the particle is assumed to have deposited and the penetration length for the particle is determined. After all the trajectories are calculated, the function of equi-penetration curves can be obtained by the method of curve-fitting. As shown in Fig. 3.6, the area enclosed by the curve BC is proportional to the penetration and the exterior area is proportional to the deposition.

Once the equi-penetration curve is determined, the deposition can be calculated by numerical integration of the product of particle concentration and the particle velocity over the shaded area.

4) Computation of Deposition

The fractional deposition in a circular tube with

$$DEPO = 1 - PENT$$

where

$$PENT = \frac{\int_{-pi/2}^{\theta}\int_{0}^{R} N_o\, Up_o\, R\, dR\, d\theta}{\int_{0}^{pi}\int_{0}^{R} N_o\, Up_o\, R\, dR\, d\theta}$$

Thus, the PENT, for Up_o = constant is

$$PENT = \frac{\int_{-pi/2}^{\theta} R^2\, d\theta}{pi} \tag{94}$$

For $Up_o = 1 - R^2$, the PENT is

$$PENT = \frac{\int_{-pi/2}^{\theta} (R^2 - 0.5\, R^4)\, d\theta}{0.5\ pi} \tag{95}$$

Eqs. (3-94) and (3-95) can be numerically integrated. The detailed numerical scheme is discussed in Appendix A.

RESULTS AND DISCUSSIONS

In this chapter, the fraction of deposition obtained from previous analysis is discussed. The results vary with fluid velocity profile and particle initial velocity in a parallel-plate channel and a circular tube. These results were obtained either by an analytical or numerical method. In the discussion , the results from the channels under the influence of viscous, gravity and inertia are presented first, then the results from additional image forces follow. Comparison on the results under the influence of inertia and viscous, gravity, and additional image forces are discussed.

4.1 Deposition in Parallel-Plate Channels

The particle deposition efficiencies obtained under the influence of inertia, gravity and image forces are discussed. The fluid velocity profiles of uniform and parabolic are assumed in the analysis. The amount of particles entering the inlet plane is computed based on the inlet particle velocity which is either a uniform or parabolic profile. To analyze the deposition, the particle initial velocity was assumed either equal to the fluid's velocity or zero.

The discussions on the deposition of fine particle in channel flow are summarized into two sections. These

involved the effects of (1) viscous, inertia and gravity and (2) image force on the deposition.

4.1.1 Viscous, Inertia, and Gravity Forces

In a parallel plate channel, particles carried by a fluid of uniform velocity profile are considered to have deposited when the particle reached the wall. At any given axial distance from the entrance, the amount of particles deposited will be affected by the particle initial velocity, fluid velocity profile, fluid viscosity, gravity, and the particle inertia. In the analysis the particle inertia is represented by the parameter Q which varied from 0.01 to 100. No image force is considered in this section.

From the governing equations (3.2) - (3.4), a set of time dependent equations are solved analytically or numerically. For a given axial distance, the particle deposition can be obtained by particle concentration integration from the penetration point to the channel wall. Results are compared with Wang's [27] which has no inertia force involved. Four cases are discussed in the following:

(A) Particles with Zero Initial Velocity and Fluid with Uniform Velocity Profile

Since the particle initial velocity is zero, the

distance of deposition predicted is smaller than those particles entering with some momentum. Therefore, the deposition is higher than that obtained for particles entering with a uniform velocity profile. The results of deposition are derived from Eq. (3-31) which is independent of Q and are given in Fig. 4.1 for gravity of unit magnitude. The dimensionless axial distance X in Fig. 4.1 is equal to the ratio of axial distance to half width of the channel. For example, at G = 1 and X= 1.0, the deposition is 0.5 for all cases of Q. From Eq.(3-31) for a completed deposition the channel requires a length of 2/G. It is noted that the deposition distance is independent of the Q value and is the same as that obtained for case without inertia as indicated in Eq. (3-35).

(B) Particles with Uniform Initial Velocity and Fluid with Uniform Velocity Profile

As indicated in Chapter 3.1 (B), an initial location Yo is found for each axial point X. The fractions of deposition are calculated analytically from Eq. (3-32). The results for a gravity parameter of G = 1 are depicted as in Fig. 4.2.

In general, a particle with higher inertia (larger Q value) will travel longer distance than those with lower inertia before depositing on the wall. Thus, particles with higher Q will be expected to have smaller deposition than

that with a smaller inertia Q as shown in Fig. 4.2. For example at X = 1.0, the deposition for Q = 0.01, 0.1, 1.0, 10, and 100 are 0.492, 0.45, 0.182, 0.022 and 0.0 respectively.

The lengths of channel required for a complete deposition of particles are 2, 2.1, 2.94, 7.05, and 20.6 for Q equal to 0.01, 0.1, 1, 10, and 100 respectively. The above results are based on G = 1.

Since particles in this case have higher inlet velocity than that in Case A, it is clear that particle with higher inlet velocity would deposit farther downstream. The deposition for Case A, therefore, is higher than that for Case B. For example, at Q = 1, the deposition at X = 1 is 0.5 and 0.182 for Upo = 0 (Case A) and Upo = U_f (Case B) respectively.

(C) Particles with Zero Initial Velocity and Fluid with Parabolic Velocity Profile

When a fluid flows in a parallel-plate channel with a parabolic velocity profile and particles enter the channel with zero velocity, the effect of gravity and inertia force on the deposition are similar to that obtained from a uniform flow; i.e. as Q increases, the deposition decrease. In Fig. 4.5, the deposition at X = 1.0 is 0.495 for Q =

0.01, 0.46 for Q = 0.1, 0.408 for Q = 1 and 0.39 for Q = 100. It is interesting to note that all the particles deposit in the region of $0 < X < 2$.

Again, particles entering at a velocity higher than zero will have lower deposition efficiency. Thus, a suspension channel flow with a parabolic velocity profile and particles with zero initial velocity have higher deposition rates.

(D) Particles with Initial Velocity of $1.5(1 - Y^2)$ and Fluid with Parabolic Velocity Profile

Deposition for this case is calculated by a numerical method as discussed in Section 3.4.2-1(A). Similar effects of inertia and gravity on the deposition described in Case B are also observed in a flow with particles entering at a parabolic velocity; i.e. particles with higher inertia have lower deposition efficiency. As shown in Fig. 4.6, the deposition at X = 1 is 0.3 for Q =0.01, .22 for Q =0.1, .052 for Q = 1 and 0.0 for Q = 10 and Q = 100. At Q = 0.01, the deposition curve is almost same as that for the case of Q = 0; this verifies that as $Q < 0.01$, the particle inertia may be neglected.

The distance required for a complete deposition for Q = 0.01, 0.1, 1, 10 and 100 is 2, 2.04, 2.99, 7.66, and 22.85 respectively. These distances are much higher than those in

a uniform flow due to the fact that particles near the centerline of the channel are initially at higher velocity than those in a uniform flow. At Q = 0.01, the deposition curve is almost same as that for case of Q = 0; this verifies that for Q < 0.01, the particle inertia may be neglected.

(E) Comparisons and Discussions

For both uniform and parabolic flows in a parallel plate channel, the fraction of deposition decreases with increasing inertia parameter and the deposition in a uniform flow is higher than that in a parabolic flow for a given inertia parameter. For example, the deposition at X = 1 and Q = 1 is 0.182 for the uniform flow and is 0.052 for the parabolic flow as shown in Fig. 4.2 and Fig 4.6 respectively.

Moreover, for both flow profiles, the deposition at Q = 0.01 is very close to that at Q = 0 as shown in Fig. 4.2 and Fig. 4.6. Therefore, when the inertia parameter Q is less than 0.01, the inertia effect may be neglected.

In practice, the initial particle velocities should lie between zero and that of the local fluid velocity; thus the deposition of the particle should fall between that obtained from Upo = 0 and Upo = U_f for both flow profiles discussed.

When the inertia parameter is decreased to a value of

0.01, the deposition calculated from the case of $Up_o = U_f$ is very close to that from the case of $Up_o = 0.0$. This is due to the fact that the viscous force accelerates the particle to a velocity equal to the fluid's in such a very short axial distance that the deposition for zero initial velocity is practically the same as that for $Up = U_f$ for a small X.

4.1.2 Viscous, Inertia, Gravity and Image Forces

In the analysis, the image parameter of $q^2/(16\ pi\ e")(f\ uo)$ and the gravity parameter are assumed as unity. The parameter is the ratio of image force to the viscous force. The force tends to attract particle to the top wall as well as to the bottom wall. At a location of Yo = 0.5191 the image force acting upward is equal to the gravity force acting downward, therefore, particles near this region travel farther before depositions occur. Also, particles entering in the region above the point Yo are attracted toward the top wall; while those entering in the region below the point Yo will deposit on the bottom wall.

In the analysis, the particle inlet velocity is assumed to be the same as that of the fluid which is either uniform or parabolic. The discussion of deposition due to additional image forces is divided into two parts as follows:

(A) Particles with Uniform Initial Velocity and Fluid with Uniform Velocity Profile

For flow with uniform velocity in a parallel-plate channel, an additional image force increases the deposition significantly. The fraction of deposition was calculated by a numerical method. The results of deposition with respect to the dimensionless axial distance X are depicted in Fig. 4.7. In the analysis, the inertia parameter Q varied from 0.01 to 100 which has a different degree of influence on the deposition of particle. For example, at Q = 1, the deposition with gravity and inertia alone, at X = 1 is .052 (see Fig. 4.2), while with the additional image force, the deposition increases to .395 (see Fig. 4.7). Significant increases are also observed for other inertia parameters. For example, at Q equal to 0.01, 0.1, 1, 10 and 100 the fraction of deposition at X = 1, with additional image force it varies from .91, .82, .39, .1 and .02 respectively and without the image force it varies from 0.5, 0.45, 0.18, 0.02 and 0.002 respectively.

There is another significant difference in the pattern of deposition when the image force is considered. A particle located at Yo = 0.5191 and G = 1 has zero net force acting in the vertical direction due to cancelation of the image force and gravity, and the particle will not be deposited on the wall theoretically. Particles entering

near Yo = 0.5191 will travel longer distances than those with inertia and gravity alone. Therefore, at a certain X downstream, the deposition for particles with additional image force is lower than that without it and there is no axial distance at which a complete deposition takes place.

(B) Particles with Initial Velocity of $1.5(1-Yo^2)$ and Fluid with Parabolic Velocity

For flow of suspension entering a parallel plate channel with a parabolic velocity, the effect of image, gravity and inertia on the deposition of particles is similar to that of uniform flow.

An increase of deposition with additional image parameter of $q^2/(4 \text{ pi } e")/(f \text{ uo})$ is observed from Fig. 4.16 and Fig. 4.14. In the region of $0 < X < 4.1$, depositions for the case with additional image force are higher than those with gravity and inertia alone. For example as gravity and the image parameter are considered as unity, the fraction of deposition at X = 1, for Q =1, is .325 and .055 for case with and without additional image force respectively. The significant increase in deposition for Q = 0.01, 0.1, 1, 10 and 100 also can be observed from Fig. 4.14 and Fig. 4.16.

Again, the opposite effect of the inertia parameter on the deposition is that particles with higher inertia forces

have lower deposition efficiency. For example, at X = 1, where Q is equal to 0.01, 0.1, 1, 10 and 100, the deposition are .785, .67, .325, .135 and .055 respectively for the magnitude of the image parameter of unity. The drop in the deposition is indeed significant.

From Fig. 4.6 and Fig. 4.8, at certain axial-locations where the deposition is greater than 0.95, the fraction of deposition for cases with additional image forces is lower than that without image forces. In the inlet plane around Yo = 0.5191, a particle with additional image force will travel longer distance than with inertia and gravity alone. For example, at Q = 1 and X = 4.3, the particle deposition for the case with additional image forces is lower than that without the image force (see Fig. 4.6 and Fig. 4.8). Similarly, near the entrance of the channel, the deposition of the particle entering under the influence of image forces is higher than those without the image forces for a parabolic flow.

(E) Comparison and Discussions

In this section we have presented the results of deposition for flow of suspensions in a parallel-plate channel under different initial particle velocities and fluid velocity profiles. The forces included are the inertia, viscous, gravity and image forces. When the gravity force

is the only force acted in the vertical direction, all particles will deposit on the wall in a finite axial distance. When the image force and the gravity are involved, the particle deposition increases greatly, but some particles will have to travel extremely far downstream before deposition occurs. The inertia of a particle tends to keep it from changing the direction of motion and thus increases the distance traveled before deposited. Therefore, as Q increases, the deposition decrease.

The fraction of deposition in a given length for flow with uniform velocity profile is higher than that of parabolic velocity profile for particles with same initial velocity.

4.2 Deposition in Circular Tubes

The analysis on the deposition efficiency in a circular tube is basically same as that in a parallel-plate channel. However, the time required to perform the analysis in a circular tube is much longer than in the parallel-plate case. For a given axial distance in a parallel-plate case only one or two points need to be determined before computing the fraction of deposition, while in a circular tube a group of points which form the equi-penetration curve have to be determined before proceeding with the computation of deposition.

In this section, the fraction of deposition under the influence of viscous, inertia, gravity and image forces are discussed. The variation with fluid velocity profile and particle initial velocity are considered and the influence of them on the deposition is also presented. In the discussion, the deposition due to inertia and gravity is discussed first, then that of additional image force.

4.2.1 Viscous, Inertia, and Gravity Forces

The fraction of deposition obtained from the Eqs. (3.49) - (3.51) are depicted in Fig. 4.11 through Fig. 4.14. The effect of gravity and inertia on the deposition is similar to the effect in the parallel-plate channel.

The variation of results variances with fluid profile and particle initial velocity are discussed as follows. In this subsection, no image force is involved.

(A) Particles with Zero Initial Velocity and Fluid with Uniform Velocity Profile

The fraction of deposition obtained from Eq. (3-47) through Eq. (3-49) is depicted in Fig. 4.11 for gravity parameter of unity. It is interesting to note that the deposition is independent of Q as in Case A in a parallel-

plate channel. From Eq. (3-52) and Eq.(3-53), it is observed that the increase of axial velocity by an amount of (Q +Exp(-T/Q)) due to increased Q is cancelled out by the increase of vertical velocity at an increment of G (Q + Exp(-T/Q)). Thus, the fraction of deposition at any given axial distance for all cases of Q is the same.

The length required for complete deposition is 2/G which is same as that in a parallel-plate channel. However, the fraction of deposition is different from that obtained in a parallel-plate channel. For example, at G = 1 and X =1 , the fraction of deposition is 0.62 for a circular tube, 0.5 for a parallel-plate channel.

(B) Particles with Uniform Initial Velocity and Fluid with Uniform Velocity Profile

As depicted in Section 3.4.3 (B), an equi-penetration curve for a given axial distance is determined first, then the amount of particle entering the tube can be obtained by integrating the product of particle concentration and inlet particle velocity over the area enclosed by the equi-penetration curve and the boundary wall. The fraction of deposition under the influence of inertia and gravity is depicted in Fig. 4.12.

Similarly, the deposition efficiency of particles with

higher inertia is smaller than those with lower inertia. For example, at G = 1 and X = 1, the deposition in a circular tube for Q equals to 0.01, 0.1, 1, 10 and 100 are .6, .55, .23, .03 and .005 respectively; while in the parallel-plate channel the depositions are .492, .45, .182, .022 and 0.0 which is lower than that in a circular tube.

As Q = 0.01, the deposition is close to that for the case of Q = 0. Thus, the particle inertia parameter is considered negligible when Q is less than 0.01. As depicted in Fig. 4.12, the deposition curve for Q = 0.01 almost conincide with the curve of Q = 0 except in the case of small axial X.

It is noted that for a suspension of uniform velocity profile the deposition curve for Up_o = 0 is exactly the same as that of Q = 0 (see Fig. 4.11 and Fig. 4.12).

As observed in Fig. 4.11 and Fig. 4.12, the fraction of deposition in this case is lower than that in case A. This is indicated by the fact that the higher particle initial velocity in Case B allows particles to travel farther than those in Case A.

The lengths required for Q equal to 0.01, 0.1, 1, 10 and 100 are 2, 2.2, 2.94, 7.05 and 20.6 respectively.

(C) Particles with Zero Initial Velocity and Fluid with Parabolic Velocity Profile

Again, the effects of gravity and inertia force on the deposition are similar to that for uniform flow. In Fig.4.13, the deposition at G = 1 and X = 1 is .6, .565, .53 and .53 for Q equal to 0.01, 0.1, 1 and 100. For Q > 1, increasing the particle inertia has little effect to the deposition efficiency.

Comparing the results obtained in a circular tube (see Fig. 4.13) with those in a parallel-plate (see Fig. 4.7), for a given X, the deposition is higher for case in a circular tube.

The complete deposition distance required is about 2.7 for all cases of Q values.

(D) Particles with Initial Velocity of 2 ($1-Y^2-Z^2$) and Fluid with Parabolic Velocity Profile

The fraction of deposition calculated numerically is depicted in Fig. 4.6. As Q increases, the deposition decreases. For example,at X =1, the fraction of deposition for Q equal to 0.01, 0.1, 1, 10 and 100 are 0.01, 0.035, 0.145, 0.4 and 0.505. Those data are higher than that obtained in a parallel-plate channel.

Since the initial particle velocity is higher than that in Case C, the fraction of deposition in this case is lower than that in Case C. It is observed in Fig. 4.13 and Fig. 4.14. For example, at X = 1, the deposition for Q = 1 is 0.53 and 0.145 for particle with initial velocity of zero and parabolic respectively.

The lengths required for completed deposition are 2.7, 3.0,4.0,7.0 and 10 for Q equal to 0.01, 0.1, 1, 10 and 100 respectively. Those lengths are much longer than in Case B of uniform velocity profile.

(E) Comparison and Discussions

The fraction of deposition, for both uniform and parabolic flows in a circular tube, increases with decreasing inertia parameter and the deposition in a uniform flow is higher than that in a parabolic flow for a given inertia parameter. For example, the deposition at X = 1 and G = 1 for the case of Q = 1 is 0.23 for the uniform flow and is .052 for the parabolic flow. The results can be observed in Fig. 4.12 and Fig. 4.14.

Similarly, as Q approaches to 0.01, the inertia effect on deposition becomes negligible. These are depicted in Fig. 4.12 and Fig. 4.14; also, the deposition of particle

practically should fall between that obtained from $Up_o = 0$ and $Up_o = U_f$ for both flow profiles discussed.

4.2 Viscous, Inertia, Gravity and Image Forces Effects

As discussed in Section 4.1.2, the image force parameter of $q^2/(16 \text{ pi } e")/f \text{ uo}$ is assumed to be unity. The image force tends to attract the particle radially toward the wall. In the analysis, the particle inlet velocity is assumed to be the same as that of the fluid. The deposition obtained due to additional image force, gravity, inertia and viscous force are discussed as follows.

(A) Particles with Uniform Velocity and Fluid with Uniform Particle Velocity

The deposition in a circular tube with additional image force is increased significantly than those with inertia and gravity alone. The results are depicted in Fig. 4.15 and Fig. 4.12. For example, at Q = 1, the deposition with gravity and inertia alone, at X = 1 is .23 (see Fig.4.12), while with additional image force, the deposition increase to .82 (see Fig.4.15). Significant increase are also observed for other inertia parameter of Q = 0.1 and 10.

No completed deposition distance is obtained due to the force balance in the vertical direction along the point

Y0 = 0.5191 for image and gravity parameters of unity.

(B) Particles with Initial Velocity of 2 (1- Y^{2-} Z_2) and Fluid with Parabolic Velocity Profile

The fraction of deposition in the flow with parabolic velocity profile is presented as shown in Fig. 4.16. For flow of a suspension entering a circular tube, additional particle image forces increase the deposition significantly. Those can be observed from Fig. 4.14 and Fig. 4.16 for Q = 0.1, 1 and 10. As example, at Q = .1, 1 and 10, the fraction of deposition at X = 1 is .035, .145 and 0.4 for the case with gravity and inertia alone, while for the case of additional image forces, the depositions are 0.82, 0.55 and 0.3 respectively.

Again, as Q increases, the depositions with additional image force decrease. For example, at x=1 and G =1 , for Q equal to 0.1, 1 and 10, the depositions are 0.82, 0.55 and 0.3 respectively. And the fraction of deposition for a fluid with a parabolic velocity profile is lower than that for uniform velocity profile (see Fig. 4.16 an Fig. 4.14). Similarly, no completed deposition can be obtained.

4.2.2 Summary and Discussions

The effects of velocity profiles and initial conditions on the deposition have been discussed in this chapter. It is observed that for both uniform and parabolic flows in a circular tube, the fractional deposition decreases with increasing inertia parameter and the deposition in a uniform flow is higher than that in a parabolic flow for a given inertia parameter. Additional image forces greatly increase the fraction of deposition. Also, as indicated in the paralle-plate, when particles in the region where gravity and image force are balanced on vertical direction will travel far downstream than those with inertia and gravity alone.

CHAPTER 5 CONCLUSIONS

The deposition of suspension (fluid-solid) flow in a parallel-plate channel and a circular tube under the influence of viscous, inertia, gravity and image forces has been studied theoretically and certain conclusions are summarized in Table 3.6 and drawn as follows:

(1) The time dependent solutions for the case with inertia and gravity forces involved are derived and given in Chapter 3. The solutions for either uniform or parabolic velocity profile and particle initial velocities of zero or the same as the fluid are included. The solutions basically are dependent upon the particle inertia and gravity which influence the particle deposition process. For particles in a parallel-plate channel and circular tube, particles with higher inertia take more time to reach the channel wall, while the gravity parameter has a reverse effect.

(2) In cases of flow of a uniform velocity profile in a parallel-plate channel, the analytical solutions of the fractional deposition are derived and given as Eq. (3-31) and Eq. (3-32) for particle initial velocities of zero and constant respectively. For a particle initial velocity of zero, the deposition obtained is independent of the partcle inertia parameter Q. As the particle

inertia is neglected, i.e. Q = 0, the equations of deposition for particles of uniform initial velocity are reduced to that given by Pich [27] for a horizontal parallel-plate channel with no inertia force involved.

(3) In a flow of uniform velocity profile in a circular tube, the solutions of fractional deposition for particles are derived and given by Eq. (3-79) and Eq. (3-82) for a particle initial velocity of zero and a constant one. It is noted that for the case of a particle initial velocity of zero, the solution of fractional deposition is independent of the particle inertia parameter. When the particle inertia is neglected, i.e. Q = 0, the solutions of deposition are reduced to those obtained by Pich [27].

(4) In a flow of parabolic velocity profile and a particle initial velocity of zero, the analytical solutions of the fractional deposition are derived as Eq. (3-36) and Eq. (3-86) for both parallel-plate channels and circular tubes respectively. It is noted that the solution of deposition in a parallel-plate channel is the same as that obtained by Wang [37] for cases with no inertia forces. However, for cases in which the particle inlet velocity is the same as the fluid, the fractional depositions are obtained numerically.

(5) Increasing the particle inertia will decrease the deposition efficiency of a particle in either a parallel-plate channel or a circular tube.

(6) If the particle initial velocity is zero or the same as that of the fluid, deposition in the flow of uniform velocity profile is higher than that in a flow of a parabolic velocity profile for flows in a parallel-plate channel and a circular tube as well. But in terms of deposition rate, for case of $Up_o = 0$, the deposition rate is zero.

(7) Results of particle deposition reveal that when the particle inertia parameter is less than 0.01, the inertia effect can be neglected as the gravity parameter is assumed to be unity.

(8) In both a parallel-plate channel and a circular tube, additional image forces greatly increase the deposition efficiency.

(9) A complete deposition of particles in a finite length of a parallel-plate channel or a circular tube is possible for the case of inertia and gravity alone. For the case with additional image forces, a complete deposition cannot be attained due to the cancellation between the downward-acting gravity and the upward-

acting image forces.

(10) In a parallel-plate channel and a circular tube, the particle trajectory solutions (time dependent solutions) can be obtained analytically for the case of gravity and inertia alone. However, for the case with additional image forces, the particle trajectory solutions are obtained numerically.

CHAPTER 6 RECOMMENDATION

A detailed analysis on the deposition of solid particles in a parallel-plate channel and a circular tube has been studied. The flows of both uniform and parabolic velocity profiles along with particle initial velocities of zero and those equal to that of the fluid were investigated. The influence on particle deposition due to viscous, inertia, gravity and image charge effects in a system of incompressible flow provided valuable information on the deposition mechanism of fine particles. The influence of the magnitude of particle size and shape on the deposition may be considered for further investigation.

Since the particle sizes are considerably small, the diffusion effect on the deposition can be investigated. The simultaneous effect of diffusion and the image charge parameter may be of importance on the research of the particle deposition mechanism.

Many experimental results on the deposition did reflect the importance of the image force on the deposition mechanism of fine particles. A recent survey by Vincent [34], John and Vincent [22] and Johnson [23] reveals that the contribution of the image charge effect on the particle deposition may not be neglected; rather, the shape of the particle with a longer aspect ratio; such as an asbestos

fiber, would be more important to the research in improving the working environment. As indicated by John [22] the amount of charge carried by the fibrous particle is more than the regular shape of particles. The emphasis on the reseach of the deposition of fibrous particle is also indicated in the 1984 Annual Conference of the British Occupational Hygiene Society at York.

Attention can also be given to the research on how the pollutant particles flow through a river or how long the pollutants suspend in the air and what the patterns of its deposition process are. It is hoped that in the near future these investigations would be useful in reducing the accumulation of pollutants and its negative impact on the ecology.

BIBLIOGRAPHY

1. Allen, M. D. and Raabe,O.G., "Re-evaluation of Millikan' Oil Drop Data for the Motion of Small Particles in Air", J. Aerosol Sci., Vol. 13, No. 6, 1982, PP. 537-547

2. Burden, R.L., Faires, J. D. and Reylonds, A. C., Numerical Analysis, 2nd ed., Chapter V, 1981

3. Carpenter, P. S. and Taulbee, D. B., "Time Dependent Gravitational Sedimentation of Aerosol Particles from Steady Laminar Flows in Channela and Ducts", J. Aerosol Sci., Vol. 11, 1982, pp. 161-178

4. Carslaw, H. S. and Jaegar, J. C., "conduction of Heat in Solids", Oxford University Press, London, 2nd ed., 1959, pp.101

5. Chan, T. L., Lipmann, M., Cohen, V. R. and Schlesinger, R. B., J. Aerosol Sci., Vol. 9,1978, pp.463-467

6. Chen, R. Y., "Deposition of Aerosol Particles in a Channel due to Diffusion and Electric Charge", J. Aerosol Sci., Vol. 9, 1978, PP. 253-260

7. Chen, R. Y., "Deposition of Charged Particle in Tube", J. Aerosol Sci., Vol. 19, 1978, pp. 449-453

8. Chen, R. Y., and Gelber, M. W., "Deposition of Suspensions in the Entrance of a Vertical Tube", Powder Technology, 28, 1981, pp.43-48

9. Chen, R. Y., Pawel, H. E. and Chen, W. C., "Inertia Effect on Deposition of Charged Particles in a Parallel-Plate Channel", Powder Technology, 34, 1983, pp.249-253

10. Cheng, L. and Soo,S. L.,"Charging of Dust Particles", J. of Applied Physics, Vol.41, No.2, 1970, pp. 585-591

11. Chu, C. Y., "Deposition of Particles in Horizontal Parallel Plate Channel due to Image Charge, Inertia, Viscosity and Gravity", Master Thesis, 1983, N. J. I. T.

12. Davies, C. N., Aerosol Science, Academic Press, London and New York, 1966

13. Diu, C. K. and Yu, C. P., "deposition from Charged Aerosol Flows Through a Pipe Bend", J. Aerosol Sci., Vol. 11, pp. 397-402

14. Dodes, I. A., Numerical Analysis for Computer Science, 1982

15. Fuchs, N. A., The Mechanics os Aerosols, Macmillan Co. New York, 1964

16. Ferron et al., "Comparison of Experimental and Calculated Data for the Toatal and Regional Deposition in the Human Lung", J. Aerosol Sci., Vol. 16, No. 2, 1983, pp. 133 - 143

17. Gelber, M. W., " Deposition of Particles in Vertical Conduits due to Electrostatic Charge, Diffusion, and Gravity", Doctoral Thesis, 1981, N. J. I. T.

18. Gentry, J. W. and Spurny, K. R., J. Aerosol Sci. Vol.8 1977, pp. 355

19. Heyder, J., and Gebhart, J. "Gravitational Deposition of Particles from Laminar Aerosol Flow through Inclined Circular Tubes", J. Aerosol Sci., Vol. 8, 1977, pp. 289-295

20. Ingham, D. B., "Deposition of Charged Particles near the Entrance of A Cylindrical Tube", J. Aerosol Sci., Vol. 11, 1981, pp. 47-52

21. Ingham, D. B., " Precipitation of Charged Particles in the Human Airways", J. Aerosol Sci. Vol. 12, No. 2, 1981, pp.131-135

22.John, W. and Vincent, J. H., "Static Electrification of Workplace Aerosol: Perspective", Ann. Occup. Hyg. 29, 1985, pp. 285-288

23. Johnson, A. M, Vincent, J. H. and Jones, A. D., "Measurement of Electric Charge for Workplace Aerosols", nn. Occup. Hyg. 29, 1985, PP. 271-284

24. Jones, A. D., Johnston, A. M. and Vincent, J. H., "Static Electrifiction of Airbone Asbestos Dust", In: Aerosol in the Mining and Industrial Work Enviroment (Edited by Morple, V. A. and Liu, B. Y. H.), Chapter 46, 1983, pp. 613-631. Ann. Arbor Science, Ann Arbor, Michigan

25. Melandri, C. et al., "Deposition of Charged Particles in the Human Airways", J. Aerosol Sci., Vol. 14, No. 5, 1983, pp. 657-669

26. Matveyev, A., Principle of Electrodynamics , 1966, Reinhold Publishing Corp.

27. Pich, J., J.,"Theory of Gravitational Deposition of Particles from Laminar Flows in Channel", J. Aerosol Sci., Vol. 3, 1972 , pp 351-361

28. Prodi, V. and Mularoni, A., "Electrostatic Lung Deposition Experiments with Humans and Animals", Ann. Occup. Hyg., Vol. 29, No.2, 1985, pp. 229-240

29. Shevchenko, A. M.G, " The Role of Some Physical and Chemical properties on Mine Dust in the Development of Pneumoconiosis". In : Inhaled Particles III (edited by Walton, W. H.), pp. 561-570, Unwin, London

30. Scott, W. R. and Taulbee, D. B., "Aerosol Deposition Along the Vertical Axis of the Lung", J. Aerosol Sci., Vol. 16, No. 4, 1985, pp. 323-333

31. Taulbee, D. B., and Carpenter, P. S., "Gravitational Deposition of Aerosol Particles Flow in a Horizontal Circular Tube", J. Aerosol Sci., Vol. 9, 1978, pp.513-519

32. Thiagarajan, V., and Yu, C. P., "Sedimentation from Charged Aerosol Flows in a Parallel-Plate and Cylindrical Channels", J. Aerosol Sci., Vol. 10, 1979, pp. 405-410

33. Thomas, J, W., J. Air Pollut. Control Ass. Vol. 8, 1958, P.32

34. Vincent, J. H., "On the Particle Significance of electrostatic Lung Deposition of Isometric and Fibrous Aerosols", J. Aerosol Sci., Vol. 16, No. 6, 1985, pp. 511-519

35. Vincent, J. H., Johnson, W. B., Jones, A. D. and Johnston, A. M., "Static Electrification of Airbone Asbestos: a Study of its cause, assessement and effects on deposition in the lungs of rats", Am. Ind. Hyg. Assoc. J. 42, 1981, pp. 711-721

36. Walton, W. H., " Theory of Size Classification of Airbone Dust Clouds by Elutriation", Br. J. Appl. Phys. Suppl. Vol. 3, S29-S39

37. Wang, C., "Gravitational Deposition of Particle from Laminar Flows in Unclined Channels", J. Aerosol Sci., Vol. 6, 1975, pp. 191-204

38. Wilidi, J. and Thomann, H., " Measurement of the Deposition of Small Particles in Stationary and Oscillating Turbulent Pipe Flow", J. Aerosol Sci., Vol. 54, No.5, 1983, pp. 615-632

39. Wongkittirock, W., " The Effect of Electrostatic Charge on the Deposition of Suspensions Flow", Master Thesis, 1980, N. J. I. T.

40. Wylie, C. R. and Kenan, W. R., Advanced Engineering Mathematics, 4th ed., 1975

41. Yu, C. P., "Precipitation of Uniformly Charged Particles in Cylindrical and Spherical Vessels", J. Aerosol Sci. Vol. 8, 1977, pp.237-241

42. Yu, C. P., "Teories of Electrostatic Lung Deposition of Inhaled Aerosols", Ann. Occup. Hyg., Vol. 29, No.2, 1985, pp. 219-227

43. Yu, C. P., " Electrostatic Effects in Aerosol Sampling and Filtration", Ann. Occup. Hyg., Vol. 29, No.2, 1985, pp. 1985, 251 - 269

44. Yu, C. P., and Chandra, K., "Precipitation of Submicron Charged Particles in Human Lung Airwaya", Bulletin of Mathematical Biology, Vol. 39, 1977, pp. 471-478

45. Yu, C. P., and Chandra, K., "Deposition of Charged Particles from Laminar Flows in Rectangular and Cylindrical Channels By Image Force", J. Aerosol Sci., Vol. 9, 1978, pp.175-180

46. Yu, C. P., and Thiagarajan, V., "Sedimentation from Charged Aerosol Flows in Parallel-Plate and Cylindrical Channels", J. Aerosol Sci., Vol. 10, 1979, pp. 405-410

APPENDIX A

NUMERICAL COMPUTATION METHODS FOR CIRCULAR TUBES

The fractional deposition in a circular tube was discussed in Section 3.5.2 Since the deposition cannot be obtained by analytical methods, a numerical method is developed to analyze the fractional deposition of the tube flow. Two cases requiring numerical methods are discussed below.

By using the solutions given in Section 3.5, the locus of particles deposited at the same axial distance can be calculated. Once the equi-penetration curve is determined, the fraction of deposition can be obtained numerically by integrating the product of the particle initial concentration and the particle initial velocity over the area enclosed by the equi-penetration curve and the boundary wall.

Based on whether the position of the equi-penetration curve lies above or below the Z-axis(depicted in Fig. 3-6 and Fig. 3-7), the fraction of deposition at any given X can be obtained by two numerical methods of integrations.

(A) Particles with Zero Initial Velocity and Fluid with Parabolic Velocity Profile

1) First Mehod

This scheme is applied to the case given in Fig.3-7(B) where part of the equi-penetration curve is below the Z-axis. The fraction of deposition (DEPO) is

$$DEPO = 1 - \frac{Qp}{Q_t} \qquad \text{(A-1)}$$

where

$$Qp = \frac{\int_{A'} No\ Up_o\ dA}{\int_{A} No\ Up_o\ dA} \qquad \text{(A-2)}$$

$$= \frac{\int_{-pi/2}^{\theta}\int_{0}^{R} (1)\ R\ dR\ d\theta}{\int_{0}^{pi}\int_{0}^{1} R\ dR\ d\theta} = \frac{\int_{-pi/2}^{\theta} R^2\ d\theta}{pi} \qquad \text{(A-3)}$$

where Q_p is the rate of penetration.

Since the penetration curve is symmetric with respect to the Y-axis, we may consider only the hemisphere on the right hand side of the tube. The numerator of Eq. (A-3) becomes

$$\Delta(Qp)_i = \frac{R_i^2\ (\Delta\theta)_i}{pi} \qquad \text{(A-4)}$$

where the angle varies from -pi/2 to pi/2.

$$\theta_i = \theta_i - \theta_{i-1}$$

Taking the summation of the increment $\Delta(Qp)_i$, the fraction of deposition can be obtained by subtracting Q_t from Q_p.

(2) Second Method

For the case as shown in Fig. 3-6 (B) in which the equi-penetration curve is located above the Z-axis, the second numerical method may be used to compute the fraction of deposition.

The method requires a new coordinate system with the origin at (0, 0.5(Y1 + Y2)) in which Y1 and Y2 are the Y-coordinates of points B and D, respectively, as shown in Fig. 3-7.

Let Zs and Ys be associated with new coordinate system and Z and Y with the old coordinate system. Then

$$Ym = 0.5\ (Y1 + Y2) \qquad (A-5)$$

$$Ys = Y - Ym \qquad (A-6)$$

$$Zs = Z \qquad (A-7)$$

If B is the only point not on the Y-axis, then Y1 is assumed to be one. The values of Y1 and Y2 can be obtained from time dependent solutions. Hence, the corresponding Ys

and Zs are calculated from Eq. (A-6) and Eq. (A-7).

Again, let

R_s= the radial distance along the equi-penetration curve in the new coodinate system.

R = the radial distance along the equi-penetration curve in the old coodinate system.

θ_s = the angle along the equi-penetration curve in the new coodinate sytem.

Then we have

$$R_s^2 = Ys^2 + Zs^2 \qquad \text{(A-8)}$$

$$R^2 = Y^2 + Z^2 \qquad \text{(A-9)}$$

From Eq.(A-6) and (A-9), we have

$$R_s^2 = R^2 - 2\ Ym\ Y + Ym^2 \qquad \text{(A-10)}$$

The penetration, Qp based on the new coordinate system can be expressed as

$$Qp = \int_{-pi/2}^{\theta_s} \int_0^{R_s} No\ Up_o\ R_s\ dR_s\ d\theta_s$$

$$= \int_{pi/2}^{\theta_s} \int_{0}^{R_s} R_s \, dR_s \, d\theta_s$$

$$= \int_{-pi/2}^{\theta_s} R_s^2 \, d\theta_s \qquad \text{(A-11)}$$

Therefore, the increment of penetration based on the new coordinate is

$$\Delta(Qp)_i = [R_s^2 \, \Delta\theta_s]_i \qquad \text{(A-12)}$$

where

$$\theta_s = \tan^{-1}\left(\frac{Ys}{Zs}\right), \text{ which varies from } -pi/2 \text{ to } pi/2$$

$$\theta_s = 0_i - 0_{i-1}$$

(B) Particle with initial velocity of $2(1 - Y^2 - Z^2)$ and Fluid with Parabolic Velocity Profile

Similarily, at given initial and boundary conditions, the fraction of deposition with a parabolic velocity can be obtained by using the same numerical approach as described in Case A.

Two numerical integration methods are used to compute the fraction of deposition for cases shown as in Fig. 3-6 (B) and Fig. 3-7. The method is presented below.

(1) First Method

For cases as shown in Figs. 3-6 and 3-7 in which part of the equi-penetration curve is located below the Z-axis, the fraction of deposition becomes

$$DEPO = 1 - \frac{Q_p}{Q_t}$$

where

$$\frac{Qp}{Qt} = \frac{\int_{A'} No\ Up_o\ dA}{\int_{A} No\ Up_o\ dA}$$

$$= \frac{\int_{-pi/2}^{\theta}\int_{0}^{R} 2(1 - R^2)\ R\ dR\ d\theta + 0.5\ (0.5\ pi - \theta_w)}{\int_{0}^{pi}\int_{0}^{1} 2(1 - R^2)\ R\ dR\ d\theta}$$

$$= \frac{\int_{-pi/2}^{\theta} (2\ R^2 - R^4)\ d\theta + (0.5\ pi - \theta_w)}{pi}$$

θ_w is the polar angle at point B where the equi-penetration curve intersects with the tube wall.

The method of numerical integration is given below to compute the integration term of penetration

$$\Delta(Q_p)_i = 2\ R_i^2\ (\ 1 - 0.5\ R_i^2)(\ \Delta\theta_i) \qquad \text{(A-14)}$$

where $\Delta\theta_i = \theta_i - \theta_{i-1}$

R_i = radial distance at point i

(2) Second Method

For the case as shown in Fig. 3-6 (B) in which the equi-penetration curve is located above the Z-axis, the second numerical method is needed to compute the fraction of deposition.

The method requires a new coordinate system centered on (0, 0.5(Y1 + Y2)) where Y1 and Y2 are the maximum and minimum values in the Y coordinate of the equi-penetration curve. The definition of the new coordinate system is as defined in Eqs. (A-8) through (A-10). From Eq. (A-10) we can derive

$$R^2 = R_s^2 + 2\ Ym\ (R_s \sin\theta) + Ym^2 \qquad \text{(A-15)}$$

The penetration, Qp based on new coordinate system can be expressed as

$$Q_p = \int_{-pi/2}^{\theta_s}\int_0^{R_s} 2\ N_o\ Up_o\ R_s\ dR_s\ d\theta_s = \int_{-pi/2}^{\theta s}\int_0^{R_s} 2(1-\ R^2)RdR\ d\theta \qquad \text{(A-16)}$$

Substituting Eq.(A-15) into Eq.(A-16),

$$Qp = \int_{-pi/2}^{\theta_s} (R_s^2 - 0.5\ R_s^4 - \frac{4}{3}(Ym\ \sin\theta_s)R_s^3 - Ym^2\ R_s^2)d\theta_s \qquad (A\text{-}17)$$

Therefore, the numerical scheme based on the new coordinate system is

$$\Delta(Q_p)_i = (R_s^2 - 0.5\ R_s^4 - \frac{4}{3}(Ym\ \sin\ \theta_s)R_s^3 - Ym^2R^2{}_s)_i(\Delta\theta_s)_i \qquad (A\text{-}18)$$

where R_s, Ym and 0_s is corresponding to the step i,

$$\theta_i = \tan^{-1}(\frac{Ys}{Zs})$$

$$(\Delta\theta_s)_i = \theta_i - \theta_{i-1}$$

(E) Constraint on the Numerical Analysis

In the numerical analysis, the increment on Y and Z are set as $Y < 0.005$ and $Z < 0.005$.

4) Computation Algorithm

The numerical scheme in the analysis is divided into three routes.

(i) Beginning at the first route

Given Zo to find Yo. Delimiter is $\theta > -1$

(ii) Followed by the second route

Given Yo to find Zo. Delimiter is $Z < 0$ or $R = 1$

(iii) Then, the third route

Given Zo to find Yo. Delimiter is $\theta = pi/2$ or $R \geq 1$

For the case as in Fig. 3-6(B), the first route and second route are applied to complete the computation. For the case as in Fig. 3-7, three routes are necessary to complete the computation.

A Bisection Method is designed to compute the deposition time T_f value for the given Yo or Zo. In routes one and two, the first calculated T_f is the value associated with the given Zo or Yo. In route three, the second computed T_f is the value associated with the given Zo.

The computation algorithm is as follows:

Step 1. For a given X and Zo or Yo, assume a T_f and calculate the corresponding Yo or Zo.

Step 2. Substitute the calculated Yo or Zo into time depenedent solutions to verify the T_f. If not satisfied, go back to step 1.

Step 3. Compute R and 0, then substitute them into Eq. (A-18) to obtain the increment of penetration.

To obtain the corresponding value of Yo or Zo, we substitute the assumed T_f value into Eq. (3-56), and when the particle is deposited on the wall , $Y_f = -(1 - Zo^2)^{1/2}$, we have

$$-(1-Zo^2)^{1/2} = Q\ G + Yo - G\ T - Q\ G\ Exp(-T/Q) \qquad (A-19)$$

Rearranging Eq. (A-19), we have

$$Yo = -(1-Zo^2)^{1/2} - Q\ G + G\ T + Q\ G\ Exp(-T/Q)$$

or

$$Zo = [1 -(Q\ G - Yo - G\ T - Q\ G\ Exp(-T/Q)]^2)^{1/2}$$

The calculated Yo or Zo is substituted into Eq. (3-58) for a particle initial velocity of zero or Eq. (3-60) for a particle initial velocity of $2\ (1 - Y_o^2 - Z_o^2)$. If the equation is satisfied, the T_f is the time value for the corresponding Yo or Zo. Once the corresponding value is obtained, we can proceed to the next increment on Y or Z. The results are presented and discussed in Chapter 4.

The numerical program is presented in Appendix C, named DEPO_3D_QG. The program is capable of handling Cases (A) and (B).

APPENDIX B

NUMERICAL COMPUTATION METHOD FOR ADDITIONAL IMAGE FORCE

The numerical schemes discussed in the following paragraphs are governed by Eqs. (3-88) through (3-90) which are given in Section 3.5.4. The numerical technique includes forth order Runge Kutta method, regression analysis and trapezoidal integration. The schemes are adopted to compute the deposition of particles discussed in Chapter 3.

(A) Computer Program

Six programs are used to compute the fraction of deposition in a circular tube. The functions of each program is explained in the following:

1. Program P3D

The program is designed to compute the trajectory of particles by the fourth order Runge-Kutta method. The typical points picked to calculate the trajectories are depicted as shown in Fig. 3.9. The points along the radial lines are totally 191 points.

Given an initial particle location, the corresponding deposited distance can be calculated. Once the corresponding distance to each set of data points located along the radial line is collected. The data set then can be transferred to

the next program for curve fitting. The data set is constructed into a function with two variable (X,R) at a given angle θ, or given as (X,R,θ).

2. Program PREGAA

This program is designed to curve-fit a set of data by the N'th order regression method.

For each data set (X,R,θ) obtained from program P3D is divided into three subsets. Each subset is then curve fitted into three polynomial functions at associated angle θ.

The function to be fitted for the first and third subsets functions are expressed as

$$F(R,\theta) = X$$ where the angle θ is constant.

The second set is expressed as

$$F(X,\theta) = R$$ where the angle θ is constant.

The data subsets and equations created are stored in a file ready for the use of next program.

3. Program DATAMK

The program is designed to compute initial coordinates of particles of same characteritic length X from the curve-fitted functions.

For a given axial distance, X , the corresponding radial distance R can be obtained by direct substitution method or Bisection Method. For functions ofthe form, F(R,θ) = X, direct substitution is employed. For functions of the form, F(X,θ) = R, a Bisection Method is utilized. The obtained data set (R,θ) are points located along the equi-penetration curve for the given axial distance X. Thedata set (R,θ) are chaqnged into the form of (Y,Z,θ).

5. Program ORDER

The program is designed to rearrange the data set (Z,Y,θ) on the order of increasing Y. The datasets are obtained from program DATAMK.

6. Program REFIT

The program is designed to curve-fit the data sets given by program ORDER for each corresponding X.

Each data set (Y,Z,θ) is readjusted to fit a new coordinatesystem. The new coordinate system is constructed with a new origin at (Ym,Z) where Ym is obtained by averaging the minimum and maximum values of Y in the data set. Z coordinate is unchanged.

The new data set is divided into three subsets, then do the curve fitting. The characteristic function of equi-

penetration curve, therefore, can be obtained for each given X.

6. Program PVOLUME

The program is designed to calculate the fraction of deposition of a suspension flow by using the Trapezoidal rule.

Overall speaking, curve-fitting a set of data requires appropriate adjustment on the order of polynomial equations, since each data set has different characteristics.

Finally, the equi-penetration curve created, after adjusted by the program ORDER, is display on the TEXTRONIC graghic terminal by using the PLOT 10 Graphics Package given in the Vax 11/780 system at NJIT. The equi-penetration curve therefore, can be verified visually for each given axial distance.

TABLE 3.1 The Magnitudes of Charge, Gravity and Inertia Parameter

Part. Dia (meter)	Cha/vi	Cha/Gr	Gr/vi	Int/vi	#Cha/part.
1.0e-7	7.88e-5	80.0	9.86e-7	4.53e-7	2.66
2.0e-7	6.30e-4	160.0	3.94e-6	1.81e-6	10.65
4.0e-7	5.04e-3	320.0	1.58e-5	7.25e-6	42.60
1.0e-6	7.88e-2	800.	9.86e-5	4.53e-5	266.2
2.0e-6	6.30e-2	--	3.94e-4	1.81e-4	--
4.0e-6	5.04	--	1.58e-3	7.25e-4	--

* Particle density 1 g/cc, h= 2 cm, Uo = 30cm/sec
vi= Viscousity; Gr = Gravity; Cha = Charge; Int= Inertia

TABLE 3.2 The Magnitudes of Image Force ,Gravity and Inertia in a Parallel-Plate Channel

Part. Dia (meter)	Gravity	Inertia	Image Force Y=.98	.99	#Cha/Part.
1.0e-7	9.86e-7	4.53e-7	4.90e-10	1.96e-9	2.66
2.0e-7	3.94e-6	1.81e-6	3.92e-9	1.57e-8	10.65
4.0e-7	1.58e-5	7.25e-6	3.13e-8	1.25e-7	42.60
1.0e-6	9.86e-5	4.53e-5	4.90e-7	1.96e-6	266.2
2.0e-6	3.94e-4	1.81e-4	3.92e-6	1.57e-5	--
4.0e-6	1.58e-3	7.25e-4	3.13e-5	1.25e-4	--

* Particle density 1 g/cc, h= 2 cm, Uo = 30cm/sec

TABLE 3.3 The Magnitudes of Image Force ,Gravity, and Inertia in a Parallel-Plate Channel

Part. Dia (meter)	Gravity	Inertia	Image Force Y=.98	.99	#Cha/Part.
1.0e-7	9.86e-7	9.06e-6	1.96e-8	7.84e-7	2.66
2.0e-7	3.94e-6	3.62e-5	1.57e-7	6.27e-6	10.65
4.0e-7	1.58e-5	1.45e-4	1.25e-6	5.02e-5	42.60
1.0e-6	9.86e-5	9.06e-4	1.96e-5	7.84e-4	266.2
2.0e-6	3.94e-4	3.62e-3	1.57e-4	6.27e-3	--
4.0e-6	1.58e-3	.015	1.25e-3	5.02e-2	--
1.0e-5	9.86e-3	.090	.196	.784	--

* Particle density 1 g/cc, h= .1 cm, Uo = 30cm/sec

Note: Charge Density 1 Electron per 1.18E-10 cm^2 Surface Area
Y = 1 is the location of wall

TABLE 3.4 The Magnitudes of Dimensionless Image Force ,Gravity, and Inertia Parameters in a Circular Tube

Part. Dia (meter)	Gravity	Inertia	Image Force Y=.98	.99	#Cha/Part.
1.0e-7	9.86e-7	9.06e-6	1.96e-8	7.84e-7	2.66
2.0e-7	3.94e-6	3.62e-5	1.57e-7	6.27e-6	10.65
4.0e-7	1.58e-5	1.45e-4	1.25e-6	5.02e-5	42.60
1.0e-6	9.86e-5	9.06e-4	1.96e-5	7.84e-4	266.2
2.0e-6	3.94e-4	3.62e-3	1.57e-4	6.27e-3	--
4.0e-6	1.58e-3	.015	1.25e-3	5.02e-2	--
1.0e-5	9.86e-3	.090	.196	.784	--

* Particle density 1 g/cc, h= .1 cm, Uo = 30cm/sec

TABLE 3.5 The Magnitudes of Dimensionless Image Force ,Gravity, and Inertia Parameters in a Circular Tube

Part. Dia (meter)	Gravity	Inertia	Image Force Y=.98	.99	#Cha/Part.
1.0e-7	9.86e-7	4.53e-7	5.00e-10	1.98e-9	2.66
2.0e-7	3.94e-6	1.81e-6	4.00e-9	1.58e-8	10.65
4.0e-7	1.58e-5	7.25e-6	3.20e-8	1.27e-7	42.60
1.0e-6	9.86e-5	4.53e-5	5.00e-7	1.98e-6	266.2
2.0e-6	3.94e-4	1.81e-4	4.00e-6	1.58e-5	--
4.0e-6	1.58e-3	7.25e-4	3.20e-5	1.27e-4	--
1.0e-5	9.86e-3	4.53e-3	5.00E-4	2.00E-3	--

* Particle density 1 g/cc, h= 2 cm, Uo = 30cm/sec

Note: Charge Density 1 Electron per 1.18E-10 cm^2 Surface Area
Y = 1 is the location of wall

Table 3.6 Summary of Analysis on the Particle Deposition due to Viscous, Inertia, Gravity and Electrostatic Charge Forces in Parallel-Plate Channels and Circular Tubes

	Fluid Velocity of Uniform Profile		Fluid Velocity of Parabolic Profile	
Item	Gravity Alone	Gravity + Image Forces	Gravity Alone	Gravity + Image Forces
Closed Form Solutions for X and Y				
$Up_o=0$	Eqs.(3-19)-(3-20)	no	Eqs.(3-23)-(3-24)	no
$Up_o=U$	Eqs.(3-21)-(3-22)	no	Eqs.(3-25)-(3-26)	no
Closed Form Solutions for Fractional Deposition				
$Up_o=0$	Eqs.(3-47)-(3-49)	no	Eqs.(3-56)-(3-58)	no
$Up_o=U$	Eqs.(3-50)-(3-52)	no	Eqs.(3-59)-(3-61)	no
Deposition	--	higher	--	higher
Complete Deposition Length	yes	no	yes	no
Q increase on Deposition	decrease	decrease	decrease	decrease
G increase on Deposition	increase	increase	increase	increase
Fp increase on Deposition	increase	increase	increase	increase

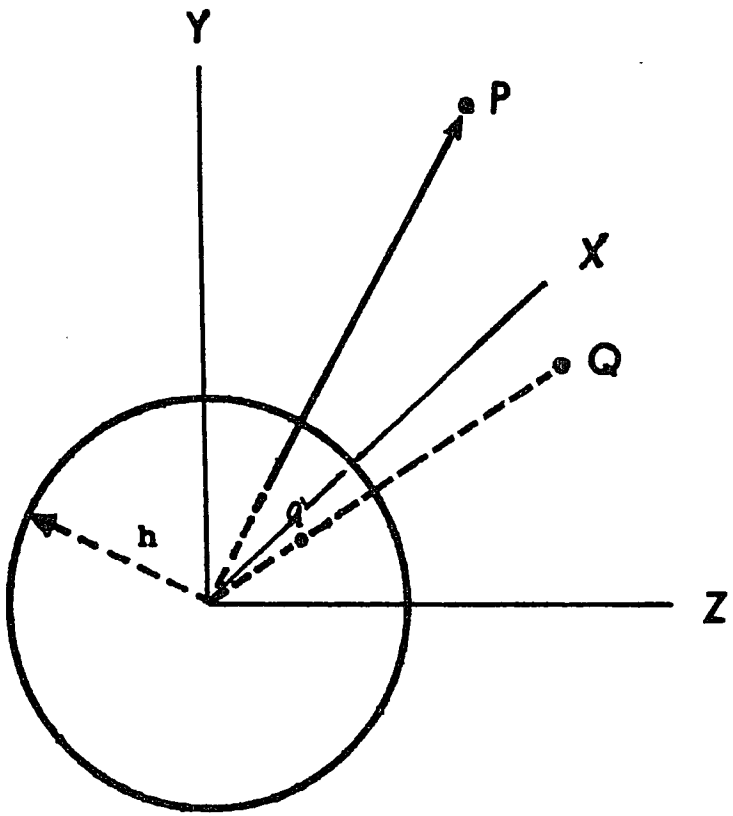

Fig. 3.1 Cartesian Coordinate System in the Analysis

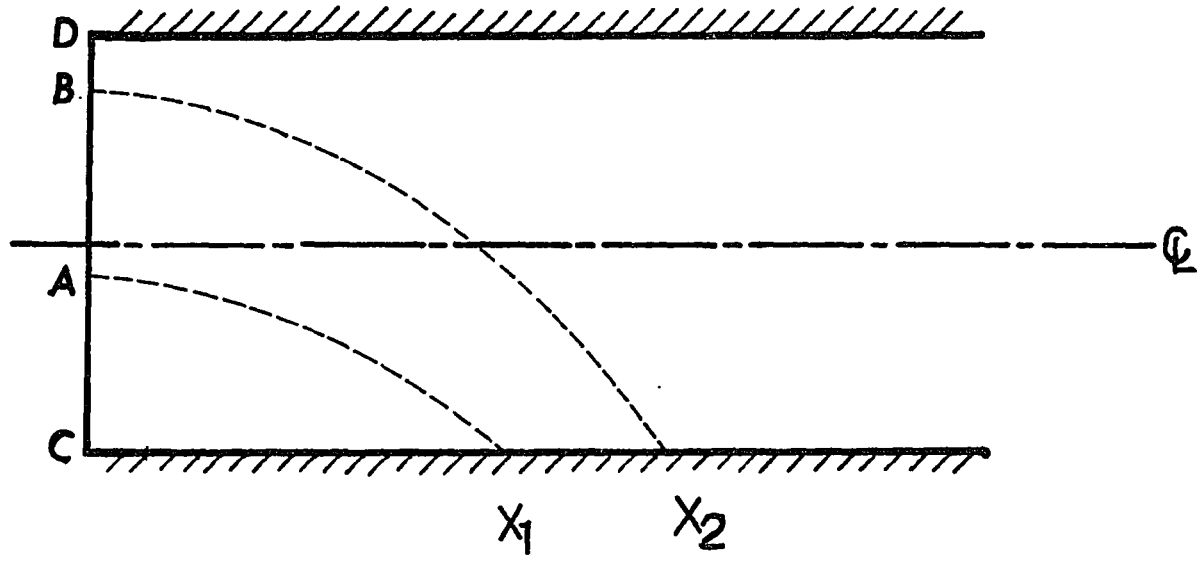

Fig. 3.2 Deposition Route of Particles in a Fluid of Uniform Velocity Profile Confined by a Parallel-Plate Channel

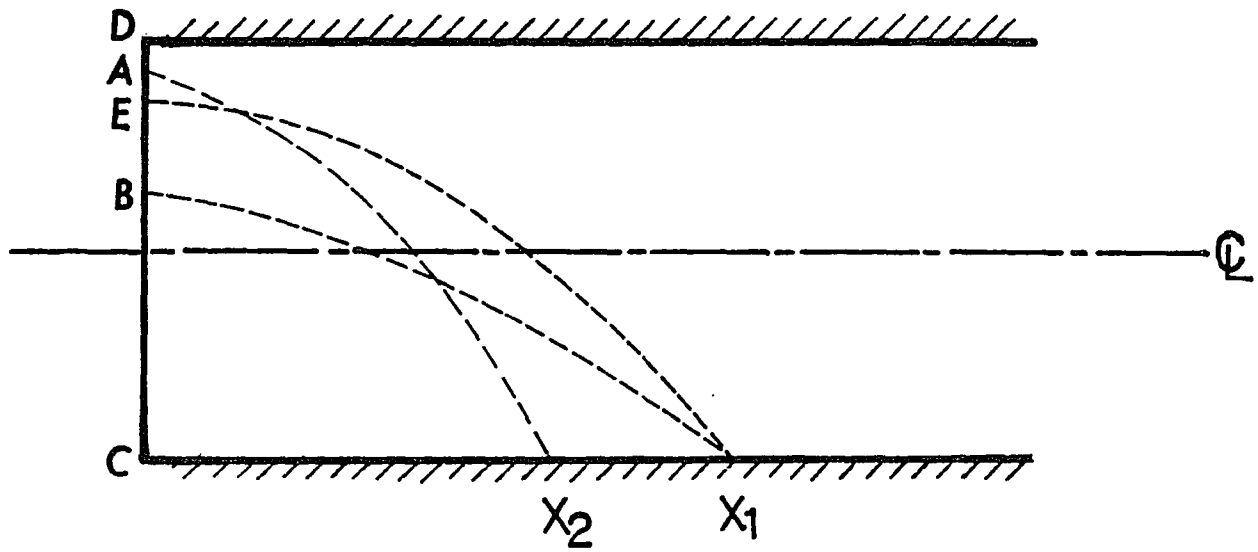

Fig. 3.3 Deposition Route of Particles in a Fluid of Parabolic Velocity Profile Confined by a Parallel-Plate Channel

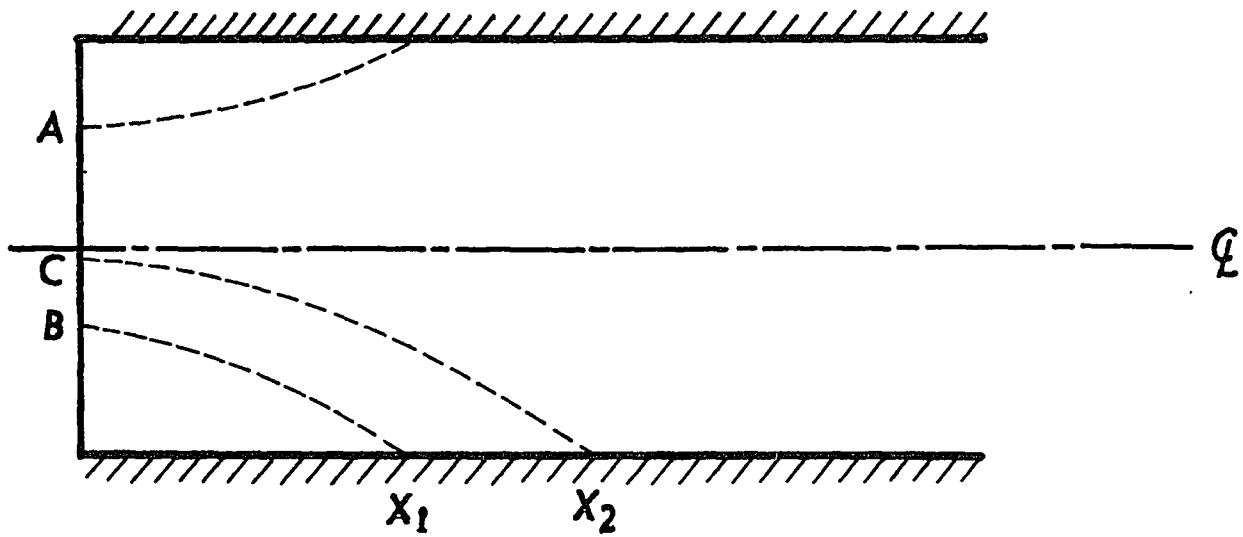

Fig.3.4 Deposition Route of Particles in a Parallel-Plate Channel with Additional Image Force

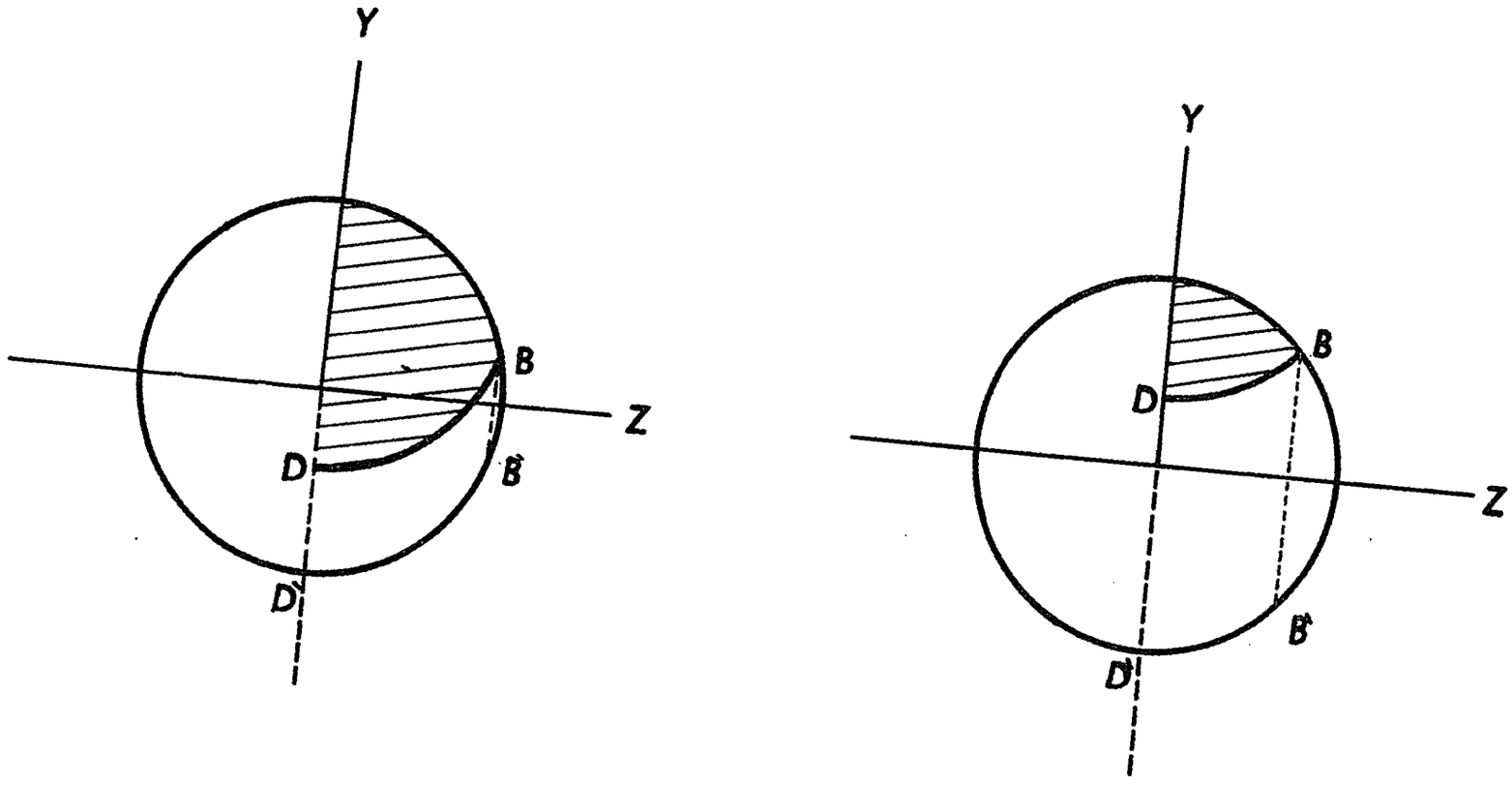

Fig. 3.5 Typical Equi-penetration Curves in a Circular Tube for a Uniform Flow with Gravity and Inertia Forces Involved

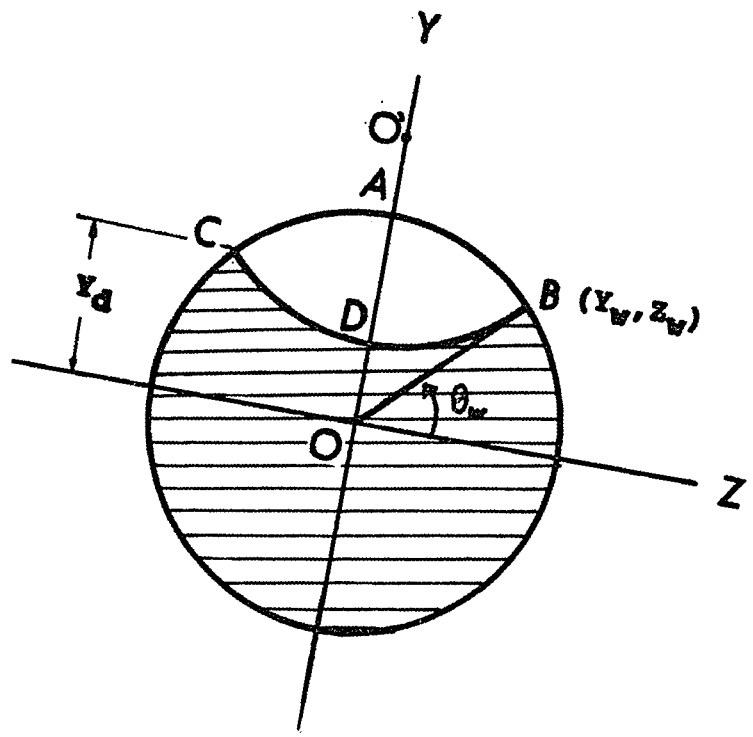

Fig. 3.6 Typical Equi-penetration Curve (CDB) Lied above the Z-axis

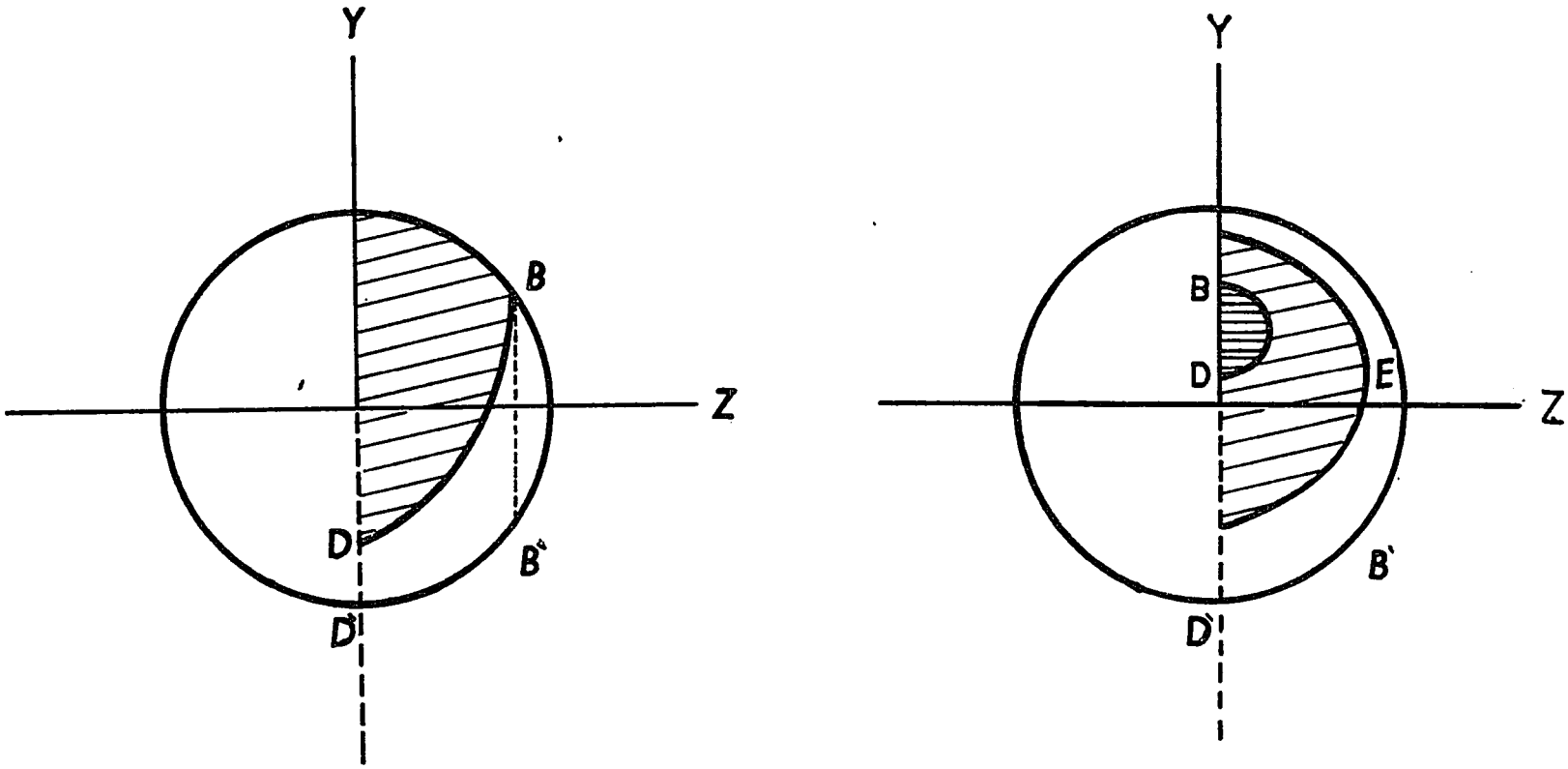

Fig. 3.7 Typical Equi-penetration Curves in a Circular Tube for a Parabolic Flow with Gravity and Inertia Forces Involved

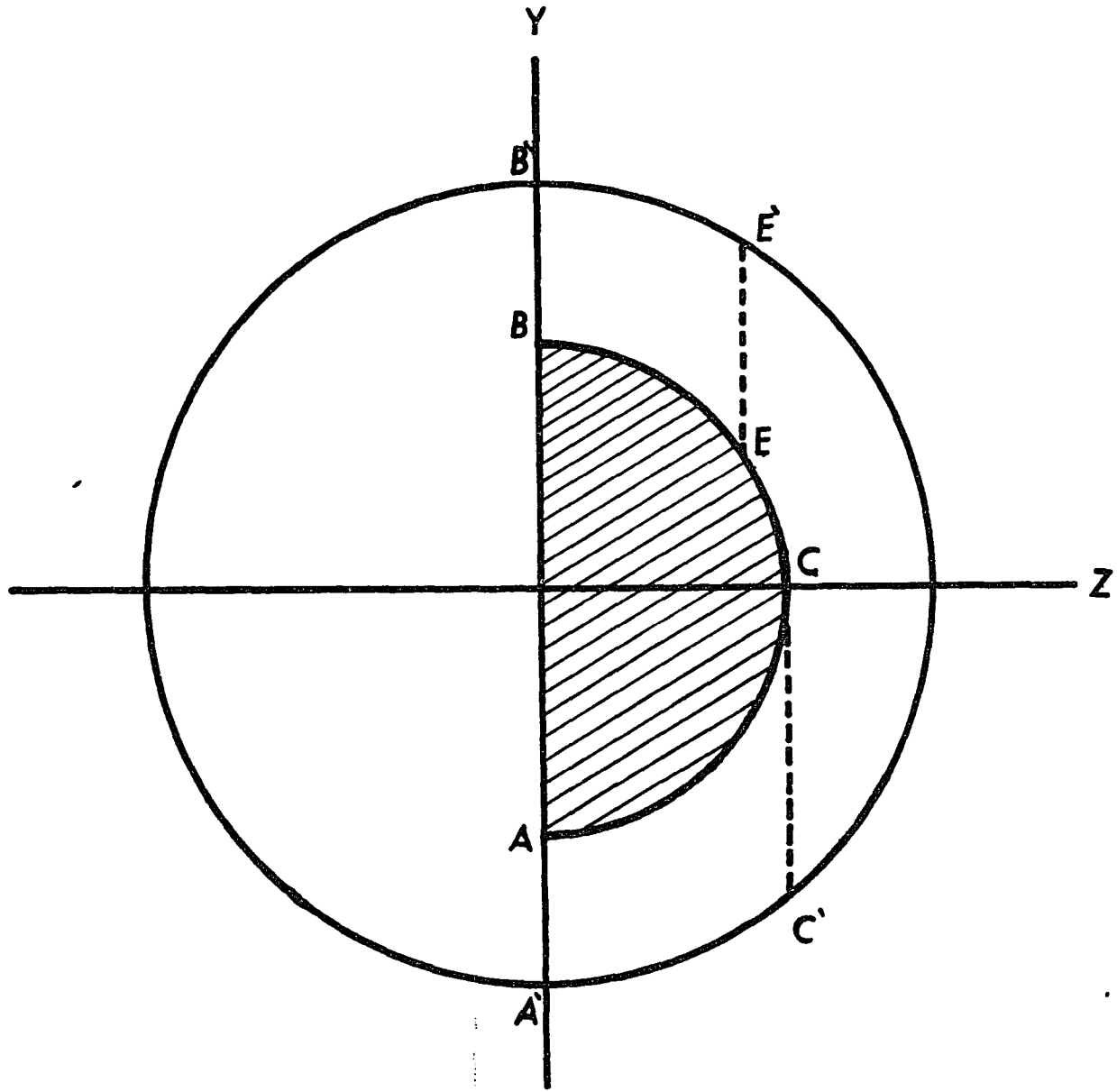

Fig. 3.8 Deposition Route of Particles in a Circular Tube with Additional Image Force Involved

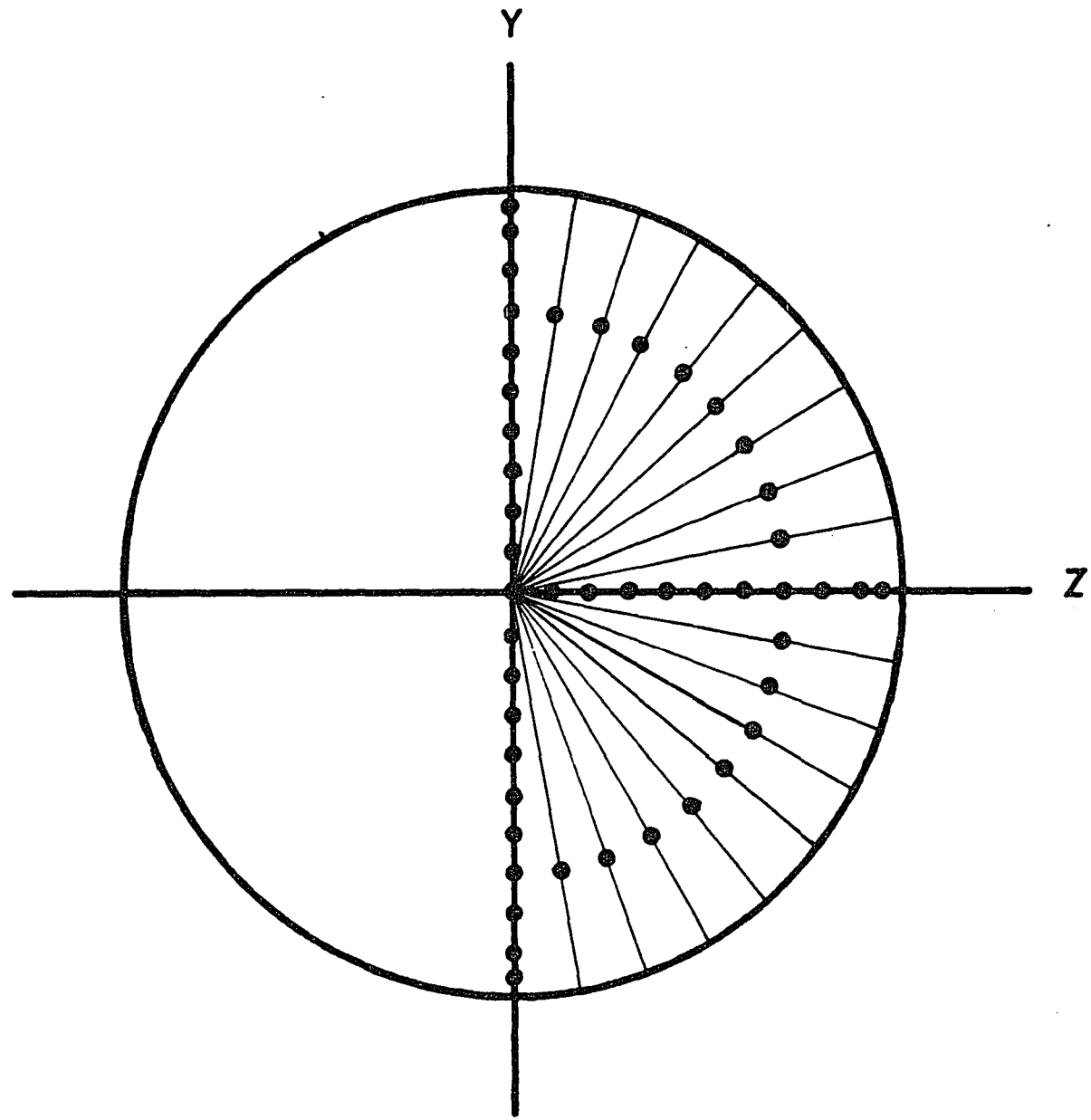

Fig. 3.9 Typical Data Points on the Inlet Plane of a Circular Tube

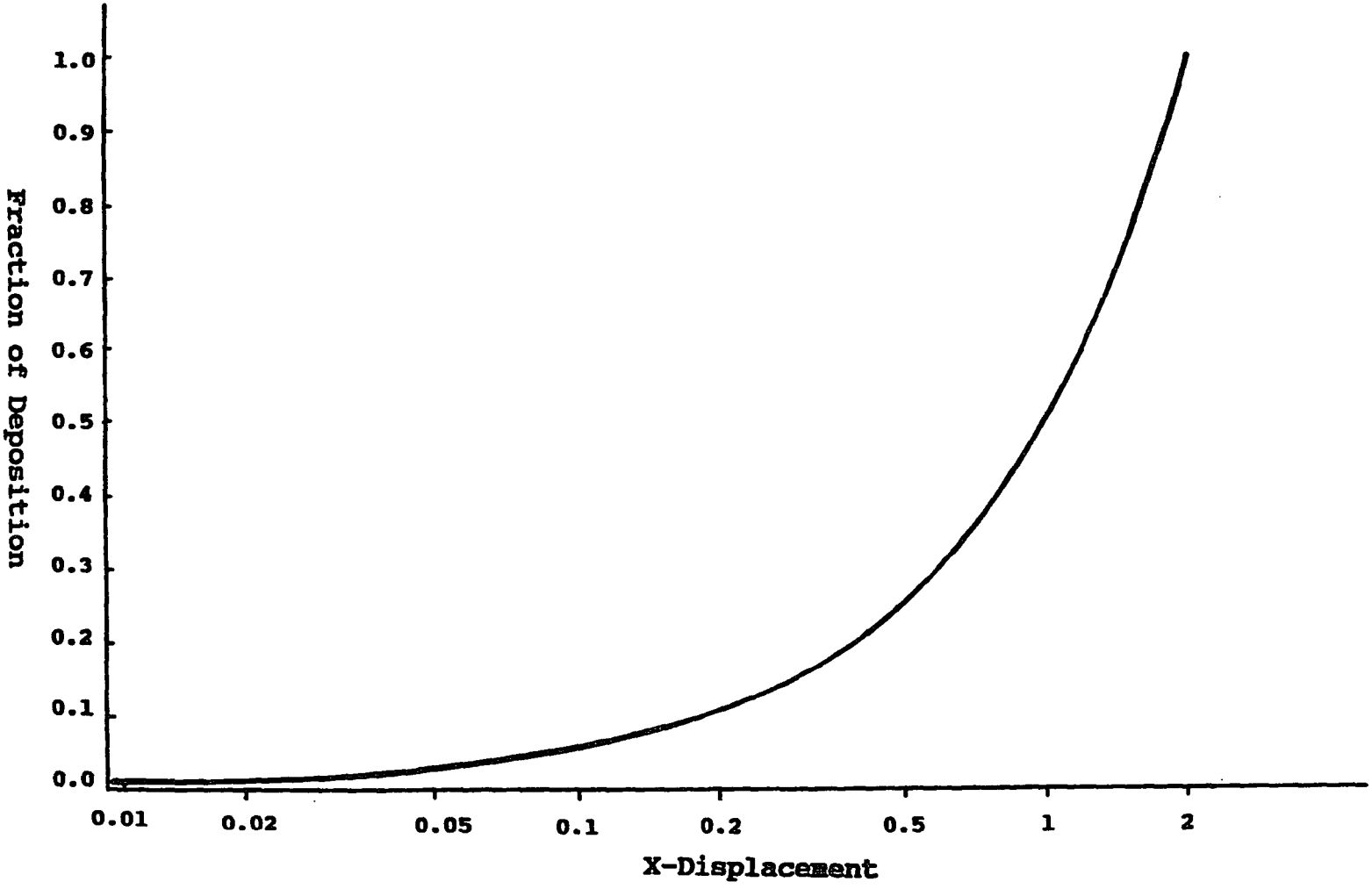

Fig. 4.1 Effect of Gravity and Inertia on Deposition for Uniform Flow in a Parallel-Plate channel; $Up_o = 0$, $G = 1$

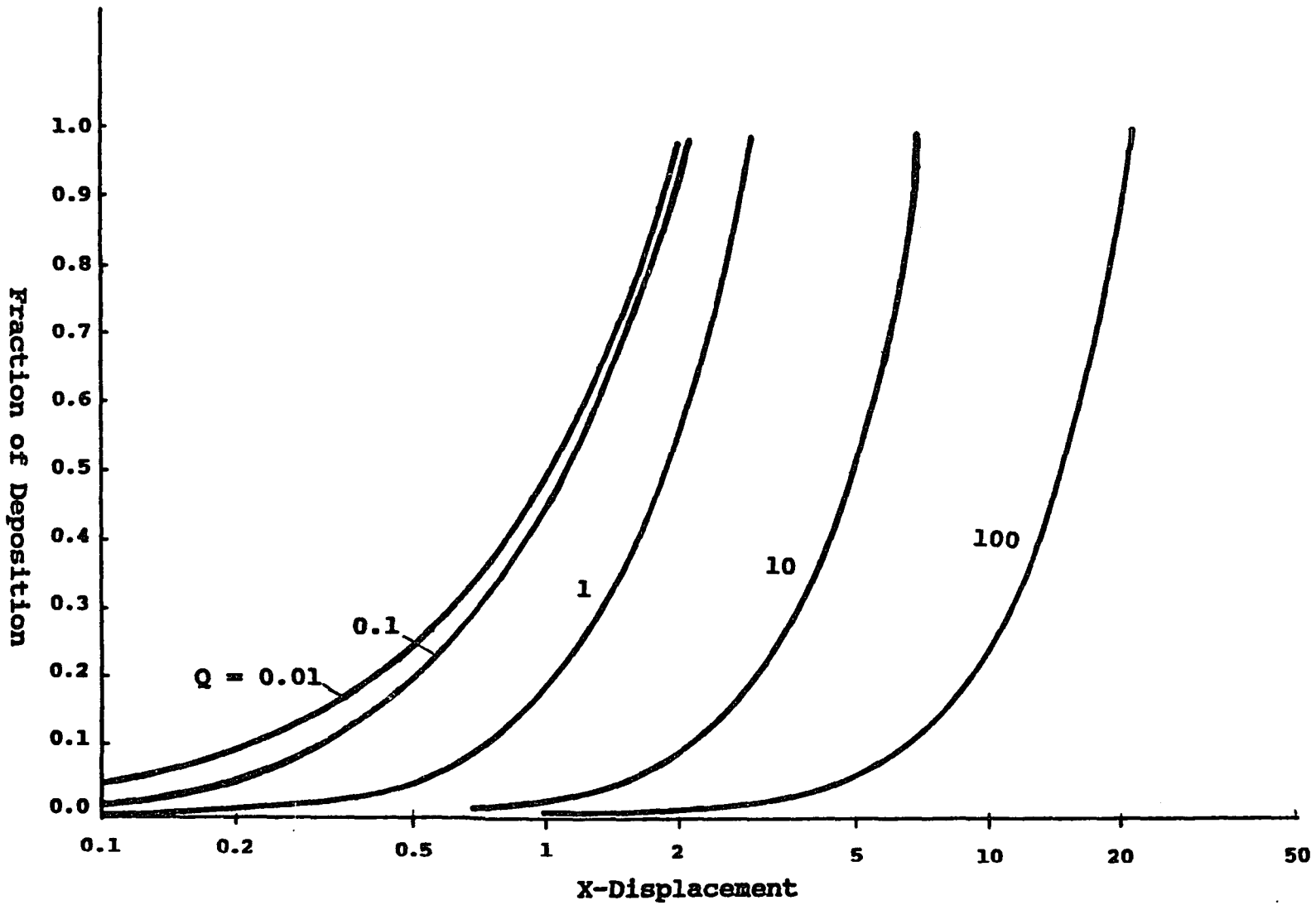

Fig. 4.2 Effect of Gravity and Inertia on Deposition for Uniform Flow in a Parallel-Plate Channel; $Up_o = U_f$, G = 1

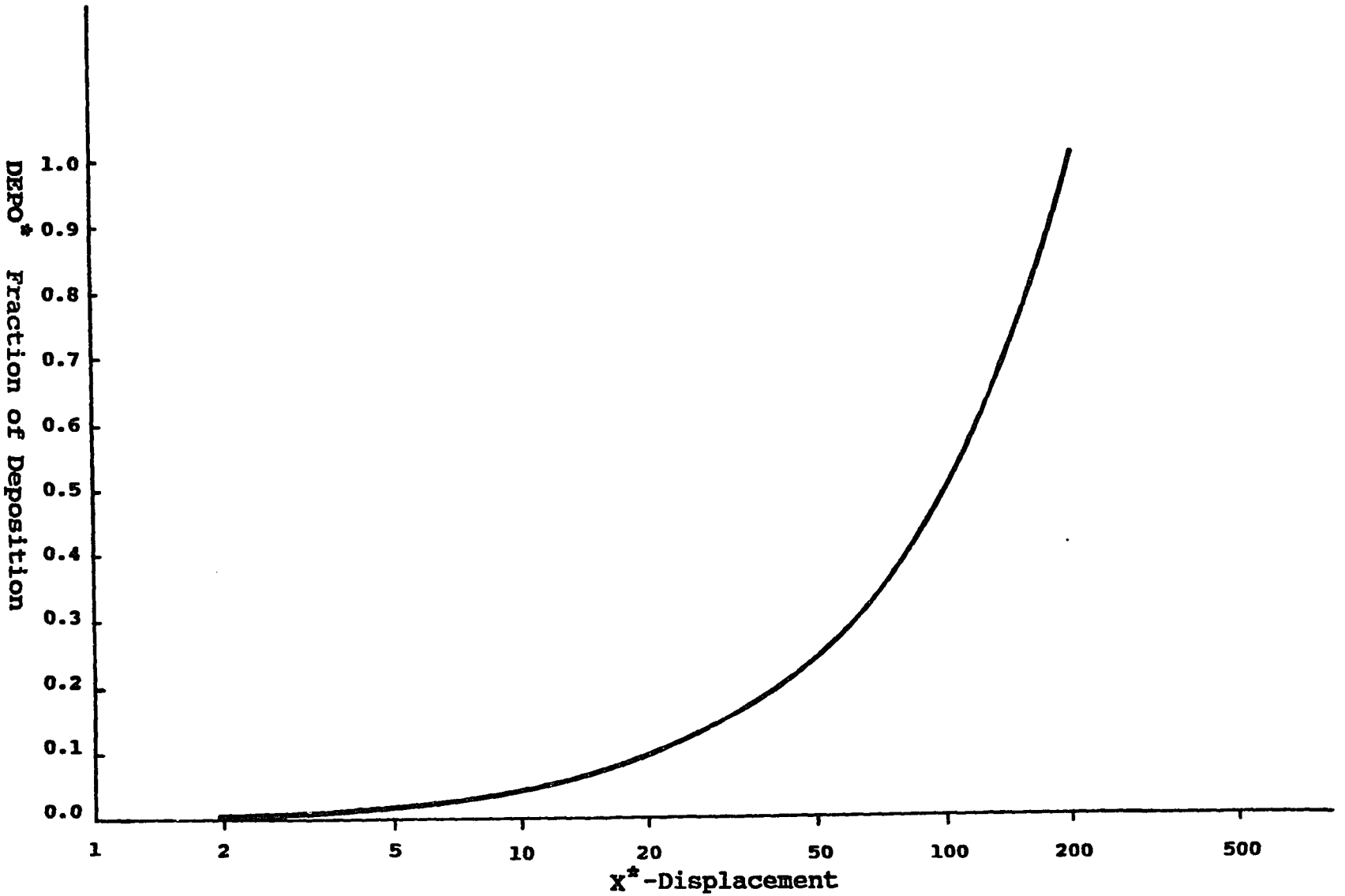

Fig. 4.3 Generalized Deposition Curve in a Parallel-Plate Channel for $X^* \leq 200$ in a Uniform Flow; $Up_o = Uf$, $G = 1$ ($X^* = X/Q$, $DEPO^* = DEPO/Q$)

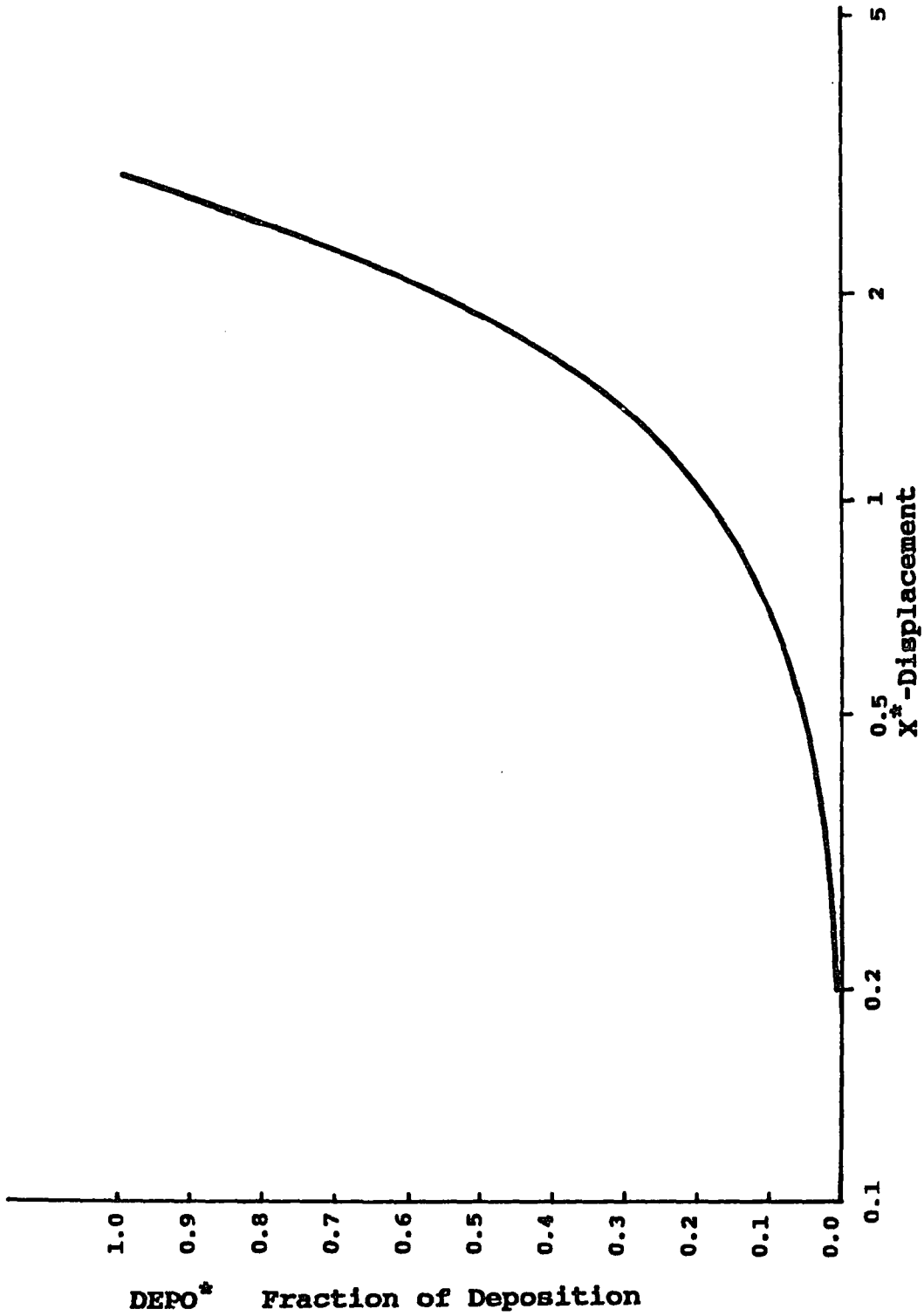

Fig. 4.4 Generalized Deposition Curve in a Parallel-Plate Channel for $X^* < 3$ in a Uniform Flow; $Up_o = Uf$, $G = 1$ ($X^* = X/Q$, $DEPO^* = DEPO/Q$)

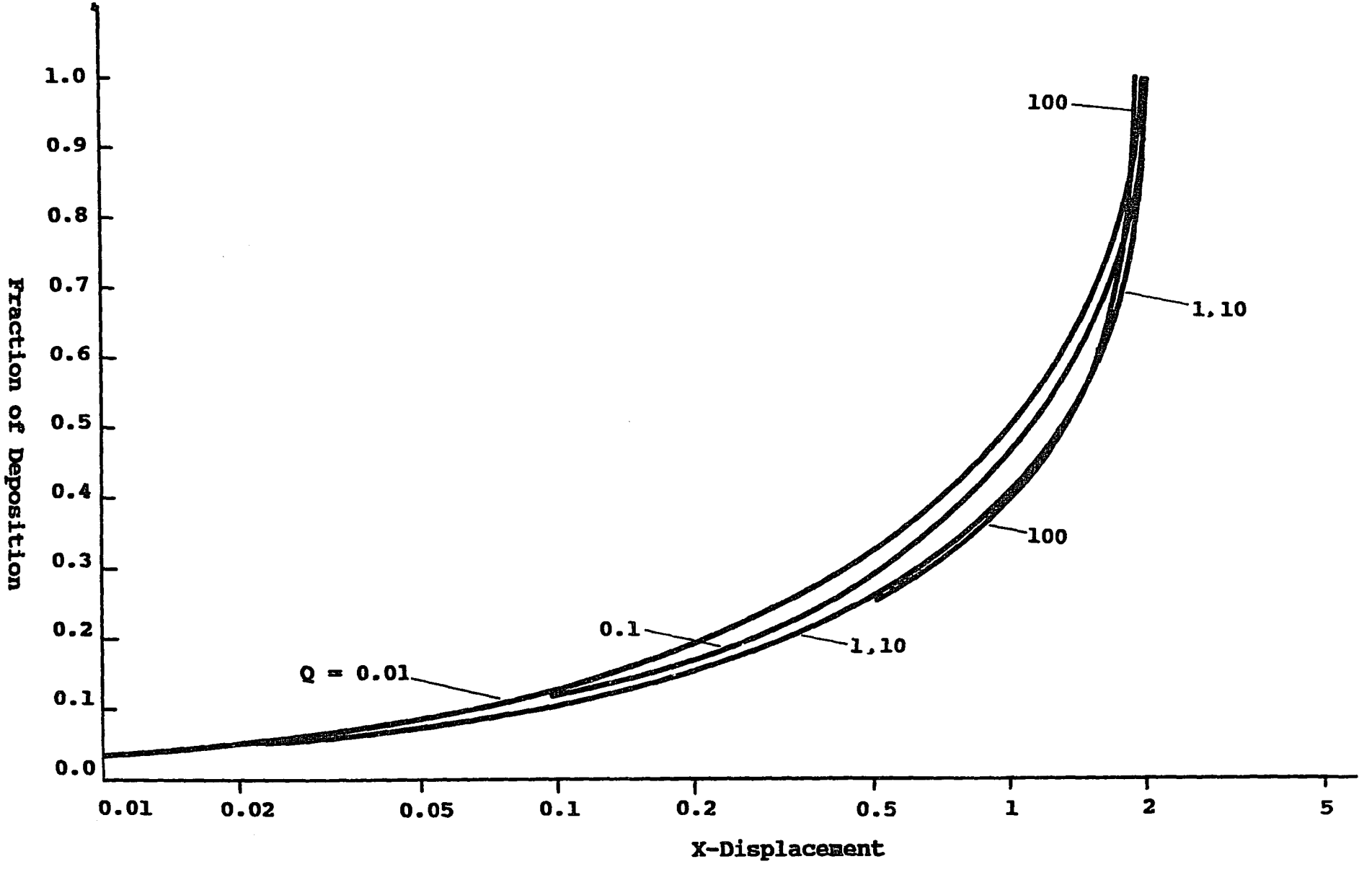

Fig. 4.5 Effect of Gravity and Inertia on Deposition for Parabolic Flow in a Parallel-Plate Channel; $Up_o = 0$, $G = 1$

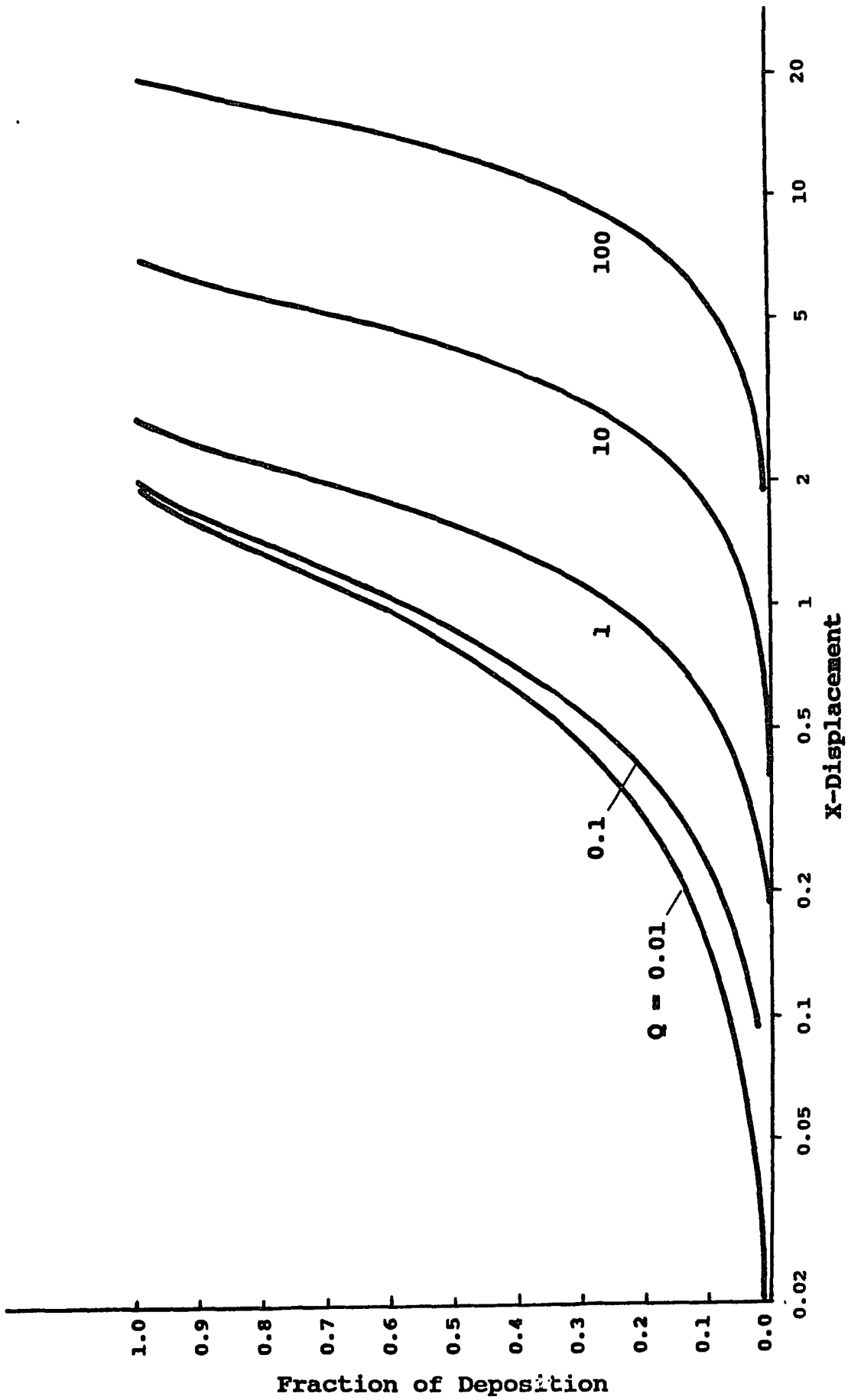

Fig. 4.6 Effect of Gravity and Inertia on Deposition for Parabolic Flow in a Parallel-Plate Channel; $Up_o = U_f$, G = 1

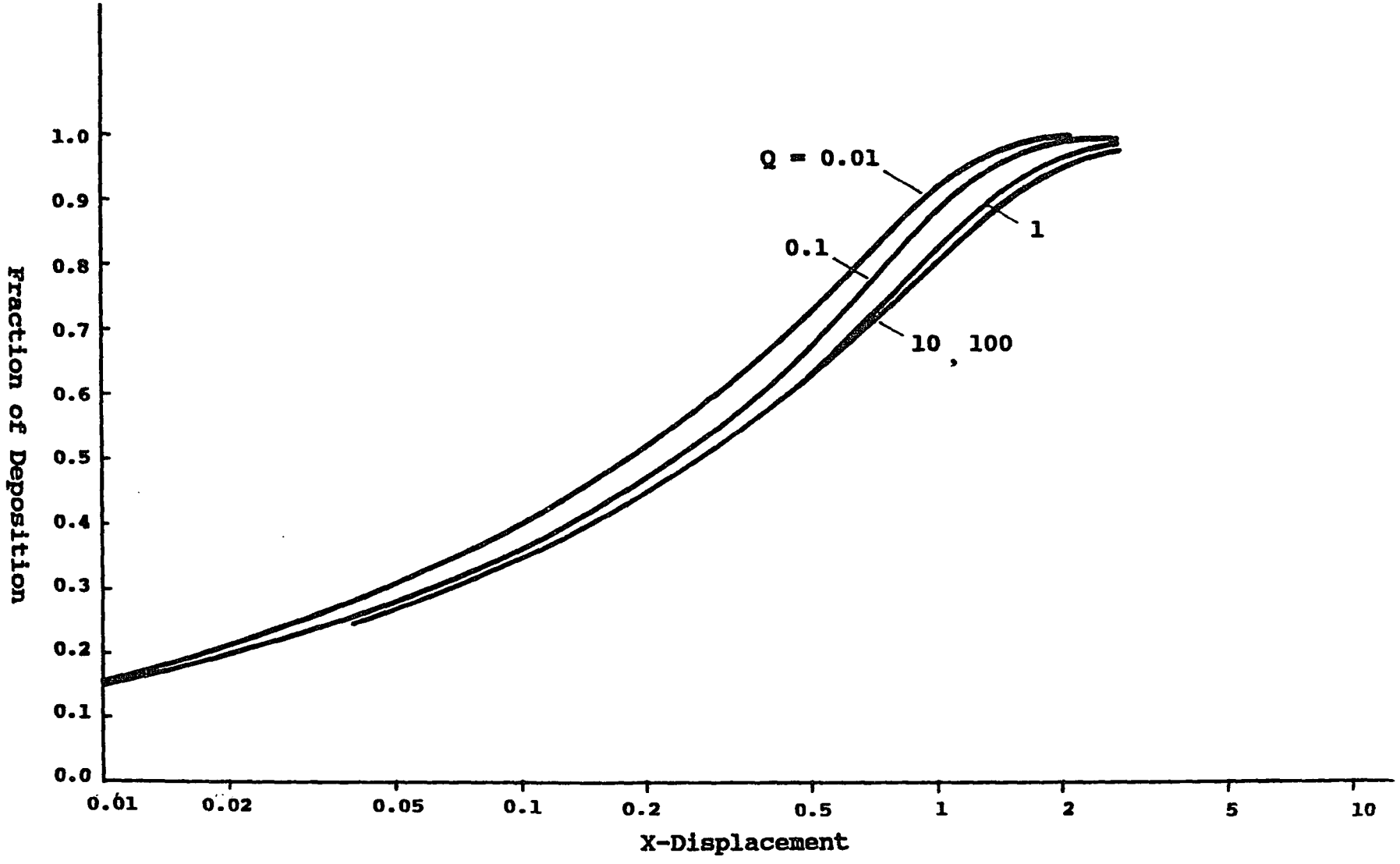

Fig. 4.7 Effect of Gravity, Inertia and Image Force on Deposition for Uniform Flow in a Parallel-Plate Channel; $Up_o = U_f$, G = 1, Fp = 1

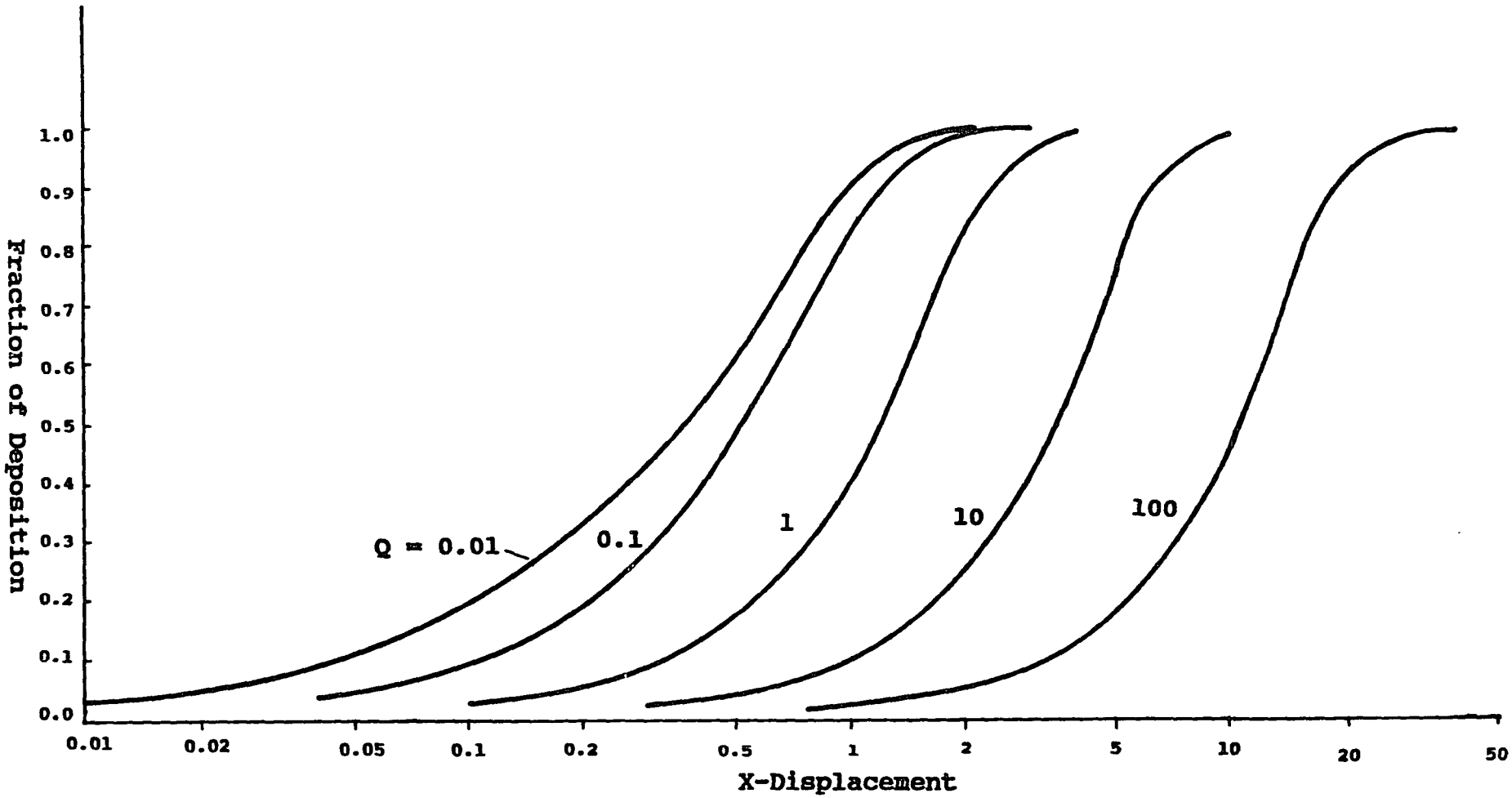

Fig. 4.8 Effect of Gravity, Inertia and Image Force on Deposition for Parabolic Flow in a Parallel-Plate Channel; $Up_o = U_f$, G = 1, Fp = 1

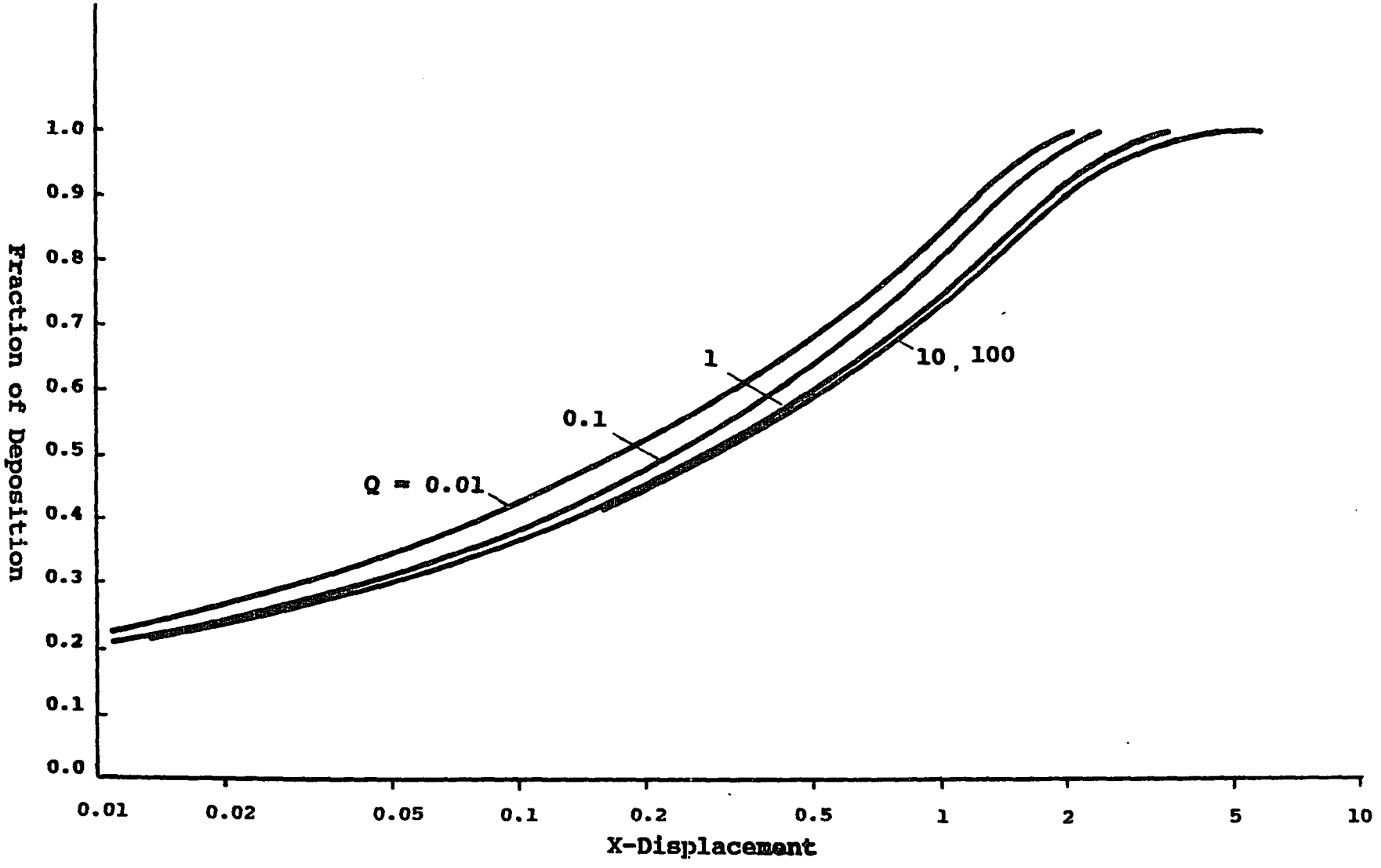

Fig. 4.9 Effect of Gravity, Inertia and Image Force on Deposition for Parabolic Flow in a Parallel-Plate Channel; $Up_o = 0$, $G = 1$, $Fp = 1$

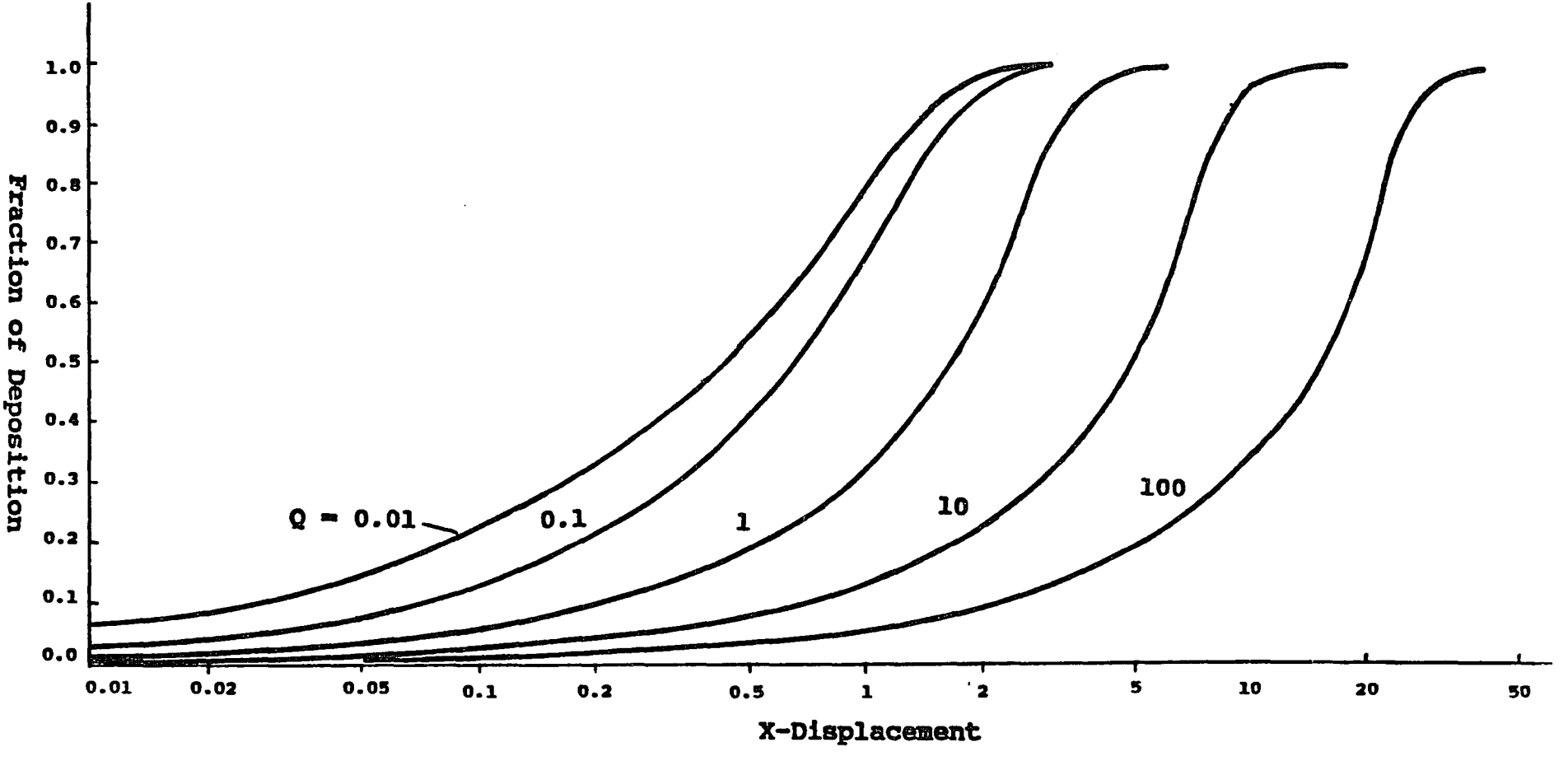

Fig. 4.10 Effect of Gravity, Inertia and Image Force on Deposition for Parabolic Flow in a Parallel-Plate; $Up_o = U_f$, G = 1, Fp = 1

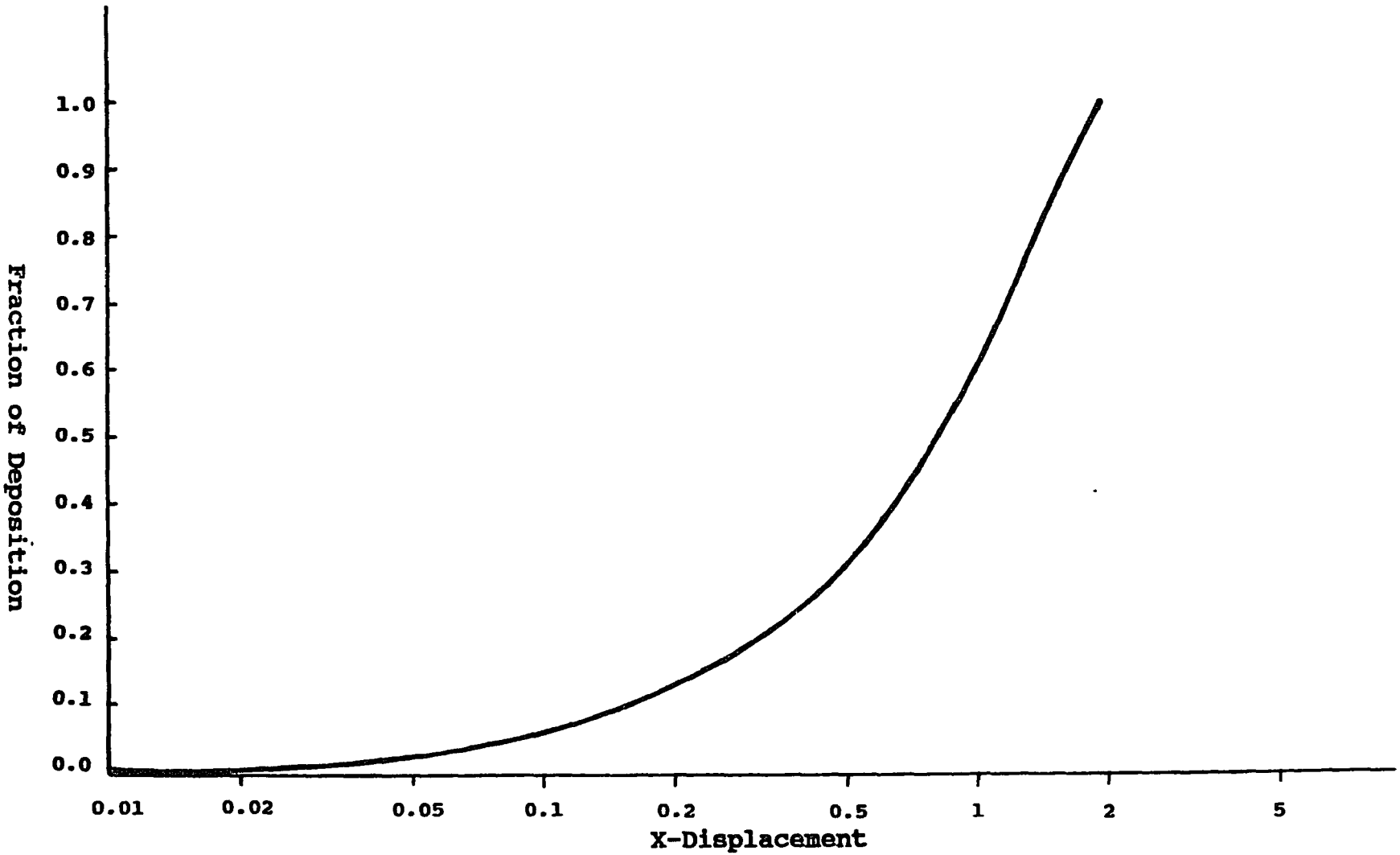

Fig. 4.11 Effect of Gravity and Inertia on Deposition for Uniform Flow in a Circular Tube; $Up_o = 0$, $G = 1$

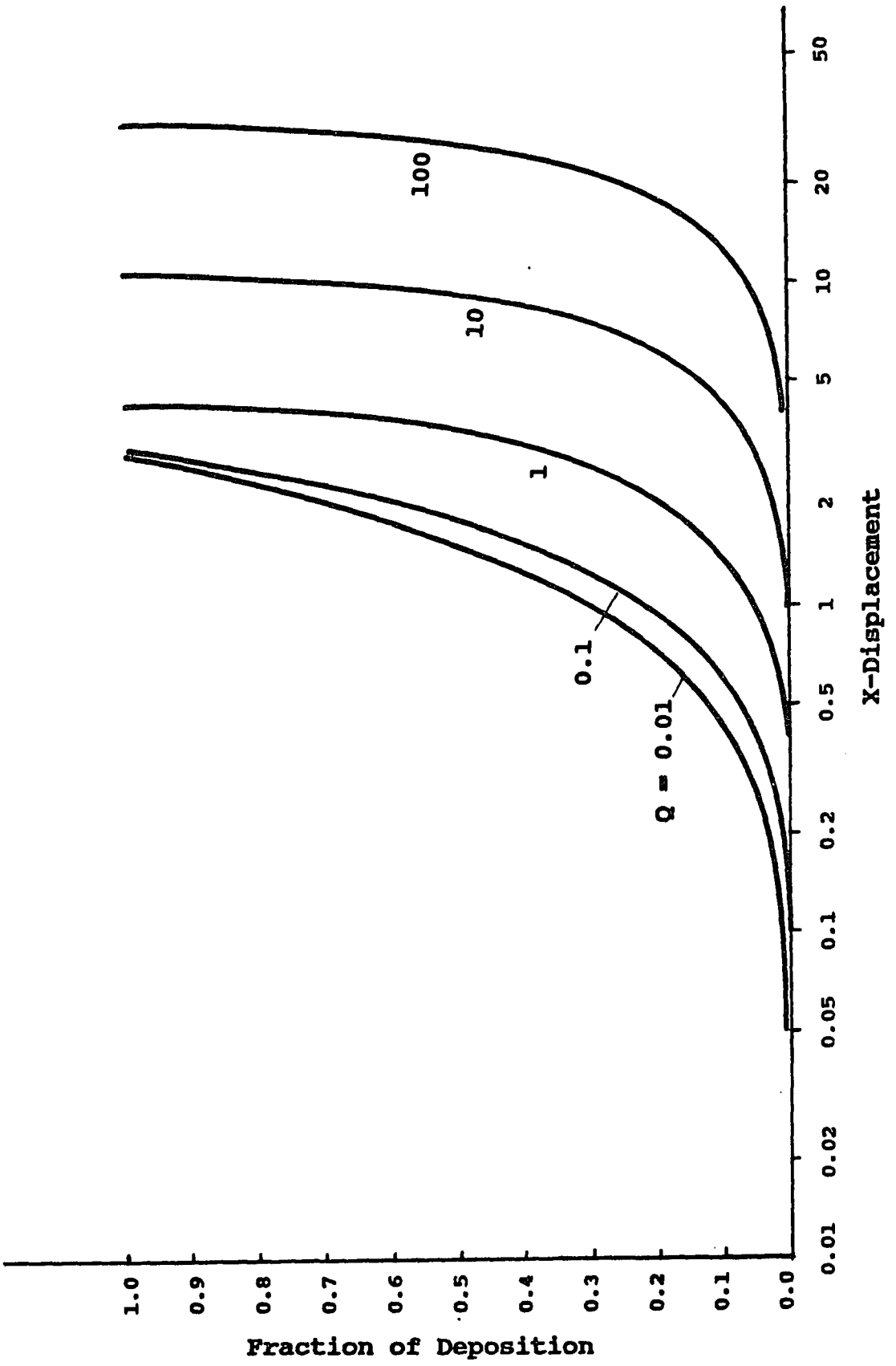

Fig. 4.12 Effect of Gravity and Inertia on Deposition for Uniform Flow in a Circular Tube; $Up_o = U_f$, G = 1

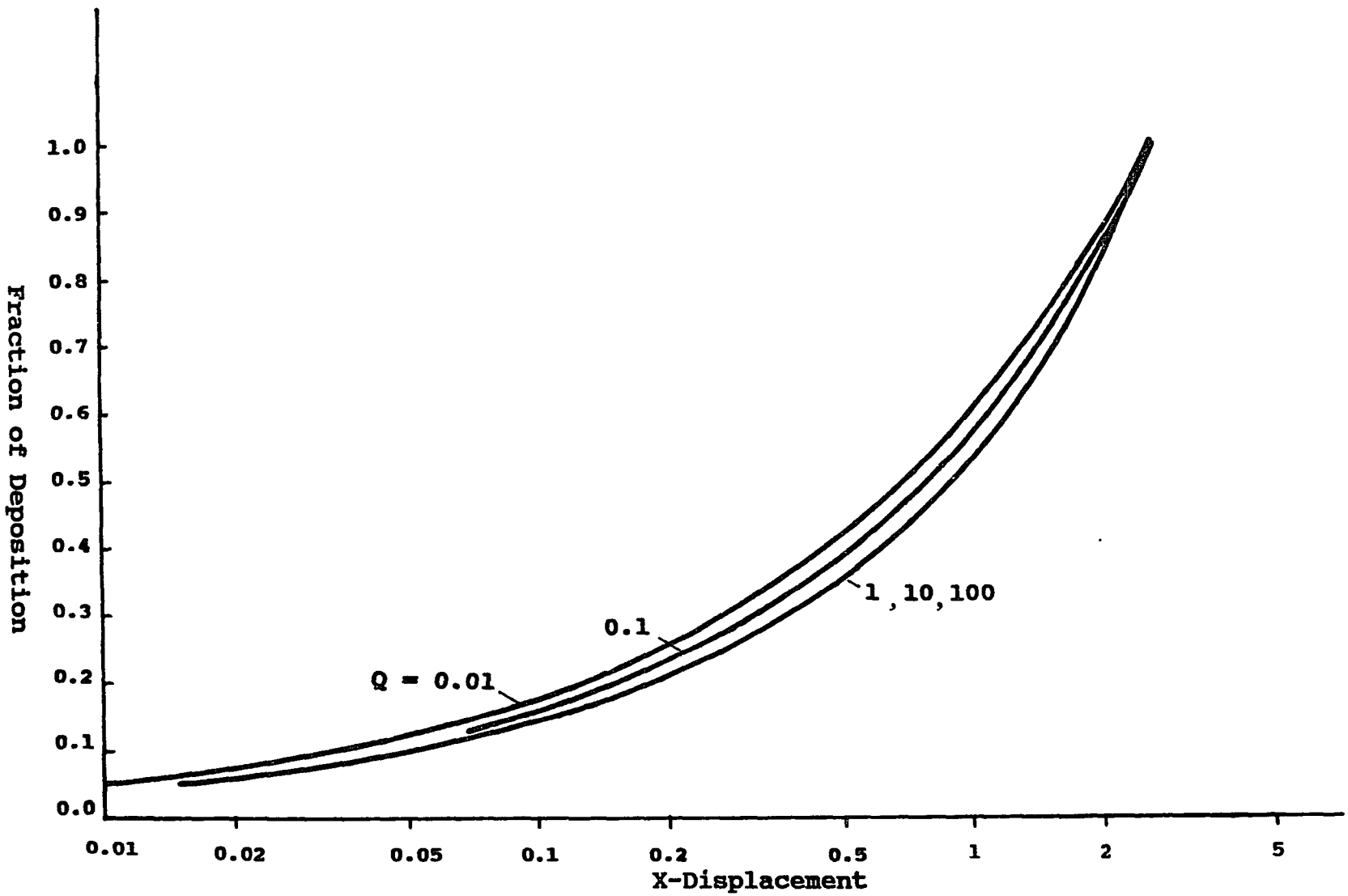

Fig. 4.13 Effect of Gravity and Inertia on Deposition for Parabolic Flow in a Circular Tube; $Up_o = 0$, $G = 1$

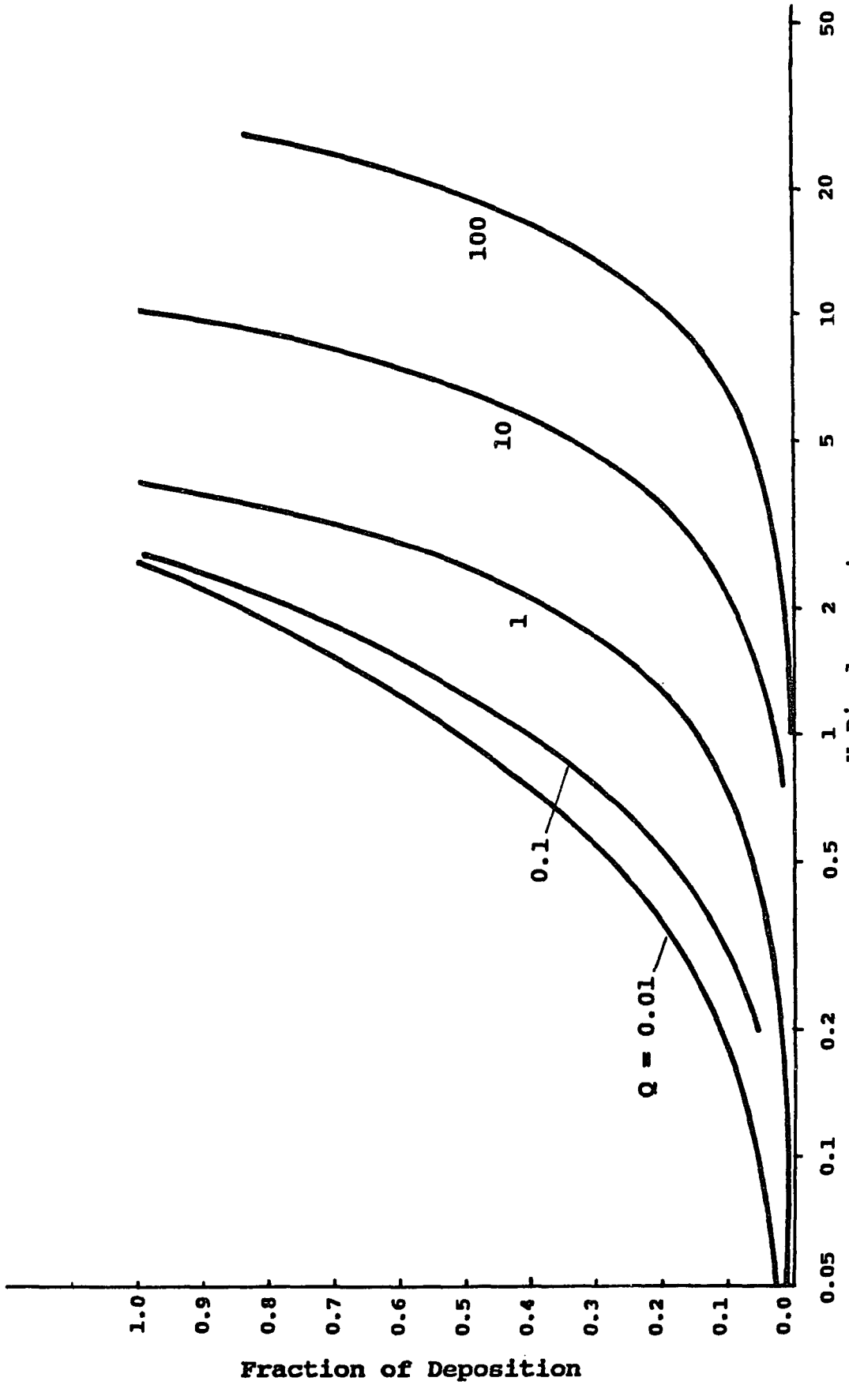

Fig. 4.14 Effect of Gravity and Inertia on Deposition for Parabolic Flow in a Circular Tube; $Up_o = U_f$, G = 1

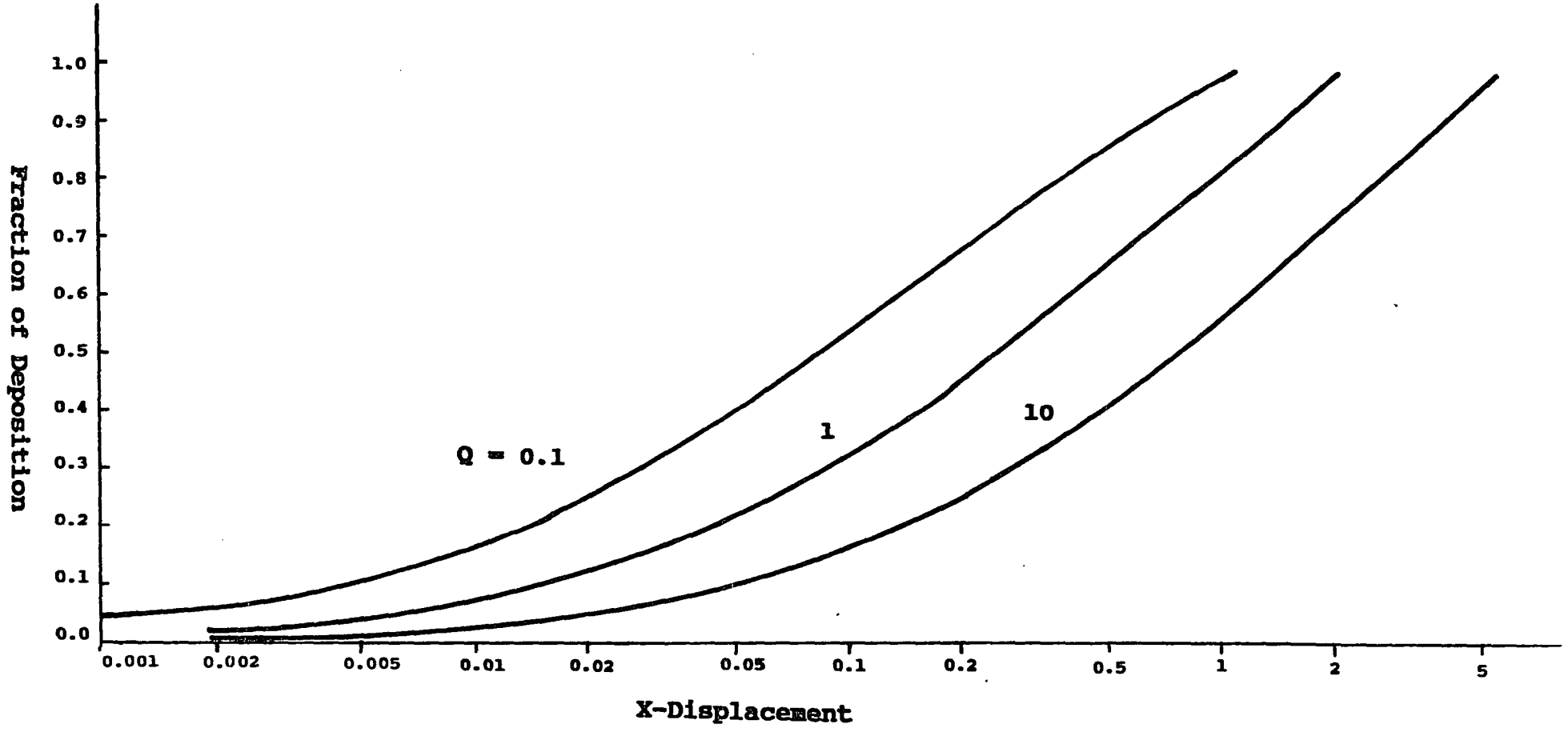

Fig. 4.15 Effect of Gravity, Inertia and Image Force on Deposition for Uniform Flow in a Circular Tube; $Up_o = U_f$, G = 1, Fp = 1

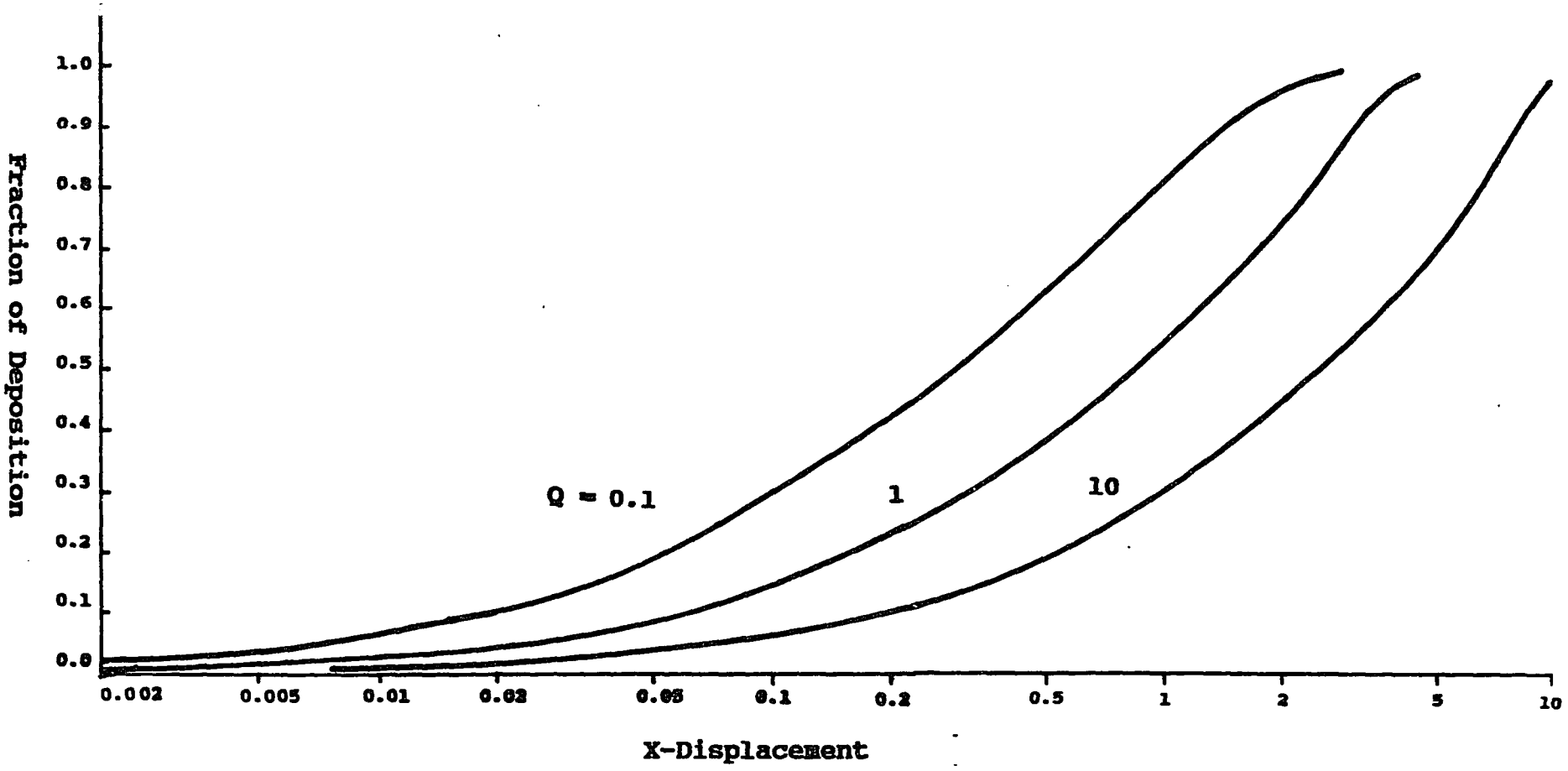

Fig. 4.16 Effect of Gravity, Inertia and Image Force on Deposition for Parabolic Flow in a Circular Tube; $Up_o = U_f$, G = 1, Fp = 1

VITA

Name : Win - Chung Chen

Degree and Date to be Conferred : Doctor of Engineering Science in Mechanical Engineering, October, 1986

Collegiate Institutions Attended	Dates	Degree (Year)
New Jersey Inst. of Tech.	1982-1986	D.Eng.Sc.1986
New Jersey Inst. of Tech.	1979-1982	M. S. 1982
National Taiwan University	1970-1974	B. S. 1974

Graduate Major : Mechanical Engineering

Undergraduate Major : Horticulture Science

Minor : Chemical Engineering, Computer Science, Chemistry

Position Held:

1/84-5/86	Teaching Assistant, N. J. I. T.
9/83-12/83	Adjunt Instructor, N. J. I. T.
4/83-8/81	Project Study Engineer Foster Wheeler Energy Corp. Livingston, New Jersey, U.S.A.
7/81-9/79	Research Assistant, N. J. I. T.

Publications:

- Inertia Effect on the Deposition of Charged Particles in a Parallel-Plate Channel.", Powder Technology, Vol. 34-2, 1983
- Oil Firing to Gas Firing Conversion with Dual Fuel Firing Capability (Eastman Kodak Co., NY)
- Evaluation of Modifications to Improve Unit Efficiency (Black Hill P&L Co., Wyoming)
- Analysis of Radiant Superheater and Waterwall Circulation at Critical Loads (PSE&G, NJ)
- Simulation of Refrigeration System with Multistage Compressor